N64-18513*
CODE-1
CR-53640
122p.

ANNUAL SUMMARY REPORT

METALLURGICAL EFFECTS OF EXPLOSIVE STRAIN RATES ON METAL ALLOYS

0513-01(02)FP

Contract NAS8-2416

27 July 1962 - 26 July 1963

OTS PRICE
XEROX $ 10.10 ph
MICROFILM $ 3.86 mf

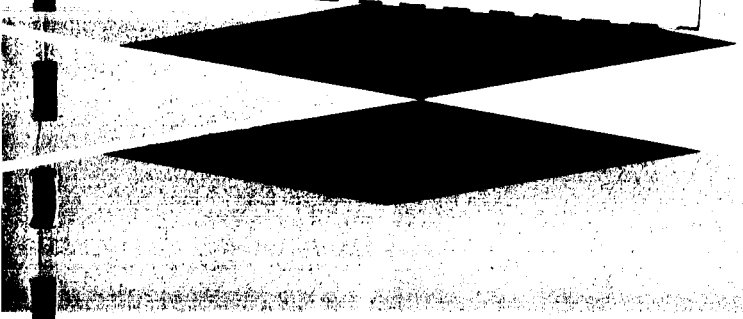

ORDNANCE DIVISION

Aerojet-General®
CORPORATION

A SUBSIDIARY OF THE GENERAL TIRE & RUBBER COMPANY
AZUSA, SACRAMENTO, AND DOWNEY, CALIFORNIA

ANNUAL SUMMARY REPORT, 27 Jul. 1962 - 26 Jul. 1963

t; METALLURGICAL EFFECTS OF EXPLOSIVE STRAIN RATES ON METAL ALLOYS

J. F. Wilkin)
E. K. Henriksen) and
I. Lieberman

26 July 1963 122 p refs

00 32672

(1) AEROJET-GENERAL CORPORATION (2)
(2) Ordnance Division
11711 Woodruff Avenue
Downey, California

Report No. 0513-01(02)FP

NASA Contract NAS8-2416
GEORGE C. MARSHALL SPACE FLIGHT CENTER
NASA, Huntsville, Alabama

26 July 1963

(NASA CR-53640; Rept. ~ site only) OTS: $ - - - See Cover

COPY NO: 09

FOREWORD

This report was prepared by Aerojet-General Corporation under Contract No. NAS8-2416 for the George C. Marshall Space Flight Center of the National Aeronautics and Space Administration. The work was administered under the direction of the Propulsion and Vehicle Engineering Division, Engineering Materials Branch of the George C. Marshall Space Flight Center with W. B. McPherson acting as project manager.

The assistance of the following Aerojet personnel whose contributions did much to aid in the successful completion of the program is acknowledged: R. E. Herfert, A. H. Hussung and C. D. Hill of the Metallurgical Laboratories.

ABSTRACT

18513 A

This program investigated the effects of explosive strain rates on the mechanical and physical properties of the following metal alloys and weldments:

2219-T37 Aluminum Alloy
2219-T87 Aluminum Alloy
5Al-2.5Sn Titanium Alloy (Annealed)
René 41 Nickel Alloy

As a result of the program, the following conclusions are drawn:

(a) Mechanical properties generally show no detrimental effects in the materials investigated when subjected to explosive strain rates.

(b) Residual stresses in 2219-T87 aluminum, formed hydraulically, approach values which may be considered hazardous, as opposed to stresses present in explosive forming which are at considerably lower levels.

(c) Changes in metallurgical structure resulting from explosive straining are not evident, and differences in structure as a result of strain rate within the range investigated can not be determined microscopically. X-ray diffraction studies, however, may be successful in detecting structural changes resulting from strain rate application for specific materials only.

Author

CONTENTS

LIST OF TABLES

LIST OF TABLES (Cont.)

LIST OF FIGURES

LIST OF FIGURES (Cont.)

LIST OF FIGURES (Cont.)

LIST OF FIGURES (Cont.)

LIST OF FIGURES (Cont.)

1. INTRODUCTION

1.1 PRIOR WORK

This contract was initiated on 27 June 1961 to investigate the metallurgical effects engendered in metal alloys by explosive forming. During the first year, the five metal alloys investigated were:

5456-0 Aluminum Alloy
AISI 301 Stainless Steel
17-7 PH Stainless Steel
6Al-4V Titanium Alloy
13V-11Cr-3Al Titanium Alloy

Test parameters included amount of strain, strain rate, temperature during straining and heat treat condition. The effects on mechanical properties and microstructural changes were observed. A comprehensive literature survey was conducted to obtain available information on the behavior of metals subjected to various strain rates. Results of these investigations are reported in the Annual Summary Report, No. 0513-01(01)FP, dated 26 July 1962, by J. F. Wilkin, E. K. Henriksen, I. Lieberman, and C. A. Landusky, Aerojet-General Corporation.

1.2 CURRENT PROGRAM

Since the size of domes required for space vehicles exceeds rolling mill width, domes must either be formed in sections and welded, or flat blanks must be welded and then formed. Explosive forming techniques are generally applied because of size limitations of other processes. The objective of this phase of the contract was to study the mechanisms that operate at high strain rates and to evaluate the effects of these mechanisms on mechanical and physical properties of metal alloys and weldments with emphasis placed on microstructural changes resulting from explosive forming.

Materials which were tested during this period were nominally 0.100-inch thick and were as follows:

Alloy	Filler Material
Aluminum Alloy 2219-T37	2319 Aluminum Alloy
Aluminum Alloy 2219-T87	2319 Aluminum Alloy
Titanium Alloy 5Al-2.5Sn (Annealed)	Parent Alloy
Nickel Alloy René 41 (Solution Treated)	Hastalloy W

Suppliers' certifications of the test materials used are given in Table I.

1.2.1 Test Procedures

For control purposes, mechanical properties tests were conducted on all materials in the as-received condition, both longitudinal and transverse to the rolling direction of the material, In addition, control tests were made on welded transverse specimens with the weld longitudinal to the roll and centered within the gage length.

Test blanks of each material were formed in such a manner that biaxial strain was developed at conventional and at explosive forming rates. The term "conventional strain rate" as applied in this report refers to the strain rate which was applied to simulate conventional forming processes such as press-working and hydro-forming, while the "explosive strain rate" is that which results from forming by the detonation of a high explosive charge. Where practicable, the materials were deformed to total strains of approximately 40 per cent and 75 per cent, expressed as per cent of maximum at fracture. A limited number of uniaxially strained specimens were also provided for correlation between uniaxial and biaxial forming. Subsequent to forming, the following mechanical properties were determined:

Proportional limit
0.2 per cent offset yield strength
Ultimate tensile strength
Notch sensitivity (NASA edge-notch test)
Per cent elongation in 2 inches
Per cent reduction of area
Modulus of elasticity
Microhardness

All prestrained specimens taken for tensile and notch tests were oriented transverse to the rolling direction. Tensile specimens had a 2-inch gage length and a 0.500-inch width. Edge-notch specimens had a 2-inch gage length, a 1.000-inch width and a 0.700-inch notch root width. Root radius of the 60°notches was 0.001-inch maximum.

The microstructural study was made by optical and electron microscopy. Lattice parameters were determined by X-ray diffraction. Residual stresses were determined by a dome sectioning method for 2219-T87 aluminum alloy.

1.2.2 Test Equipment

Biaxial straining of the test materials was accomplished by use of a forming die which may utilize either a high explosive charge as in Figure 1 or hydraulic fluid as in Figure 2 to form the test blank. All test blanks were photogridded with a combined 0.2-inch quadrille and 0.1-inch polar grid to provide for measuring strain. The die allowed for deep free-forming to fracture for determining fracture strain. Then, adjusting die depth by placing a spacer and an insert in the die, domes with a flat center section were formed. This provided flat balanced biaxially strained material from which tensile, edge-notch, and microstructural specimens were cut. A number of spacers and inserts were provided to allow for a wide range of strains as required to form the various test materials.

Three hydraulic pump units were used with the die for hydraulic bulge forming, depending on the pressure required. A Rucker Circuit-Pak hydraulic unit provided a maximum pressure of 1,500 psi and a flow rate of 3 GPM. A Worthington Reciprocating Pump furnished 3,000 psi, and a Sprague Pneumatic Diaphragm could deliver up to 30,000 psi, but at a very limited flow rate. For time-pressure plots, a Bristol Circular Chart Recorder was used in conjunction with the Worthington Pump, and a Bristol Strip Chart Recorder was used with the Sprague Pump. No recording device was used with the Rucker unit, but a stop-watch was used to obtain total time of pressure application, and maximum pressure was read from a pressure gage. Average strain rate was calculated by dividing strain at the center of the dome by the total time of forming. The explosive strain rate was previously found to be on the order of 100 in/in/sec.

Uniaxial prestraining of test specimens at the conventional strain rate was performed in the tensile testing machine with a cross-head velocity of 10 in/min. With approximately 3 inches of effective

length between grips, the resultant strain rate developed in the specimen was 0.05 in/in/sec. All control and uniaxially prestrained specimens were photogridded with parallel lines spaced 0.100-inch apart transverse to the specimen. This facilitated measurement of strain distribution in addition to elongation in 2 inches. Specimens machined with excess width in the gage length were strained at the 0.05 in/in/sec rate to fracture and to approximately 75 per cent of fracture. After prestraining the wide specimens, tensile specimens were remachined to the standard 0.500-inch width, edge-notch specimens were remachined to the 1.000-inch width, and the notches were added. Additional specimens were sectioned and mounted for microstructural study.

The Dynamic Test Fixture, Figure 3, was used for the explosive straining. Fracture strain only was developed in uniaxial specimens at the explosive strain rate of approximately 100 in/in/sec.

1.2.3 Comparison of Test Results

In order to evaluate and compare test results from uniaxially and biaxially stressed material, the prestrain was converted to octahedral shear strain. The octahedral shear strain is the shear strain found in the octahedral plane. The normal to this plane forms equal angles of $54^{\circ}\ 44'$ with the directions of the three principal strains. The true octahedral shear strain,

$$\bar{\gamma} = \frac{2}{\sqrt{3}} \sqrt{\bar{\varepsilon}_1^{\,2} + \bar{\varepsilon}_2^{\,2} + \bar{\varepsilon}_3^{\,3}}$$

where $\bar{\varepsilon}_1$, $\bar{\varepsilon}_2$, and $\bar{\varepsilon}_3$ are the principal true strains. In the case of uniaxial stress, $\bar{\gamma} = \sqrt{2}\ \bar{\varepsilon}_1$, and for balanced biaxial stress, $\bar{\gamma} = 2\sqrt{2}\ \bar{\varepsilon}_1$. The true strain,

$$\bar{\varepsilon} = \ell n\,(1 + \varepsilon)$$

where ε is the measured strain.

2. DISCUSSION

2.1 2219 ALUMINUM ALLOY

The 2219 aluminum sheet material was received in the T37 condition. A recommended heat cycle for aging to the T87 condition was evaluated on a representative sample. The aging cycle employed was 325°F for 14 hours. Since the resulting mechanical properties given in Table II agree closely with published properties, the above heat cycle was adopted for use in this program where T87 condition material was required.

2.1.1 Welding Procedure

Qualification welds of 2219-T87 aluminum conformed to Specification ABMA-DD-R27A, A-1, Class II, upon radiographic inspection. Blanks were then prepared for biaxial forming. Welding was done on an Airline Stake Welder with 3/4-inch finger spacing, using a Vickers "Controlarc" 300DC Welder power supply and a Linde "Heliarc" Automatic Welding Machine. The weld schedule used was as follows:

Preparation:	Draw file edges, remove wire edge.
Etch:	Caustic and nitric solutions.
Hold-Down:	Table with 2-inch x 2-inch run-in and run-out tabs.
Equipment:	Automatic Direct Current Single Pole.
Backup Material:	Copper with groove 0.250-inch wide x 0.062-inch deep.
Amperes:	145
Volts:	15
Travel Speed:	14 IPM
Filler Metal Type:	2319
Filler Metal Size:	0.045-inch diameter.

Filler Metal Feed:	60 IPM
Atmosphere:	Helium
Flow Rate:	50 CFH
Electrode:	2% thoriated tungsten, 0.125-inch diameter.
Electrode Holder Angle:	Vertical

After welding was completed, the welds were machined flush with the sheet material and radiographically inspected. The composite polar and quadrille photogrid was then applied to the test blanks.

2.1.2 Forming Unwelded Blanks

In preliminary testing of the forming die, unwelded hot rolled steel blanks were used in 7 shots to assist in determining explosive charge sizes and details of die setup without using the more expensive test materials. After fracturing two blanks, five symmetrical domes were then formed, including three using an insert as shown in Table III. The same size charge, which fractured a blank in free-forming produced an integral dome when an insert was used. Four 2219-T37 and two 2219-T87 aluminum unwelded blanks were then formed. These included four domes for a preliminary experiment to determine the effect on mechanical properties of explosive forming before and after aging 2219 alloy from T37 to T87 condition. Comparison was also made with unstrained material. The four domes used in the experiment are shown in Figure 4 and the tensile specimens are marked on each dome as they were subsequently cut. Prestrain and mechanical properties data are presented in Table IV and are plotted in Figure 5.

Strain was equally distributed throughout the flat portion of the domes. The fracture in Dome No. 12 was basically longitudinal and off-center a sufficient distance to allow the cutting of three longitudinal specimens from the center of the dome. To avoid confounding the effects of directionality and per cent prestrain, all specimens from the four domes were cut in the longitudinal direction, as there was variation in prestrain among domes.

In referring to Domes No. 10 and No. 11 in Table IV, it may be observed that the yield and ultimate strengths of material aged subsequent to forming appear to be practically insensitive to the degree of prestrain. There is only a very slight increase in strength over the unstrained material.

Domes No. 12 and 13, formed after aging, gained in both yield and ultimate strengths. The average yield strength increased 15 per cent and the average ultimate strength increased 4.5 per cent when forming was done in the T87 temper. It would, therefore, be advantageous to form in the aged condition for improvement of strength if a reduction in elongation from 13.7 to 10.5 per cent could be tolerated in the blank material as indicated in Tables IV and XIV.

2.1.3 Forming Welded Blanks

A welded hot-rolled steel blank was free-formed in the die using the identical charge of a previously formed unwelded blanks as reported in Table III. The resulting deflection was less than the unwelded dome, as reinforcement was apparently provided by the weld, but the dome formed symmetrically without fracture. A welded 2219-T87 aluminum blank was set up and fired in the same manner as a previously formed unwelded blank. The weld fractured, and the sheet material fractured below and roughly concentric with the draw radius. The flange drew in on the weld diameter but increased on the diameter perpendicular to the weld, indicating that the weld fractured early in the process and the pressures forced the material outward transverse to the weld seam. On subsequent tests, the charge and the blank diameter were reduced, but the weld fractured in each case from the apex into the flange area. One blank was formed with a hot-rolled steel cover sheet, but the weld fractured. A blank was then hydraulically formed to determine if the weld fracturing was a strain rate effect. With a very moderate deflection of 0.4-inch, the weld fractured for a length of 10.5 inches, indicating that weld failure is not to be ascribed to the explosive strain rate which was employed.

Strain was measured on three of the domes, transverse to the weld and across the fracture shown in Table V. It was found that the strain was concentrated within the weld area, and no strain could be detected outside of an original 0.4-inch width. Therefore, this zone was used as the basis for comparing elongation of the weld in the three domes. In comparing the two explosively formed domes with

the hydraulically formed dome (the last three domes shown in Table V), there appears to be a definite strain rate effect on elongation but with the strain confined to the weld zone. This elongation will not reflect itself appreciably in any increase in deflection as it is confined to a very narrow zone of only 0.4-inch as shown in Table V. It is apparent that the ultimate strength of the weld is lower than the yield strength of the sheet material in the T87 condition. The larger deflections shown for the explosively formed units are due to kinetic energy imparted to the material by the explosive charge which is still acting after fracture has occurred. With hydraulic forming, all pressure is released immediately upon fracture and resulting deflection appears much smaller.

2.1.4 Control and Uniaxial Strain Tests

Control tests for unwelded and welded material in Table XVI show that elongation in 2 inches is 10 per cent for unwelded material and 3.5 per cent for welded. Ultimate tensile strength of welded specimens is 38 ksi, while the yield strength of the unwelded specimens is 59 ksi. This fully accounts for the concentration of strain in the weld zone and confirms the explanation given above for the observed behavior.

Unwelded and welded specimens were explosively strained to fracture, and the per cent elongation is given at the end of Table XVI. Strain distribution curves are given for each specimen in Figures 6 and 7. The unwelded specimens show uniform strain except in the necked region adjacent to fracture, while strain in the welded specimens is concentrated entirely in the original 0.4 to 0.5-inch at the weld zone.

Uniaxially strained specimens displayed the same strain rate effect as the biaxially formed blanks in that elongation increased substantially at the higher strain rate for both unwelded and welded material.

Additional tensile tests were made on T87 welded material with the weld oriented on the longitudinal axes of the specimens. Specimens were also strained to fracture at conventional and explosive strain rates to reveal any possible strain rate effects on ductility. Results of these tests are given in Table VI. In comparing with the transverse welded control specimens in Table XVI, yield strengths are essentially the same, while ultimate tensile strengths varied from 38 ksi in transverse welds to 48 ksi in the longitudinal welds. Elongation in the longitudinal welds exceeds that of unwelded material in the standard tensile test and at the conventional strain rate, while elongation at the

explosive strain rate is slightly less in the longitudinal welds than in unwelded material. Where the parent material serves to reinforce the structural integrity of a welded unit, the elongation and mechanical properties will be improved over that specimen where the forces act only on the weldment and the parent material does not make a contribution.

2.1.5 Forming Welded Blanks in the T42 Condition

In view of the high strength differential between parent metal and weld metal in 2219-T87 welded aluminum blanks, an effort was made to increase the formability of the material by post-weld heat treating to achieve approximately equal yield strength in the sheet and weld material -- a necessary condition for uniform forming.

Recommendations received from Alcoa indicated that welded material should be re-solution heat-treated to the T42 condition for best forming. This lowers the strength below a useful level, but aging the material to the T62 condition increases the strength level while achieving equal yield strength in the sheet and weld.

To check formability of welded blanks in the T42 condition, four T87 condition blanks were re-solution heat-treated at 1000°F for 40 minutes and cold water quenched. Welds were machined flush on two of the blanks, while the weld bead was left on two blanks to take advantage of the area reinforcement; however, the weld bead was ground flush in the flange area to avoid interference when clamping in the die. One blank with the flush weld and one with the retained weld bead were formed explosively, and one with each type of weld was formed hydraulically. All blanks were cut 19 inches in diameter, and identical forming conditions were applied to each explosively formed blank. The results of forming two blanks in the T87 condition with flush weld, formed under the same conditions and reported in Table V, are included in Table VII and Figure 8 for comparative purposes.

The T87 dome, formed explosively, fractured early in the process and was driven out as well as down, causing the flange to increase on a diameter perpendicular to the weld, as shown in Table VII. A similar blank, formed hydraulically, fractured along the weld with only 0.4-inch deflection. The explosively formed T42 blank with flush weld formed deeper than the blank in the T87 condition with

small fracture dimensions and no increase in flange width, which would indicate that the fracture occurred later in the forming process. A similar blank, formed hydraulically, drew 5.4 inches deep, and the fracture intersected the weld but did not progress along it. The T42 blank, with weld reinforcement and formed explosively, fractured adjacent to the weld and appeared to fracture earlier in the forming process than the blank with the flush weld. The comparable blank, formed hydraulically, did not fracture but continued to draw to 6-inch deflection until one side of the flange drew past the draw radius, and hydraulic pressure was lost. In comparing formability of the four T42 domes, it may be concluded that increased forming was obtained by the hydraulic process, while greater forming was accomplished by the explosive method in T87 material. The apparent reversal of strain rate sensitivity may be ascribed to the change in heat treat condition. Prior to a solid conclusion, additional investigation on behavior of this material under various conditions is recommended.

Tensile specimens were cut from unformed 2219-T42 material from which the welded blanks were prepared. As shown in Table VIII, parent material exhibited very little scatter in mechanical properties values, but the welded specimens showed very wide scatter in ultimate tensile strength, per cent elongation in 2 inches, and per cent reduction of area, although yield strength was consistent and comparable to the values obtained for parent material. All welds passed radiographic inspection per Specification ABMA-DD-R27A-1, A-1, Class II. It was anticipated that some evaluation could be made of the contribution offered by the unground bead over the flush weld; however due to the wide scatter observed for the welded material, no valid conclusion can be drawn.

Metallographic specimens were cut from the apex area of each dome shown in Figure 8, and selected photomicrographs of the parent metal, the heat-affected zone, and the fracture are shown in Figures 9 through 12. There were no visible differences between explosively formed and hydraulically formed materials. Figure 9 clearly shows the grain growth in the parent material due to the re-solution heat treatment from T87 to the T42 condition. In Figure 10, a precipitate appears as an intermittent line at the edge of the heat-affected zone in the T42 material and change in grain size is abrupt at this plane. Fracture surfaces are shown in Figure 11 from a T87 and a T42 dome, both explosively formed. In the T42 material, there are a number of intergranular cracks extending into the material from the major fracture. Evidence of this is also observed in Figure 12A in a hydraulically formed dome.

2.1.6 Forming Unwelded Blanks

Because of the difficulties experienced in forming welded 2219 aluminum alloy in the conditions described above, further investigation of this material was directed towards forming unwelded specimens in the T37 and T87 conditions. Explosive forming data for T37 and T87 domes are presented in Tables IX and X, and the hydraulic forming data for all materials are presented in Table XI. Four aluminum domes in each condition and formed by each of the two processes were selected for sectioning into tensile, edge-notch, and microstructural specimens. Two additional domes in the T87 condition were free-formed by each process for the residual stress study. The data presented in Tables IX, X, and XI are cross-referenced through the column designated "Blank Number" to the results presented in Tables XV and XVII.

2.1.7 Discussion of Test Results With Unwelded 2219-T37 Aluminum Alloy

Tensile properties of 2219-T37 aluminum are given in Tables XIV and XV, and microhardness values for all materials are listed in Table XXIII. Values of ultimate strength, yield strength, notch strength, and proportional limit are plotted in Figures 13, 15, and 17. From these graphs, ultimate, yield, and notch strength values for common points of strain are listed in Table XXII and notch-to-yield strength and notch-to-ultimate strength ratios are calculated. These ratios together with elongation and reduction of area are plotted in Figures 14, 16, and 18.

Ultimate strength, yield strength, proportional limit and Knoop hardness consistently increased with strain while notch strength decreased with uniaxial conventional and biaxial explosive straining, but increased with biaxial conventional straining. Elongation and reduction of area decreased with strain in all cases. $\frac{N}{U}$ and $\frac{N}{Y}$ ratios also decreased with strain in uniaxial conventional and biaxial explosive forming while remaining nearly constant with biaxial conventional strain.

In photomicrographs, Figures 19 through 22, no change in structure due to strain or strain rate is visible. Figure 19A shows the general structure of the unstrained material at 100X. Elongated grains, due to rolling, and a fine precipitate are visible. At 2000X,

Figure 19B, intragranular inclusions are observed. Comparing to Figures 20 and 21, no significant difference is seen in material with biaxial explosive strain of 10 per cent elongation or biaxial conventional strain with 10.5 per cent elongation. The electron micrograph in Figure 22 shows grain boundaries and intragranular inclusions but no effects of straining.

X-ray diffraction data are listed in Table XXIV. The lattice parameter, taken in the (420) direction, indicated no significant change from the control level in uniaxial conventional straining, but in biaxial conventional straining the lattice parameter decreased, while in biaxial explosive straining there was a marked increase. In the case of uniaxial conventional forming, sufficient time and direction were available for energy transfer by crystal slip. Decrease in notch strength of biaxial conventional strained specimens may be accounted for by the decreased lattice parameter, indicating the formation of intergranular precipitation which would serve to act as fracture initiating sites. The increase in lattice parameter for biaxial explosive strained specimens may be attributed to energy absorption by the unit crystallographic cells, resulting in a lattice distortion and expansion. No precipitation is indicated, and the notch strength increased.

Measurements of the half-height width of the diffraction peaks indicate a given microstress level and are measures of dislocation densities and atomic site displacements. There was no significant change in microstress level induced by straining or strain rate. A change of 0.20^{o} may be regarded as significant.

2.1.8 Discussion of Test Results with 2219-T87 Aluminum Alloy

Mechanical properties for the aluminum in the T87 condition are tabulated in Tables XVI, XVII, and XXIII, and are plotted in Figures 23 through 28. Ultimate strength increased slightly with strain in uniaxial and biaxial straining with no difference due to strain rate. Yield strength increased markedly with initial strain and remained fairly constant with additional strain, regardless of strain rate. Proportional limit increased with strain in uniaxial and biaxial conventional straining but decreased with biaxial explosive straining. Notch strength decreased with strain in uniaxial conventional and biaxial explosive straining but increased and then decreased slightly with biaxial conventional strain. Knoop hardness did not change appreciably with strain or strain rate.

Elongation and the $\frac{N}{Y}$ ratio decreased with strain in all cases. Reduction of area increased slightly in uniaxial and biaxial conventional straining while decreasing slightly with biaxial explosive straining, but the spread of values is too wide to accurately define these trends. $\frac{N}{U}$ ratio decreased with uniaxial conventional and biaxial explosive straining while remaining nearly constant with biaxial conventional straining.

Comparing major trends of the mechanical properties for 2219 aluminum in the T87 condition to the properties for the T37 condition plotted in Figures 13 through 18, it is observed that the T87 condition being at a higher strength level in the initial condition behaves as expected and the increases due to straining are at a reduced rate as compared to the T37 which is at lower strength values in its initial condition. The properties of the material in the T37 condition after straining tend to approach the values of the properties shown for the T87 condition but never do reach the same levels.

As in the T37 condition material, there were no visible differences in the photomicrographs at any magnification due to strain or strain rate. Figure 29 shows the parent material with grain boundaries, and intragranular inclusions visible at 2000X are shown in Figure 29B. Figure 30A shows a welded specimen in the weld zone near the parent material where a coarse structure of dendritic grains is seen. In Figures 31A and 31B, thickening of the grain boundaries and the formation of a secondary fine precipitate may be seen in the heat-affected zone at 2000X, while additional precipitate came out of solution in the weld zone as the result of the increase in temperature.

Micrographs to 24,000X were processed for specimens strained biaxial conventionally and biaxial explosively, and no evidence of strain rate effects are observed.

As may be observed in Table XXIV, there were no significant changes in the lattice parameter. Microstresses are uniform with the exception of the welded specimen which shows a decrease in the half-height width. This may be attributed to stress relievement or substructure grain refinement due to heat application at welding.

2.1.9 Residual Stress Testing and Analysis

Experimental residual stress analysis was performed on domes 87-16 and 87-17 which were explosively formed, and domes 87-13 and 87-15 which were hydraulically formed.

The investigation method is based on measuring deformations after sectioning in two steps. The first step is cutting the domes into rings and measuring the diameter change, D_1, of each ring. The second step is cutting the rings open and measuring the relative motions of the free ends. The method is described in full detail in Appendix B in the Annual Summary Report, No. 0513-01(01)FP, dated 26 July 1962.

The measured deformations and the calculated stresses are shown graphically in Figures 32 through 39. All graphs for deformations as well as for stresses show the wavy variation pattern which is characteristic for effects of edge disturbances on shells.

The deformations and stresses increase with dome deflection. The stresses are very much lower in the explosively formed domes than in the hydraulically formed domes. The stresses may be highly sensitive to even minute changes in the dome contour. An example is the local peak of 64,000 psi (approximately) near the apex of dome 87-17 (Figure 35). This dome has developed a very slight dimple at the center. The dimple was barely noticeable to the eye, but could be traced clearly by analysis of the measured points.

The severity of residual stresses is evaluated by comparison with the yield stress of the material -- in this case approximately 60,000 psi.

For the explosively formed domes, the stresses (apart from the localized peak described above) are generally below 20-25 per cent of yield and may be characterized as low to moderate. The stresses in the explosively formed domes present no structural hazard.

They may cause problems in one-sided metal removal, such as in the case of chemical milling or surface machining. Depending on the susceptibility of the material to stress corrosion, which was not determined within this program, the stress peaks may be high enough to cause such type of chemical attack.

The hydraulically formed domes are stressed to the yield point over large areas. This stress condition represents a structural hazard, and will cause severe warping in the case of a one-sided metal removal operation. It is certain to cause serious chemical attack if the metal in this condition is exposed to aggressive liquids.

The striking difference between the stress levels and distributions for the two forming methods is fundamentally a result of the difference in strain distribution. A comparison between the scale drawings of the domes inserted in the graphs shows that the hydraulically formed domes have greater deflections without correspondingly greater flange diameter reductions, and the dome contours also have large, rather flat areas in the center. The contours of the explosively free-formed domes are much closer approximations to the ideal contour for a pressure vessel closure than hydraulically formed domes and are therefore less susceptible to the build-up of residual stress.

2.2 5Al-2.5Sn TITANIUM ALLOY

Acceptable qualification welds were obtained by using the welding schedule given below.

	Pass 1	Pass 2	Pass 3
Hold-Down	Table with 2-inch x 2-inch run-in and run-out tabs		
Equipment	Automatic Direct Current Single Pole		
Backup Material	Copper with groove 0.625-inch wide x .080-inch deep		
Amperes	100	115	120
Volts	9	10	10.5
Travel Speed	6 IPM	6 IPM	6 IPM
Filler Metal Type	--	5Al-2.5Sn Ti	5Al-2.5Sn Ti
Filler Metal Size	--	.043	.043
Filler Metal Feed	--	14 IPM	8 IPM
Purge Gas - Argon	20 CFH	20 CFH	20 CFH
Torch Gas - Argon - Helium	15 CFH 15 CFH	30 CFH --	30 CFH --
Trail Cup Gas - Argon	50 CFH	50 CFH	50 CFH
Electrode	2% thoriated tungsten, 0.125-inch diameter.		
Electrode Holder Angle	Vertical	Vertical	Vertical

The edges were beveled 45° with a 0.020-inch square land. The same equipment was used as on the aluminum, and three passes were made; one fusion pass and two with filler wire. Edges were wire brushed and cleaned with alcohol prior to welding.

All welds were subjected to radiographic inspection. The sheets warped in welding which prevented the welds from being machined flush; thus some weld reinforcement was available in the joint. Welds in blanks used in biaxial forming were ground flush outward from a 12-inch diameter, however, to prevent interference in the die and to allow for equal clamping over the entire flange area.

Five welded titanium blanks were explosively formed as shown in Table XII. Three of the domes fractured in the heat-affected zone, and a maximum of 1 per cent elongation developed in the apex area of one of the two non-fractured domes.

Five welded blanks were hydraulically formed. Two of these fractured along the heat-affected zone with only minimal strains.

Two non-fractured, explosively formed domes and two non-fractured, hydraulically formed domes were sectioned for tensile testing and microstructural examination. Microstructure of two of the fractured domes was also examined. One dome formed by each method was free-formed, but the apex area was sufficiently flat to obtain tensile specimens. No edge-notch tests were made of the biaxially stressed material due to limited available area in the formed units from which test specimens could be obtained.

Although welded blanks fractured along the weld in biaxial forming, all welded control and uniaxially strained specimens fractured in parent material at least 1/2-inch from the weld area. Tensile specimens cut from the domes also fractured in parent material.

Necking occurred in uniaxially prestrained specimens at generally less than half of fracture strain and as low as 39 per cent of fracture strain. Therefore, the prestrain to which uniaxial specimens were subjected was kept below the value at which necking would take place. However, this condition is generally found in the earlier types of material, but should be eliminated or at least greatly reduced in the newer forms of titanium alloys which are more closely controlled in the interstitials, hydrogen, oxygen, and nitrogen, and are reputed to strain in a more uniform manner.

2.2.1 Discussion of Test Results, 5Al-2.5Sn Titanium

Mechanical properties are listed in Tables XVIII, XIX, XXII, and XXIII and are plotted in Figures 40 through 47. In unwelded material subjected to uniaxial straining, ultimate strength, yield strength, notch strength, proportional limit, and hardness increased moderately while elongation, reduction of area, $\frac{N}{U}$ and $\frac{N}{Y}$ decreased slightly with strain. Welded specimens which were uniaxially strained exhibited increased ultimate strength, yield strength, and proportional limit similar to results obtained with unwelded material but showed a decrease in hardness and in reduction of area. The elongation remained nearly constant for the welded material inasmuch as the weld served as a reinforcement at the center of the gage length. The reduced gage width occurred on both sides of the weld, and a larger contribution to the elongation was made by the bisected gage length over the integral gage length of the unwelded bar.

Of the four domes which were sectioned and tested, only one sustained enough strain in the apex area to be measurable. This strain was found to be 1 per cent in an explosively formed dome. Tests were made to determine whether mechanical properties had been affected either by gradual or impulsive loading. There are only slight differences in properties between unformed and the biaxially formed material and these may not be significant. For both forming processes, ultimate strength, proportional limit, and elongation increased after forming while yield strength remained constant. Hardness and reduction of area decreased with biaxial conventional forming while they remained constant with explosive forming. The small changes in value truly reflect the minimal strains which could be found after forming in both processes.

Photomicrographs revealed no change in structure due to strain or strain rate, but the structure resulting from the welding indicated the probable cause of fracture at the low strain levels. Figures 48A and 48B show the parent metal, heat-affected zone and the weld material with precipitate tending to coalesce in the heat-affected zone. Microstructure of the weld shows typical Widmannstatten structure of alpha titanium. Figure 49 shows the parent metal and weld zone at a higher magnification with intergranular precipitate visible in the parent material. In the electron micrographs, Figure 50, the intergranular structure of the parent metal shows striations of twinning, and the weld material shows chevrons due to Widmannstatten structure. Within the scope of this program,

examination of welded specimens taken from formed domes, formed by conventional and explosive techniques, does not show any structural effects as a result of the forming process. Careful comparisons of unstrained and strained specimens did not reveal effects due to forming.

The data obtained from X-ray diffraction of selected specimens are shown in Table XXIV.

In obtaining lattice parameter values, the a-axis values were taken in the (103) direction, and the c-axis values were taken in the (002) direction. The increase of lattice parameter values for specimens listed over the theoretical values for pure alpha titanium of 4.686 for the c-axis and 2.950 for the a-axis are due to solution of the aluminum-tin matrix. The decrease in a-axis values results in identical crystallographic volumes. The scatter in the parameter data is due to inhomogeneities and segregation, and are not related to the straining conditions. Decrease in microstress levels of the welded and strained specimens from that of the unwelded control specimen is due to stress relievement during the welding process.

2.3 RENÉ 41

Qualifying welds which were acceptable in radiographic inspection were produced by the following schedule. Test blanks for biaxial forming were then welded according to the same procedure.

Preparation:	Sand weld areas, disc sand mating edges, remove wire edge, wash with alcohol.
Hold-Down:	Airline Seamwelder with 2-inch x 2-inch run-in and run-out tabs.
Joint:	Flush and square.
Equipment:	Automatic Direct Current Single Pole.
Filler Material:	Hastalloy W
Filler Material Diameter:	0.062-inch
Backup Material:	Copper
Backup Configuration:	0.062-inch x 0.250-inch groove.

Amperes:	140-145
Volts:	10-11
Weld Speed:	10 IPM
Atmosphere:	Argon-Helium
Flow Rate (Torch):	10 CFH Argon, 10 CFH Helium
Backup Gas:	Argon
Flow Rate (Backup):	20 CFH
Electrode:	2% Thoriated Tungsten, 0.062-inch diameter.

Very little warping resulted from the welding, and the welds were machined flush. All straining of this material was done in the solution-treated condition and all testing was done after an aging treatment of 1400°F for 16 hours and air-cooled. All specimens were aged simultaneously to eliminate possible variations in properties due to heat-treatment.

Three unwelded blanks and six welded blanks were explosively formed, and the data are given in Table XIII. Maximum elongation achieved without fracture was 15 per cent in unwelded material and 7 per cent in welded domes. As shown in Table XX, unwelded specimens uniaxially strained conventionally and explosively to fracture, elongated from 45 to 50.5 per cent while welded specimens, similarly strained, elongated from 10 to 20 per cent.

An unwelded blank (RU-4) was formed, using the Worthington Pump, but the 3,000 psi capacity was sufficient to produce only 6 per cent elongation at the apex of the dome. The remainder of the Rene 41 blanks were hydraulically formed using the Sprague Pump with the very low flow rate, which in turn produced a very low strain rate. As the blanks formed, wrinkles in the flange developed which separated the pressure plate from the blank sufficiently to allow the O-ring seal to fail. Failure of the O-ring was the limiting factor in the amount of elongation achieved. Efforts were made to form René 41 unwelded blanks to the high elongations of which the solution-treated material is capable, but the hydraulic seal could not be maintained. As the result of asymmetric draw-in, excessive wrinkling occurred in the narrow side of the eccentric flange.

Although biaxially formed blanks which were strained to fracture parted along the weld, tensile specimens which were cut from formed domes and aged did not fracture in the weld area, but parted in the parent material and, on occasion, outside of the 2-inch gage length. This behavior was also observed in the titanium alloy previously described, but was not confined to the biaxially strained specimens. Fracture during tensile testing consistently occurred within the parent material but not in the weld, for the biaxially and uniaxially strained specimens.

Within the limits of the tests performed, it is not possible to advance an explanation for the inconsistent behavior between materials in the location of the fracture. It is suggested that additional work may be desirable with highly polished tensile specimens to determine whether a notch effect may account for the behavior.

2.3.1 Discussion of Test Results, René 41

Mechanical properties are listed in Tables XX through XXIII and are plotted in Figures 51 through 58. Ultimate strength, yield strength, proportional limit, notch strength, hardness, elongation and reduction of area increased with increased strain for unwelded, uniaxially strained material, while the $\frac{N}{Y}$ and $\frac{N}{U}$ ratios decreased. For welded, uniaxially strained specimens, ultimate strength, yield strength and proportional limits increased; hardness, notch strength, $\frac{N}{Y}$ and $\frac{N}{U}$ ratios, and reduction of area decreased, and elongation remained constant with increase in strain. Welded, biaxially strained material, whether conventionally or explosively formed, follow the same general trend. Ultimate strength, yield strength, proportional limit and hardness increase with straining while elongation and reduction of area generally decrease.

Rene 41 is a heat-resisting nickel base alloy containing 19 per cent chromium, 11 per cent cobalt, and 10 per cent molybdenum as the primary alloying elements. It is an austenitic type alloy which is strengthened by solid solution hardening. The high strength at high temperatures is obtained by precipitation hardening of a gamma prime phase of the same crystallographic structure as the matrix. Boron is added to the material to reduce carbon segregation and subsequent carbide formation at the grain boundaries.

Microstructure of parent metal in Figure 59A shows banding of austenitic grains with the presence of some twinning. In Figure 59B, the parent metal is protruding into the Hastalloy W filler metal and microcracks are apparent in the heat-affected zone and parent material. This cracking was prevalent throughout the weld area. Figure 60 shows this intergranular cracking adjacent to the weld in specimens from two of the conventionally formed domes. In Figure 61 at 2000X, gamma prime precipitate is visible in the grain boundaries of the parent metal. In the weld zone, the precipitate has thickened at the grain boundaries with gamma prime precipitate coming out of solution near the grain boundaries. In Figure 62A, the electron micrograph shows gamma prime precipitate along a grain boundary in gamma matrix. In Figures 62B and 62C, the gamma prime precipitate is seen in the gamma matrix.

In the X-ray diffraction data, Table XXIV, the lattice parameter values were obtained in the (220) direction, and do not indicate any changes in cellular dimensions. Energy absorption was accomplished by precipitation of the gamma prime phase. Differences observed in the values for lattice parameter and microstress are not considered significant.

3. CONCLUSIONS

3.1 A marked increase in strength properties of 2219 aluminum may be achieved by aging the blank to the T87 condition and then forming. Forming in the solution-treated T37 condition and then aging produces negligible change in strength. Yield strength of T87 condition material was increased from 59 ksi to 68 ksi by moderate cold working. This increase in strength may be taken advantage of only where the decrease in formability does not adversely affect the fabrication of the specific part.

3.2 A post-weld heat treatment is required to form welded 2219-T87 aluminum sheet material. Weld reinforcement also enhances forming characteristics.

3.3 Residual stresses in explosively and hydraulically formed 2219-T87 aluminum domes were found to increase with dome

deflection. The general stress level was much lower for the explosively formed domes and will not represent a structural hazard. However, this stress level can constitute a problem for materials which are highly sensitive to stress corrosion. The stresses in the hydraulically formed domes were at the yield point. This stress level may be considered hazardous from the structural viewpoint as well as from the viewpoint of chemical attack in materials sensitive to stress corrosion. In the Annual Summary Report, No. 0513-01(01)FP, dated 26 July 1962, high residual stresses were observed for explosively formed hot rolled steel. Indications are that the residual stresses which are generated as a result of forming by any process must be evaluated for that specific material for the condition of forming which had been used.

3.4 No detrimental effects were observed in the 5Al-2.5Sn titanium due either to gradual stressing or to impulsive stressing.

3.5 In general, within the limits of the materials tested, the mechanical properties are affected favorably as a result of increased strain rates. This is applicable to uniaxial and biaxial straining. While some of these properties show some marked changes as a result of strain rate, the values reported are not to be construed as definitive design type criteria since additional testing conducted under statistical design will be required to generate this type of information.

3.6 Within the limits of examinations employed in this program, there are not visible changes in structure to be observed as a result of the strain rates used to form materials. This generalization is applicable to electron microscopy up to 36,000X with the replication technique. With X-ray diffraction techniques, some evidence of lattice parameter changes may be ascribed to unit cell distortion varying with rate of strain.

3.7 An analysis of data obtained from the uniaxial Dynamic Test Fixture during the course of this and the preceding investigation has demonstrated that this data can serve to predict the trends that a particular material will exhibit when subjected to biaxial explosive straining. It is therefore suggested that the uniaxial Dynamic Test Fixture be employed for preliminary testing of new materials which are proposed for use.

4. RECOMMENDATIONS

4.1 Because of the unique response by each material to explosive forming, each material proposed for fabrication involving explosive techniques should be subjected to a testing procedure similar to the one developed in this program prior to standardizing on a material and on the fabrication technique to be employed. This should include residual stress analyses and the effects of stress corrosion for the specific materials as processed.

4.2 To complete the picture on the materials which were investigated in this program, it would be desirable that additional residual testing be performed on those materials not previously tested and that actual stress corrosion comparisons be made for conventional and explosive forming procedures.

4.3 Because of the valuable information supplied on the behavior of a material when subjected to high strain rates in the Dynamic Test Fixture for uniaxial straining, it is recommended that the Dynamic Test Fixture for imposing high strain rates on uniaxial specimens be modified and improved to serve as a standard test fixture for standardizing a high strain rate test specification to be used by the services and by industry.

TABLE I

SUPPLIERS' CERTIFICATIONS OF CHEMICAL ANALYSIS OF TEST MATERIALS

Si	Fe	Cu	Mn	Mg	Zn	Ti	V	Zr	Al	Be	Sn	C	H	N	O	Cr	Ni	Co	Mo	S	B	P	Others Ea.	Others Total
2219-T37 ALUMINUM ALLOY, 0.100-INCH SHEET, ALUMINUM COMPANY OF AMERICA																								
.20	.30	5.8-6.8	.20-.40	.02	.10	.02-.10	.05-.15	.10-.25	Rem.														.05	.15
2319 ALUMINUM ALLOY, 0.045-INCH FILLER WIRE, ARCOS CORPORATION																								
.20	.30	5.8-6.8	.20-.40	.02	.10	.10-.20			Rem.	.0008														
5Al-2.5Sn TITANIUM ALLOY, 0.100-INCH SHEET, AFFILIATED METAL PRODUCTS COMPANY																								
	.22					Rem.			5.10		2.46	.038	.0102	.017										.18
5Al-2.5Sn TITANIUM ALLOY, 0.043-INCH FILLER WIRE, ASTRO-FAB, INC.																								
	.09		.12			Rem.			5.3		2.5	.022	.0121	.008	.131									
RENÉ 41, 0.100-INCH SHEET, HAYNES STELLITE COMPANY																								
.18	2.63		.06			3.20			1.49			.07				19.39	Rem.	11.22	9.79	.009	.006			
HASTALLOY W, 0.045-INCH FILLER WIRE, HAYNES STELLITE COMPANY																								
.64	3.91		.57				.27					.015				4.74	Rem.	.42	24.76	.011		.002		

TABLE II

ALLOY 2219 MECHANICAL PROPERTIES

Property	T37			T87 [3]		
	Table [1] (ksi)	Test (psi)	σ [2] (psi)	Table [1] (ksi)	Test (psi)	σ [2] (psi)
Ultimate Tensile [4]						
L	56	60,149	361	68	67,871	99
T	57	61,249	202	69	68,398	54
Yield Tensile [5]						
L	47	49,863	1,042	57	54,595	440
T	46	45,486	491	57	55,294	715
Elongation (% in 2")						
L	12	14.9	1.2	10	11.0	0
T	11	13.8	0.3	10	10.2	0.3

(1) L. W. Mayer, Alcoa Aluminum Alloy 2219, Aluminum Co. of America, Sales Development Division, January 1962, Table III.

(2) Standard deviation, $\sigma = \sqrt{\frac{\Sigma (Y - \bar{Y})^2}{N - 1}}$ where sample size, N = 5.

(3) T87 tested material was aged from the T37 condition at 325° for 14 hours.

(4) L = longitudinal to rolling direction.
T = transverse to rolling direction.

(5) Yield tensile test values are by 0.2% offset method.
Table values are not specified.

TABLE III

FORMING DATA - UNWELDED BLANKS

Standoff Distance: 12" to center of charge.
Aerex Liquid Explosive.

Material	Blank No.	Charge (ml)	Spacing at Hold-Down + Stock Thickness (in.)	Blank Diameter		Elongation at Apex (%)	Results
				Before Forming (in.)	After Forming (in.)		
HRS	1	500	.003	21	18.4	-	Multiple fractures
	2	200	.003	21	19.5	12.4	4 radial fractures
	3	100	.007	21	20.1	12.5	Symmetrical dome, 3.7" deflection.
	4	100	.005	21	19.8	13.0	Symmetrical dome, 4.05" deflection.
	5	150	.005 (1)	21	19.2	24.0	6.5" dia. flat
	6	150	.005 (1)	21	19.3	19.6	5.0" dia. flat
	7	200	.005 (1)	21	19.1	16.4	7.0" dia. flat
2219 T37	8	100	.005	21	20.1	9.0	Fracture near draw radius.
	9	50	.005	20	18.8	6.0	3.35" deflection
	10	50	.005 (2)	20	19.1	6.0	Flat 6" diameter.
	11	75	.005 (2)	20	18.9	3.5	Flat 8.2" diameter.
2219 T87	12	75	.005 (2)	20	19.1	5.0	Fracture, flat 8.3" diameter.
	13	50	.005 (2)	20	19.3	7.0	Flat 5" diameter.

(1) Formed with spacer and insert for 3.38" deflection.

(2) Formed with spacer and insert for 2.44" deflection.

TABLE IV

PRELIMINARY EXPERIMENT ON 2219-T37 ALUMINUM

(All specimens longitudinal to roll)

T37 AGED TO T87

Specimen No.	.2% Yield Strength psi	Ultimate Strength psi	% Elongation in 2"
A0-1	58,708	69,276	10.5
A0-2	58,708	69,472	10.5
A0-3	58,641	69,903	10.5

T37 DOME BLANKS EXPLOSIVELY FORMED AND AGED TO T87

Dome No.	Specimen No.	Prestrain, % Elong.	0.2% Yield Strength psi	Ultimate Strength psi	% Elong. in 2"
10	A10-1	6	59,823	70,199	10.0
10	A10-2	6	59,487	70,089	7.5
10	A10-3	6	59,211	69,737	10.0
11	A11-1	3.5	59,355	70,323	11.0
11	A11-2	3.5	58,955	68,230	6.5
11	A11-3	4.0	55,794	69,957	10.5

T37 DOME BLANKS AGED TO T87 AND EXPLOSIVELY FORMED

Dome No.	Specimen No.	Prestrain, % Elong.	0.2% Yield Strength psi	Ultimate Strength psi	% Elong. in 2"
12	A12-1	5	69,079	73,246	6.5
12	A12-2	5	68,018	73,649	5.0
12	A12-3	5	66,630	73,085	6.0
13	A13-1	6	66,079	72,687	7.0
13	A13-2	7	67,281	72,350	6.0
13	A13-3	6	67,329	72,406	7.5

TABLE V

FORMING DATA - WELDED BLANKS

Standoff Distance: 12" to center of charge.
Aerex Liquid Explosive.

Material	Blank No.	Charge (ml)	Spacing at Hold-Down + Stock Thickness (in.)	Blank Diameter (1) Before Forming (in.)	Blank Diameter (1) After Forming (in.)	Elongation (2) at Apex (% El. in 0.4")	Results
HRS	1	100	.005	W 21.080 ⊥ 21.105	19.962 19.990	-	No fracture. 3.90" deflection.
2219 T87	22	50	.005	W 19.993 ⊥ 19.993	18.432 20.941	-	Fractured length of weld & below draw radius.
	28	25	.005	W 19.015 ⊥ 19.031	17.950 19.580	-	Weld fractured. 1.5" wide, 2.7" deflection.
	26	25	.005	W 16.994 ⊥ 17.010	15.455 17.635	12.7	Weld fractured, 2.4" wide, 3.2" deflection.
	30	50	.008 - formed with HRS cover sheet.	W 19.020 ⊥ 19.030	18.537 19.026	13.0	Weld fractured, 0.8" wide, 2.3" deflection.
	25	(3)	.008	W 18.996 ⊥ 19.000	18.992 18.979	6.5	Weld fractured, 0.1" wide, 0.4" deflection.

(1) W Diameter with weld.
⊥ Diameter perpendicular to weld.

(2) Elongation measured transverse to weld.

(3) This blank was hydraulically formed. Maximum pressure was 300 psi. Fracture occurred in 4 sec.

TABLE VI

MECHANICAL PROPERTIES OF LONGITUDINAL WELDED SPECIMENS

2219-T87 ALUMINUM ALLOY

Specimen No.	Strain Rate	Mechanical Properties					
		Proportional Limit ksi	0.2% Yield Strength ksi	Ult. Tensile Strength ksi	% Elong. in 2"	% Red. of Area	E, Mod. of Elasticity psi x 10^{-6}
A7-1	Control	16.4	24.5	46.9	13.0	20.0	10.9
A7-2	↓	17.2	27.6	49.1	14.5	18.8	10.8
A7-3	↓	16.2	27.5	49.6	14.5	16.2	10.7
A9-1	Conv.				13.0		
A9-2	↓				14.0		
A9-3	↓				13.5		
A16-1	Expl.				11.5		
A16-2	↓				13.0		
A16-3	↓				9.5		

TABLE VII

TEST RESULTS

2219-T87 ALUMINUM BLANKS, 19-INCH DIAMETER
DIAMETRAL WELD PARALLEL TO ROLLING DIRECTION

MATERIAL CONDITION	WELD	FORMING METHOD	
		EXPLOSIVE 12-Inch Standoff 25 ML. Aerex	HYDRAULIC
T87 As Welded	Flush	DOME NO. 28 2.7-inch Deflection Weld Diameter 17.9 inches ⊥ Weld Diameter 19.6 inches Fracture 17.7 inches long 1.5-inch Maximum Opening	DOME NO. 25 0.4-inch Deflection Weld Diameter 19.0 inches ⊥ Weld Diameter 19.0 in. Fracture 10.4 inches long 0.1-inch Maximum Opening Maximum Pressure 300 psi 4 seconds to Fracture
Post Weld Re-Solution Heat-Treated to T42	Flush	DOME NO. 2 3.5-inch Deflection Weld Diameter 17.6 inches ⊥ Weld Diameter 18.9 inches Fracture 16.9 inches long 1.4-inch Maximum Opening	DOME NO. 23 5.4-inch Deflection Weld Diameter 15.6 inches ⊥ Weld Diameter 15.7 in. Fracture 8.8 inches long 0.35-inch Maximum Opening Fracture does not coincide with weld Maximum Pressure 1300 psi 35 seconds to Fracture
Post Weld Re-Solution Heat-Treated to T42	With Bead	DOME NO. 40 3.6-inch Deflection Weld Diameter 17.4 inches ⊥ Weld Diameter 19.4 inches Fracture 16.5 inches long 2.2-inch Maximum Opening	DOME NO. 41 6.0-inch Deflection Weld Diameter 14.1 inches ⊥ Weld Diameter 14.0 in. No Fracture - blank pulled through draw radius on one side. Maximum Pressure 1250 psi 47 seconds to pull through

TABLE VIII

MECHANICAL PROPERTIES OF BLANK MATERIAL - TRANSVERSE SPECIMENS

2219-T42 ALUMINUM ALLOY

Blank No.	Specimen No.	Welded or Unwelded	Mechanical Properties						Area of Fracture
			Proportional Limit ksi	0.2% Yield Strength ksi	Ult. Tensile Strength ksi	% Elong. in 2"	% Reduction of Area	E, Mod. of Elasticity psi x 10^{-6}	
2 Flush Weld	2-1	Unwelded	17.6	31.5	58.5	19.5	27.0	10.1	
	2-2	↓	15.8	31.7	58.1	20.5	28.2	10.3	
	2-3	↓	17.0	30.5	56.7	20.0	29.0	10.1	
	2-5	Welded	19.0	32.4	51.5	7.5	21.6	10.6	Weld
	2-6	↓	19.0	32.6	54.9	9.5	20.0	11.3	Weld
	2-7	↓	18.0	31.1	42.9	4.0	12.2	10.0	HAZ Line
23 Flush Weld	23-1	Unwelded	18.8	30.1	57.6	22.0	26.9	10.0	
	23-2	↓	19.3	30.6	57.9	21.0	31.0	9.9	
	23-3	↓	15.7	30.5	57.9	21.0	23.2	10.2	
	23-5	Welded	16.5	30.1	56.6	23.0	31.0	9.8	Parent
	23-6	↓	16.6	29.6	56.8	22.0	28.5	9.9	Weld
	23-7	↓	15.5	30.5	46.5	6.0	8.4	10.3	Edge of Weld
40 With Weld Bead	40-1	Unwelded	18.5	30.2	57.9	21.0	28.3	9.9	
	40-2	↓	17.6	29.4	57.0	22.0	27.2	10.1	
	40-3	↓	16.0	29.8	57.4	21.0	26.9	10.8	
	40-5	Welded	17.4	26.9	26.9	--	3.4	8.8	Parent
	40-6	↓	17.6	30.5	38.9	3.0	3.3	9.6	HAZ Line
	40-7	↓	16.6	31.3	57.4	15.0	26.1	9.9	Parent
41 With Weld Bead	41-1	Unwelded	19.2	30.5	57.5	21.0	28.1	10.0	
	41-2	↓	19.8	30.2	56.9	19.0	26.3	10.2	
	41-3	↓	19.0	30.2	56.9	21.0	29.2	9.9	
	41-5	Welded	18.5	30.6	56.8	16.0	26.3	10.1	Parent
	41-6	↓	18.7	33.0	59.3	16.5	25.7	10.4	Parent
	41-7	↓	19.6	32.0	41.6	3.0	7.5	10.3	HAZ Line
Typical Alcoa Values (1)		Unwelded	--	27	53	20	--	10.6	

(1) L. W. Mayer, Alcoa Aluminum Alloy 2219, Aluminum Co. of America, Sales Development Division, January 1962, Table III.

TABLE IX

FORMING DATA - UNWELDED BLANKS
2219-T37 ALUMINUM ALLOY

Standoff Distance: 12" to center of charge.
Aerex Liquid Explosive

Blank No.	Charge (ml)	Spacing at Hold-Down + Stock Thickness (in.)	Die Depth (in.)	Blank Diameter (1)	Blank Diameter Before Forming (in.)	Blank Diameter After Forming (in.)	Elong. Apex (%)	Elong. Periph. (%)	Results
37-1	75	.008	Free Form	L T	21.000 21.002	20.663 19.407	15.0	7.8	Fractured on transverse diameter. Deflection 4.5".
37-2	75	.008	4.13	L T	21.004 21.033	20.065 20.400	10.0	--	5 Radial Fractures.
37-3	50	.008	3.00	L T	20.980 20.997	20.301 20.267	18.0	4.8	1.5" diameter flat.
37-4	60	.008	2.44	L T	21.000 20.959	20.249 20.260	5.0	4.3	6" diameter flat.
37-5	75	.008	2.44	L T	21.032 21.009	20.143 20.116	5.0	4.9	8" diameter flat.
37-6	75	.008	3.00	L T	20.986 21.014	20.068 20.140	10.0	6.0	6" diameter flat.
37-7	75	.008	3.00	L T	21.022 21.000	20.024 19.958	9.0	6.2	6" diameter flat.

(1) L Longitudinal to roll.
T Transverse to roll.

TABLE X

FORMING DATA - UNWELDED BLANKS

2219-T87 ALUMINUM ALLOY

Standoff Distance: 12" to center of charge.
Aerex Liquid Explosive

Blank No.	Charge (ml)	Spacing at Hold-Down + Stock Thickness (in.)	Die Depth (in.)	Blank Diameter (1)	Blank Diameter Before Forming (in.)	Blank Diameter After Forming (in.)	Elong. Apex (%)	Elong. Periph. (%)	Results
87-1	50	.008	Free Form	L T	21.010 21.005	--- ---	8.0	--	Multiple fractures.
87-2	35	.008	Free Form	L T	21.000 21.002	20.698 20.713	7.0	2.5	2.19" Deflection.
87-3	65	.008	2.44	L T	20.005 20.003	19.222 19.180	5.0	4.0	6" diameter flat.
87-4	75	.003	2.44	L T	20.016 20.014	19.191 19.171	5.0	4.2	6" dia. flat.
87-5	100	.003	3.00	L T	19.982 19.995	18.958 19.058	10.0	11.5	8" dia. flat.
87-6	100	.003	3.00	L T	19.976 20.012	--- ---	12.0	--	Fractured on diameter. (Blank was scratched.)
87-7	100	.003	3.00	L T	19.955 19.964	18.838 18.884	8.0	6.1	8" dia. flat.
87-16	40	0	Free Form	L T	20.004 20.023	19.536 19.547	5.0	2.5	2.25" deflection. Symmetrical dome.
87-17	50	0	Free Form	L T	20.018 20.023	19.454 19.438	8.0	3.1	2.54" deflection. Symmetrical dome.

(1) L Longitudinal to roll.
T Transverse to roll.

TABLE XI

HYDRAULIC FORMING DATA

Blank No.	Spacing at Hold-down + Stock Thickness (in.)	Die Depth (in.)	Maximum Pressure (psi)	Time (sec)	Blank Diameter (1)	Before Forming (in.)	After Forming (in.)	Elong. Apex (%)	Elong. Periph. (%)	Results
2219-T37 Aluminum Alloy Unwelded										
37-8	.003	Free Form	1560	408	L T	21.000 21.004	19.861 19.824	12.5 10.5	6.8 7.0	4.05" deflection. Transverse diametral fracture 11" long.
37-9	.003	3.00	2150	156	L T	20.996 21.028	19.896 19.931	6.0 5.0	5.6 4.9	Fracture at edge of insert. 5" dia. flat.
37-10	.003	3.38	2600	90	L T	21.088 21.002	19.438 19.402	8.0 7.5	6.4 6.8	6" dia. flat.
37-11	.003	3.75	2280	50	L T	21.001 21.005	19.275 19.301	10.5 10.0	7.9 7.8	Transverse diametral fracture 2.8" from center.
37-12	.003	3.75	2450	43	L T	21.049 21.011	19.354 19.263	10.5 10.0	7.9 7.9	5.5" dia. flat.
37-13	.003	3.23	2600	45	L T	21.013 21.080	19.604 19.588	7.0 6.0	6.6 5.7	Fracture at edge of insert. 6.5" dia. flat.
37-14	.003	3.23	2650	51	L T	21.010 21.019	19.625 19.638	7.0 6.5	6.9 6.2	Fracture at edge of insert. 6.0" dia. flat.
2219-T87 Aluminum Alloy Unwelded										
87-8	.003	Free Form	1650	31	L T	19.992 20.023	18.626 18.702	8.0 8.0	6.3 5.6	3.83" deflection. Longitudinal diametral fracture 15" long.
87-9	.003	2.44	2620	38	L T	19.800 20.040	19.071 19.095	3.0 3.0	4.6 3.4	6" dia. flat.
87-10	.003	2.44	2825	45	L T	20.019 20.004	19.082 19.020	3.0 3.0	3.7 3.6	6.5" dia. flat.
87-11	0	3.00	2380	29	L T	20.042 20.011	18.955 18.871	6.0 4.5	5.2 4.8	Fracture at edge of insert. 5" dia. flat.
87-12	0	3.00	2375	50	L T	20.006 20.020	18.934 18.822	5.5 5.0	4.9 5.1	Fracture at edge of insert. 5" dia. flat
87-13	0	Free Form	1400	36	L T	20.022 20.028	19.196 19.155	4.0 3.5	3.7 3.4	2.73" deflection. Symmetrical dome.
87-14	0	Free Form	1350	30	L T	19.964 20.018	19.136 19.217	4.0 3.0	3.5 3.2	Longitudinal fracture 2.7" from center, 12" long.
87-15	0	Free Form	1500	40	L T	19.989 20.025	18.903 18.900	5.0 4.0	4.5 4.2	3.09" deflection. Symmetrical dome.

(1) L Longitudinal to roll.
T Transverse to roll.

TABLE XI (Cont.)

HYDRAULIC FORMING DATA

Blank No.	Spacing at Hold-down + Stock Thickness (in.)	Die Depth (in.)	Maximum Pressure (psi)	Time (sec) * (min)**	Blank Diameter (1)	Before Forming (in.)	After Forming (in.)	Elong. Apex (%)	Elong. Periph. (%)	Results
5Al-2.5Sn Titanium Alloy Welded										
T-1	.001	Free Form	1480	68 *	L T	19.078 19.043	18.745 18.691	0.0 0.0	0.4 0.9	1.5" deflection. Transverse fracture at draw radius, 4" long.
T-8	.001	Free Form	2590	80 *	L T	19.014 19.040	17.872 18.036	0.0 1.0 in weld	2.7 3.4	2.57" deflection. Symmetrical dome.
T-22	.002	2.34	2950	87 *	L T	19.053 19.025	18.136 18.263	1.5 0.5	2.5 2.3	Fracture in HAZ 16" long.
T-19	.001	2.34	1925	70 *	L T	18.896 19.050	18.210 18.560	0.5 0.0	1.6 1.7	Fracture in HAZ 16" long.
T-5	0	1.34	1900	70 *	L T	18.970 19.004	18.726 18.753	0.0 0.5 in weld	0.7 0.8	1.16" deflection. Symmetrical dome.
René 41										
RU-4 Unwelded	0	Free Form	3000	64 *	L T	21.030 20.948	20.039 19.931	5.0 6.0	5.7 5.5	3.29" deflection. Symmetrical dome. Maximum pressure available.
R-3 Welded	.001	Free Form	3700	20 **	L T	21.025 20.981	18.702 18.681	9.0 11.0	11.9 11.2	5.45" deflection. Fracture in HAZ 10" long.
R-5 Welded	.002	4.13	4200	21.7**	L T	21.011 21.028	19.065 19.232	8.5 11.0	9.1 10.0	4" dia. flat. 0-ring failed.
R-11 Welded	No Spacer	4.13	4600	19.4**	L T	21.087 21.003	19.153 19.143	9.0 10.0	10.1 10.6	5" dia. flat. 0-ring failed.
R-8 Welded	No Spacer	2.44	4800	11 **	L T	21.012 21.036	20.236 20.226	5.0 4.5	4.7 4.7	7" dia. flat. 0-ring failed.
RU-5 Unwelded	No Spacer	Free Form	3950	19.5**	L T	20.992 21.012	17.842 18.074	15.0 15.0	13.5 14.4	5.66" deflection. 0-ring failed. Severe flange wrinkles. Asymmetrical flange.
RU-6 Unwelded	No Spacer	5.18	4600	19.3**	L T	21.008 21.015	18.795 18.792	13.0 17.0	14.0 13.7	2" dia. flat. 0-ring failed. Asymmetrical flange.

(1) L Longitudinal to roll.
T Transverse to roll.

TABLE XII

FORMING DATA - WELDED BLANKS

5Al-2.5Sn TITANIUM

Standoff Distance: 12" to center of charge.
Aerex Liquid Explosive.

Blank No.	Charge (ml)	Spacing at Hold-Down + Stock Thickness (in.)	Die Depth (in.)	Blank Diameter (1)	Before Forming (in.)	After Forming (in.)	Elong. Apex (%)	Elong. Periph. (%)	Results
15	50	.008	Free Form	L	19.222	18.875	.5	1	1.6" deflection - nearly flat dome.
				T	19.165	18.829		1	
25	100	.008	Free Form	L	19.350	18.334	1	2.9	Fractured length of weld.
				T	19.325	19.275		1.7	
11	75	.008	Free Form	L	19.183	18.403	1	2.6	Fractured length of weld.
				T	19.320	19.315			
12	65	.008	Free Form	L	19.063	18.170	1	2.5	Fractured length of weld.
				T	18.962	19.072			
20	65	.007	1.34	L	19.028	18.771	1	0.8	1.24" maximum deflection. Apex dimpled .22". (Evidence of air burn
				T	18.973	18.667			

(1) L Longitudinal to roll (weld).

T Transverse to roll.

TABLE XIII

FORMING DATA - UNWELDED AND WELDED BLANKS

RENÉ 41

Standoff Distance: 12" to center of charge.
Aerex Liquid Explosive

Blank No.	Welded or Unwelded	Charge (ml)	Spacing at Hold-Down + Stock Thickness (in.)	Die Depth (in.)	Blank Diameter (1)	Before Forming (in.)	After Forming (in.)	Elong. Apex (%)	Elong. Periph. (%)	Results
RU-1	Unwelded	150	.008	Free Form	L T	21.052 21.024	20.012 19.955	11	7.5	3.94" deflection.
RU-2		200	.008	Free Form	L T	21.047 21.027	19.693 19.725	15	8.9	4.41" deflection.
RU-3		300	.003	Free Form	L T	20.940 21.020	19.553 19.631	15	9.0	3 radial fractures. (Die bottom fractured).
17	Welded	100	.001	Free Form	L T	21.034 21.040	20.527 20.598	7	4.5	2.82" deflection.
7		200	0	Free Form	L T	21.008 21.001	20.053 20.083	9	6.0	3 radial fractures
15		200	.003	3.00	L T	21.011 21.031	19.925 20.140	7	7.0	Fracture in HAZ 16" long. 7" dia. flat.
13		150	.002	2.44	L T	21.000 21.030	20.224 20.263	4	4.0	2.39" maximum deflection. Apex dimpled 0.14". 6.5" dia. flat.
10		150	.002	2.44	L T	21.036 21.002	20.348 20.304	5	4.9	6.5" dia. flat.
18		200	.002	2.44	L T	20.992 21.040	20.165 20.225	4	5.0	7" dia. flat.

(1) L Longitudinal to roll (weld).
T Transverse to roll.

TABLE XIV

STRAIN DATA AND MECHANICAL PROPERTIES OF CONTROL AND UNIAXIALLY STRAINED SPECIMENS

2219-T37 ALUMINUM (Unwelded)

Specimen No.	Specimen Type	Prestraining Conditions					Mechanical Properties					
		Strain Rate in/in/sec	Applied Strain % of Max.	Measured Strain % Elong. in 2"	Actual Strain % of Max.	Octahedral Shear Strain $\bar{\gamma}$	Prop. Limit ksi	0.2% Yield Strength ksi	Ultimate Strength ksi	% Elong. in 2"	% Red. of Area	E, Mod. of Elasticity psi x 10^{-6}
A101	Tensile Long.	None					34.1	50.5	60.7	13.0	22.5	10.0
A102	↓	↓					37.2	50.6	60.6	14.0	25.0	10.0
A103	↓	↓					30.0	50.4	61.0	14.0	24.8	10.2
A104	Tensile Trans.	↓					26.3	46.2	61.1	13.0	24.3	10.7
A105	↓	↓					26.9	45.8	60.9	13.5	25.3	10.1
A106	↓	↓					28.0	45.6	60.9	13.0	25.4	10.1
A120	Notch Trans.	↓							53.5			
A121	↓	↓							53.5			
A122	↓	↓							54.1			
A112	Tensile Fracture	.05	100	12.0								
A113	↓	↓	↓	13.0								
Avg.	↓	↓	↓	12.5	100							
A115	Tensile	↓	75	7.5	60	.102	51.1	60.0	64.7	9.0	17.1	9.8
A118	↓	↓	↓	8.0	64	.109	45.3	59.5	64.2	10.0	19.0	10.5
A119	↓	↓	↓	8.0	64	.109	49.5	59.5	63.7	10.5	21.5	9.9
A125	Notch	↓	↓	8.5	68	.115			32.6			
A126	↓	↓	↓	8.5	68	.115			54.3			
A127	↓	↓	↓	8.5	68	.115			44.4			
A107	Tensile Fracture	100	100	14.0								
A108	↓	↓	↓	13.5								
A110	↓	↓	↓	13.5								
A111	↓	↓	↓	14.5								

TABLE XV

STRAIN DATA AND MECHANICAL PROPERTIES OF BIAXIALLY STRAINED SPECIMENS

2219-T37 ALUMINUM (Unwelded)

Specimen No.	Specimen Type	Prestraining Conditions					Mechanical Properties					
		Strain Rate in/in/sec	Applied Strain % of Max.	Measured Strain % Elong. in 2"	Actual Strain % of Max.	Octahedral Shear Strain $\bar{\gamma}$	Prop. Limit ksi	0.2% Yield Strength ksi	Ultimate Strength ksi	% Elong. in 2"	% Red. of Area	E, Mod. of Elasticity psi x 10^{-6}
37-8	Fracture	.0003	100	12.5	100							
37-11-1	Tensile	.002	75	10.5	84	.283	47.3	59.5	68.0	7.0	15.8	9.0
37-11-3	↓	.002	↓	↓	↓	↓	39.8	57.1	66.7	7.5	18.3	8.7
37-12-2	↓	.002	↓	↓	↓	↓	40.6	58.5	67.4	7.5	18.4	8.8
37-11-2	Notch	.002	↓	↓	↓	↓			62.1			
37-12-1	↓	.002	↓	↓	↓	↓			58.1			
37-12-3	↓	.002	↓	↓	↓	↓			58.7			
37-13-1	Tensile	.002	40	7.0	56	.192	42.2	58.0	66.5	8.5	18.7	8.7
37-13-3	↓	.002	↓	↓	↓	↓	43.7	58.4	67.0	9.5	17.9	9.2
37-14-2	↓	.001	↓	↓	↓	↓	38.5	58.0	67.0	8.5	17.2	9.0
37-13-2	Notch	.002	↓	↓	↓	↓			62.6			
37-14-1	↓	.001	↓	↓	↓	↓			61.8			
37-14-3	↓	.001	↓	↓	↓	↓			60.6			
1	Fracture	100	100	15								
2	↓	↓	↓	10								
3	↓	↓	↓	18								
Avg.	↓	↓	↓	14.3	100							
37-6-1	Tensile	↓	75	10.0	70	.270	43.3	58.3	68.3	8.0	14.8	9.9
37-6-3	↓	↓	↓	10.0	70	.270	39.8	57.8	67.9	7.0	19.0	10.4
37-7-2	↓	↓	↓	9.0	63	.244	41.2	60.0	67.9	6.0	15.8	10.6
37-6-2	Notch	↓	↓	10.0	70	.270			41.3			
37-7-1	↓	↓	↓	9.0	63	.244			20.3			
37-7-3	↓	↓	↓	9.0	63	.244			17.9			
37-4-1	Tensile	↓	40	5.0	35	.138	37.2	56.7	66.3	5.5	16.1	11.0
37-4-3	↓	↓	↓	5.0	35	↓	43.0	57.1	66.9	7.0	13.0	10.0
37-5-2	↓	↓	↓	5.0	35	↓	42.9	56.2	65.7	9.5	16.3	10.0
37-4-2	Notch	↓	↓	5.0	35	↓			32.7			
37-5-1	↓	↓	↓	5.0	35	↓			56.7			
37-5-3	↓	↓	↓	5.0	35	↓			17.2			

TABLE XVI

STRAIN DATA AND MECHANICAL PROPERTIES OF CONTROL AND UNIAXIALLY STRAINED SPECIMENS

2219-T87 ALUMINUM

Specimen No.	Specimen Type		Prestraining Conditions					Mechanical Properties					
			Strain Rate in/in/sec	Applied Strain % of Max.	Measured Strain % Elong. in 2"	Actual Strain % of Max.	Octahedral Shear Strain $\bar{\gamma}$	Prop. Limit ksi	0.2% Yield Strength ksi	Ultimate Strength ksi	% Elong. in 2"	% Red. of Area	E, Mod. of Elasticity psi x 10^{-6}
A32	Tensile Long.	U	None					46.2	59.5	70.4	10.5	14.3	10.7
A33		U						44.9	60.4	71.2	11.0	21.7	10.4
A34		U						47.3	60.4	71.0	10.5	21.4	10.5
A23	Tensile Trans.	U						51.2	59.8	72.2	10.0	18.5	10.9
A24		U						42.1	59.2	70.3	10.0	19.3	10.6
A44		U						48.0	53.4	72.4	9.5	10.9	10.9
A36	Notch Trans.	U								59.2			
A37		U								53.7			
A38		U								52.4			
A60	Tensile Trans.	W						12.1	26.9	37.9	3.5	13.8	9.9
A61		W						14.8	27.6	38.9	3.5	18.5	8.9
A62		W						13.4	27.2	39.3	3.5	15.2	9.7
A76	Notch Trans.	W								35.9			
A77		W								32.8			
A78		W								32.9			
A29	Tensile Fracture	U	.05	100	11.0								
A30		U			11.5								
A48		U			10.0								
A49		U			10.0								
Avg.		U			10.6	100							
A31	Tensile	U		75	5.0	47	.069	56.0	71.8	73.5	7.5	17.3	10.0
A45		U			5.0	47	.069	43.9	70.8	72.4	7.0	16.7	10.2
A46		U			6.0	57	.082	46.7	71.4	72.7	7.0	16.5	10.2
A41	Notch	U			4.7	44	.065			21.4			
A42		U			3.5	33	.049			15.0			
A43		U			3.5	33	.049			23.5			
A25	Tensile Fracture	U	100	100	12.0								
A26		U			13.5								
A27		U			12.5								
A28		U			15.0								
A63		W			5.0			Elongation confined to weld area.					
A64		W			4.0								
A65		W			5.5								

U Unwelded
W Welded

TABLE XVII

STRAIN DATA AND MECHANICAL PROPERTIES OF BIAXIALLY STRAINED SPECIMENS

2219-T87 ALUMINUM (Unwelded)

Specimen No.	Specimen Type	Prestraining Conditions					Mechanical Properties					
		Strain Rate in/in/sec	Applied Strain % of Max.	Measured Strain % Elong. in 2"	Actual Strain % of Max.	Octahedral Shear Strain $\bar{\gamma}$	Prop. Limit ksi	0.2% Yield Strength ksi	Ultimate Strength ksi	% Elong. in 2"	% Red. of Area	E, Mod. of Elasticity psi x 10^{-6}
87-8	Fracture	.003	100	8.0								
87-11-1	Tensile	.002	75	6.0	75	.165	44.3	67.4	73.3	7.0	19.1	9.9
87-11-3	↓	.002	↓	6.0	75	.165	51.6	68.2	72.9	8.5	16.8	9.1
87-12-2	↓	.001	↓	5.5	69	.152	51.1	68.9	73.4	7.5	19.8	9.2
87-11-2	Notch	.002	↓	6.0	75	.165			51.9			
87-12-1	↓	.001	↓	5.5	69	.152			46.5			
87-12-3	↓	.001	↓	5.5	69	.152			51.7			
87-10-1	Tensile	.0007	40	3.0	38	.084	45.3	68.4	73.4	8.5	19.6	9.3
87-10-3	↓	.0007	↓	3.0	38	.084	49.6	67.2	73.0	8.0	19.4	9.3
87-9-2	↓	.0008	↓	3.0	38	.084	52.8	69.8	73.5	8.5	19.9	9.0
87-10-2	Notch	.0007	↓	3.0	38	.084			57.7			
87-9-1	↓	.0008	↓	3.0	38	.084			60.0			
87-9-3	↓	.0008	↓	3.0	38	.084			57.4			
87-1	Fracture	100	100	8.0								
87-6	↓	↓	↓	12.0								
Avg.	↓	↓	↓	10.0	100							
87-5-1	Tensile	↓	75	10.0	100	.270	35.8	67.3	72.2	6.0	10.4	10.6
87-5-3	↓	↓	↓	10.0	100	.270	32.7	66.0	71.8	6.0	11.6	11.6
87-7-2	↓	↓	↓	8.0	80	.218	47.8	68.2	72.2	5.5	20.0	10.5
87-5-2	Notch	↓	↓	10.0	100	.270			24.7			
87-7-1	↓	↓	↓	8.0	80	.218			39.4			
87-7-3	↓	↓	↓	8.0	80	.218			14.4			
87-3-1	Tensile	↓	40	5.0	50	.138	52.1	67.8	72.4	7.0	15.5	10.1
87-3-3	↓	↓	↓	5.0	50	.138	46.2	67.1	72.4	5.5	14.4	10.6
87-4-2	↓	↓	↓	5.0	50	.138	37.0	68.2	72.9	5.5	14.6	11.2
87-3-2	Notch	↓	↓	5.0	50	.138			28.9			
87-4-1	↓	↓	↓	5.0	50	.138			22.9			
87-4-3	↓	↓	↓	5.0	50	.138			17.1			

TABLE XVIII

STRAIN DATA AND MECHANICAL PROPERTIES OF CONTROL AND UNIAXIALLY STRAINED SPECIMENS

5Al-2.5Sn TITANIUM

Specimen No.	Specimen Type		Prestraining Conditions: Strain Rate in/in/sec	Applied Strain % of Max.	Measured Strain % Elong. in 2"	Actual Strain % of Max.	Octahedral Shear Strain $\bar{\gamma}$	Mechanical Properties: Prop. Limit ksi	0.2% Yield Strength ksi	Ultimate Strength ksi	% Elong. in 2"	% Red. of Area	E, Mod. of Elasticity psi x 10-6
T1	Tensile Long.	U	None					79.8	122.4	127.0	17.0	39.9	15.5
T2	↓	U	↓	↓	↓	↓	↓	96.4	123.4	127.3	16.5	40.2	15.6
T3	↓	U	↓	↓	↓	↓	↓	73.0	123.6	127.8	16.5	37.5	15.6
T4	Tensile Trans.	U	↓	↓	↓	↓	↓	74.7	124.8	127.3	17.0	40.2	16.1
T5	↓	↓	↓	↓	↓	↓	↓	67.6	125.5	127.8	16.5	39.8	15.9
T6	↓	U	↓	↓	↓	↓	↓	62.4	124.8	127.2	17.0	41.8	16.0
T17	Notch Trans.	U	↓	↓	↓	↓	↓			151.4			
T18	↓	U	↓	↓	↓	↓	↓			151.8			
T19	↓	U	↓	↓	↓	↓	↓			151.9			
T30	Tensile Trans.	W	↓	↓	↓	↓	↓	99.6	124.6	128.6	11.5	42.9	17.3
T31	↓	W	↓	↓	↓	↓	↓	73.7	120.3	124.9	12.5	44.7	16.2
T32	↓	↓	↓	↓	↓	↓	↓	87.1	124.0	129.4	12.0	41.3	15.1
T46	Notch Trans.	W	↓	↓	↓	↓	↓			150.1			
T47	↓	W	↓	↓	↓	↓	↓			150.2			
T48	↓	W	↓	↓	↓	↓	↓			140.2			
T56	Tensile Fracture	U	.05	100	12.0								
T57	↓	U	↓	↓	10.5	↓	↓						
T58	↓	U	↓	↓	19.0	↓	↓						
Avg.	↓	U	↓	↓	13.8	100	↓						
T12	Tensile	U	↓	75	6.5	47.1	.089	90.3	138.6	139.2	11.5	37.8	14.1
T15	↓	U	↓	↓	6.5	47.1	.089	88.1	139.1	139.3	7.5	19.5	13.8
T16	↓	U	↓	↓	5.5	39.8	.076	83.5	138.3	138.5	12.5	40.1	13.9
T61	Notch	U	↓	↓	4.5	32.6	.062			153.6			
T62	↓	U	↓	↓	4.5	32.6	.062			153.3			
T63	↓	U	↓	↓	4.5	32.6	.062			158.9			
T38	Tensile Fracture	W	↓	100	8.5								
T39	↓	W	↓	↓	8.5	↓	↓						
Avg.	↓	W	↓	↓	8.5	100	↓						
T41	Tensile	W	↓	75	4.5	53.0	.062	93.5	138.9	142.6	12.5	34.1	15.1
T43	↓	W	↓	↓	4.5	53.0	.062	93.3	135.9	139.3	11.5	34.3	14.7
T44	↓	W	↓	↓	3.5	41.2	.049	108.9	139.0	141.9	13.5	37.8	15.0
T49	Notch	W	↓	↓	3.5	41.2	.049						
T50	↓	W	↓	↓	4.0	47.1	.056						
T51	↓	W	↓	↓	3.5	41.2	.049						
T8	Tensile Fracture	U	100	100	15.0								
T9	↓	U	↓	↓	15.5	↓	↓						
T13	↓	U	↓	↓	14.5	↓	↓						
T14	↓	U	↓	↓	16.0	↓	↓						
T33	↓	W	↓	↓	10.0	↓	↓						
T34	↓	W	↓	↓	10.0	↓	↓						
T35	↓	W	↓	↓	10.5	↓	↓						
T36	↓	W	↓	↓	10.0	↓	↓						
T37	↓	W	↓	↓	9.5	↓	↓						

U Unwelded
W Welded

TABLE XIX

STRAIN DATA AND MECHANICAL PROPERTIES OF BIAXIALLY STRAINED SPECIMENS

5Al-2.5Sn TITANIUM (Welded)

Specimen No.	Specimen Type	Prestraining Conditions			Mechanical Properties					
		Strain Rate in/in/sec	Measured Strain % Elong. in 2"	Octahedral Shear Strain $\bar{\gamma}$	Prop. Limit ksi	0.2% Yield Strength ksi	Ultimate Strength ksi	% Elong. in 2"	% Red. of Area	E, Mod. of Elasticity psi x 10^{-6}
T-19	Fracture	Conv.	0.5							
T-22	↓	↓	1.5							
T-1-1	Tensile		0.0	0	90.0	123.3	128.8	14.5	44.4	15.0
T-1-2	↓	↓	↓	↓	85.2	126.5	132.6	13.0	41.2	15.7
T-1-3	↓	↓	↓	↓	96.3	123.5	128.7	14.5	41.6	14.7
T-1-4	↓	↓	↓	↓	106.9	126.8	132.1	14.0	40.5	15.0
T-5-1	↓	↓	↓	↓	98.6	121.9	127.6	14.0	41.2	15.1
T-5-2	↓	↓	↓	↓	98.4	120.1	126.6	13.0	37.3	14.0
T-5-3	↓	↓	↓	↓	96.5	119.7	126.6	12.0	29.5	14.6
T-5-4	↓	↓	↓	↓	77.8	119.4	125.9	12.5	44.2	15.2
T-12	Fracture	Expl.	1.0							
T-25	↓	↓	1.0							
T-15-1	Tensile		0.0	0	92.4	125.0	130.1	14.0	45.0	14.3
T-15-2	↓	↓	↓	↓	88.0	120.0	130.6	13.0	44.0	14.1
T-15-3	↓	↓	↓	↓	89.3	122.7	132.0	13.0	40.5	14.7
T-15-4	↓	↓	↓	↓	89.4	124.0	132.3	14.0	40.7	14.5
T-20-1	↓	↓	1.0	.028	90.7	120.8	129.9	12.0	43.8	14.4
T-20-2	↓	↓	↓	↓	97.8	122.8	131.9	11.5	45.8	13.8
T-20-3	↓	↓	↓	↓	98.4	121.3	129.9	11.5	44.3	14.9
T-20-4	↓	↓	↓	↓	89.3	119.9	129.5	11.5	45.3	13.7

TABLE XX

STRAIN DATA AND MECHANICAL PROPERTIES OF CONTROL AND UNIAXIALLY STRAINED SPECIMENS

RENÉ 41

Specimen No.	Specimen Type		Prestraining Conditions					Mechanical Properties					
			Strain Rate in/in/sec	Applied Strain % of Max.	Measured Strain % Elong. in 2"	Actual Strain % of Max.	Octahedral Shear Strain $\bar{\delta}$	Prop. Limit ksi	0.2% Yield Strength ksi	Ultimate Strength ksi	% Elong. in 2"	% Red. of Area	E, Mod. of Elasticity psi x 10^{-6}
R1	Tensile Long.	U	None					116.4	144.2	169.5	7.0	9.4	26.7
R2		U						119.4	144.2	168.1	7.0	5.4	27.2
R3		U						118.7	144.0	169.0	6.5	6.7	27.3
R4	Tensile Trans.	U						101.8	137.8	165.4	6.0	5.9	26.8
R5		U						103.9	137.5	162.9	6.0	5.0	26.5
R6		U						99.6	136.8	167.6	7.5	8.0	27.1
R18	Notch Trans.	U								147.2			
R19		U								143.6			
R20		U								150.8			
R26	Tensile Trans.	W						101.3	138.3	160.2	5.0	1.5	26.0
R27		W						105.9	138.9	164.6	5.5	3.6	26.5
R28		W						111.9	139.4	164.4	5.5	4.1	26.1
R42	Notch Trans.	W								94.1			
R43		W								105.4			
R44		W								130.3			
R12	Tensile Fracture	U	.05	100	46.0								
R13		U			46.5								
Avg.		U			46.2	100							
R14	Tensile	U		75	31.5	68.2	.388	151.4	199.8	221.1	8.5	8.5	28.2
R15					32.0	69.3	.393	160.2	202.4	220.6	4.5	5.8	28.3
R16					32.0	69.3	.393	158.4	199.9	218.2	7.5	8.3	28.0
R21	Notch	U			26.0	56.3	.328			158.7			
R22		U			29.5	63.9	.366			160.1			
R25		U			20.5	44.4	.264			169.1			
R34	Tensile Fracture	W		100	17.0								
R35		W			10.0								
Avg.		W			13.5	100							
R38	Tensile	W		75	4.0	29.6	.055	121.9	156.4	175.6	5.5	1.9	26.1
R39		W			4.5	33.4	.062	111.3	153.2	172.4	5.5	2.1	26.6
R40					4.5	33.4	.062	115.4	154.6	171.0	5.0	2.3	26.1
R45	Notch	W			5.0	37.0	.069			87.0			
R46		W			5.0	37.0	.069			98.7			
R47		W			5.5	40.7	.076			97.7			
R8	Tensile Fracture	U	100	100	47.0								
R9		U			50.5								
R10		U			45.0								
R11		U			48.5								
R29		W			17.5								
R32		W			20.0								
R33		W			12.5								

U Unwelded
W Welded

TABLE XXI

STRAIN DATA AND MECHANICAL PROPERTIES OF BIAXIALLY STRAINED SPECIMENS

RENÉ 41 (Welded)

Specimen No.	Specimen Type	Prestraining Conditions				Mechanical Properties					
		Strain Rate in/in/sec	Measured Strain % Elong. in 2"	Actual Strain % of Max.	Octahedral Shear Strain $\bar{\gamma}$	Prop. Limit ksi	0.2% Yield Strength ksi	Ultimate Strength ksi	% Elong. in 2"	% Red. of Area	E, Mod. of Elasticity psi x 10^{-6}
R-3	Fracture	.00008	9.0	100							
R-8-1	Tensile		5.0	56	.138	119.5	155.0	171.8	3.0	3.9	30.0
R-8-2						113.4	158.8	177.7	3.0	2.5	29.7
R-8-3						117.0	158.5	179.5	3.5	6.2	28.9
R-8-4						111.3	155.9	175.3	3.0	2.9	31.1
R-11-1			9.0	100	.244	136.7	178.6	183.7	1.5	0.9	32.4
R-11-2						126.8	178.9	193.9	2.5	2.1	32.4
R-11-3						124.7	--	195.4	3.0	2.8	30.8
R-7	Fracture	100	9.0								
R-15			7.0								
Avg.			8.0	100							
R-10-1	Tensile		5.0	62	.138	124.9	176.2	197.6	3.5	3.2	31.0
R-10-2						130.8	169.8	187.1	2.0	6.1	33.5
R-10-3						133.0	169.5	186.7	2.5	7.1	36.4
R-10-4						123.1	177.4	198.7	5.0	1.3	29.9
R-18-1			4.0	50	.111	119.7	158.8	172.2	2.0	1.7	31.7
R-18-2						140.4	162.9	176.3	3.0	4.2	31.5
R-18-3						117.1	159.6	178.0	2.5	3.8	32.8
R-18-4						131.7	177.0	188.9	2.5	1.7	30.1

TABLE XXII

NOTCH STRENGTH RATIOS

Material	Welded or Unwelded	Mode of Strain	Strain Rate	Octahedral Shear Strain $\bar{\gamma}$	0.2% Yield Strength ksi	Ultimate Strength ksi	Notch Strength ksi	Notch-Yield Strength Ratio $\frac{N}{Y}$	Notch-Ultimate Strength Ratio $\frac{N}{U}$
2219-T37 ALUMINUM	Unwelded	--	--	--	45.9	61.0	53.7	1.17	0.88
	↓	Uniaxial	Conv.	.100	58.5	63.9	44.9	0.77	0.70
	↓	Biaxial	↓	.192	58.1	66.8	61.7	1.06	0.92
	↓	↓	↓	.283	58.4	67.4	59.6	1.02	0.88
	↓	↓	Expl.	.138	56.7	66.3	35.5	0.63	0.54
	↓	↓	↓	.250	58.3	67.9	27.3	0.47	0.40
2219-T87 ALUMINUM	Unwelded	--	--	--	57.5	71.6	55.1	0.96	0.77
	↓	Uniaxial	Conv.	.050	66.4	72.2	20.0	0.30	0.28
	↓	Biaxial	↓	.084	68.5	73.3	58.4	0.85	0.80
	↓	↓	↓	.150	68.0	73.2	50.7	0.75	0.69
	↓	↓	Expl.	.138	67.7	72.6	23.0	0.34	0.32
	↓	↓	↓	.250	67.7	72.0	25.1	0.37	0.35
5Al-2.5Sn TITANIUM	Unwelded	--	--	--	125.0	127.4	151.7	1.21	1.19
	↓	Uniaxial	Conv.	.062	135.1	136.8	155.3	1.15	1.14
	Welded	--	--	--	123.0	127.6	146.8	1.19	1.15
RENÉ 41	Unwelded	--	--	--	137.4	165.3	147.2	1.07	0.89
	↓	Uniaxial	Conv.	.300	185.5	207.0	160.5	0.87	0.78
	Welded	--	--	--	138.9	163.1	109.9	0.79	0.67
	↓	Uniaxial	Conv.	.050	152.0	171.0	98.5	0.65	0.58

TABLE XXIII

STRAIN DATA AND MICROHARDNESS OF SPECIMENS FOR MICROSTRUCTURAL ANALYSIS

Material	Specimen No.	Welded or Unwelded	Prestraining Conditions				Microhardness Knoop Hardness Number		
			Mode of Strain	Strain Rate	Measured Strain % Elong. in 2"	Octahedral Shear Strain $\bar{\gamma}$	Parent	HAZ	Weld
2219-T37 ALUMINUM	A128	Unwelded	None				92		
	A117		Uniaxial	Conv.	8.5	.115	97		
	37-11-4		Biaxial		10.5	.283	117		
	37-11-5				10.5	.283			
	37-13-4				7.0	.192	106		
	37-6-4			Expl.	10.0	.270	113		
	37-6-5				10.0	.270			
	37-4-4				5.0	.138	110		
2219-T87 ALUMINUM	A84	Unwelded	None				124		
	A85	Welded					99	78	58
	A86								
	A87						119	--	--
	A47	Unwelded	Uniaxial	Conv.	5.2	.072	121		
	87-11-4		Biaxial		6.0	.165	124		
	87-11-5				6.0	.165			
	87-10-4				3.0	.084	120		
	87-5-4			Expl.	10.0	.270	128		
	87-5-5				10.0	.270			
	87-3-4				5.0	.138	130		
5Al-2.5Sn TITANIUM	T54	Unwelded	None				266		
	T55	Welded					271	307	323
	T10	Unwelded	Uniaxial	Conv.	7.5	.102	300		
	T40	Welded			6.0	.082	265	269	312
	T-1-5		Biaxial		0.0	0	266	255	299
	T-5-5				0.0	0			
	T-11-1			Expl.	0.0	0	279	281	347
	T-25-1				1.0	.028	294	303	345
RENÉ 41	R50	Unwelded	None				455		
	R51	Welded					439	435	383
	R17	Unwelded	Uniaxial	Conv.	28.3	.355	511		
	R41	Welded			4.5	.062	423	443	393
	R-8-5		Biaxial		5.0	.135	439	455	468
	R-11-4				9.0	.244	481	507	483
	R-11-5				9.0	.244			
	R-10-5			Expl.	5.0	.138	456	475	497
	R-18-5				4.0	.111			

TABLE XXIV

X-RAY DIFFRACTION DATA

Material	Specimen No.	Test Condition	Lattice Parameter Å		Half-Height Width θ°
2219-T37 ALUMINUM	A128	Control	4.0376		0.84
	A117	Uniaxial 8.5%	4.0378		0.95
	37-11-5	Biax. Conv. 10.5%	4.0357		0.92
	37-6-5	Biax. Expl. 10%	4.0424		0.99
2219-T87 ALUMINUM	A84	Unwelded Control	4.0468		0.92
	A87	Welded Control	4.0433		0.73
	87-11-5	Biax. Conv. 6%	4.0468		1.01
	87-5-5	Biax. Expl. 10%	4.0485		0.94
5Al-2.5Sn TITANIUM			c	a	
	T54	Unwelded Control	4.6912	2.9328	.45
	T55	Welded Control	4.6996	2.9231	.30
	T10	Unwelded Uniax. 7.5%	4.6912	2.9433	--
	T40	Welded Uniax. 6%	4.7012	2.9225	.30
	T-5-5	Welded Biax. 0	4.6842	2.9421	.32
RENÉ 41	R50	Unwelded Control	3.6014		0.66
	R51	Welded Control	3.6025		0.94
	R41	Welded Uniax. Conv. 4.5%	3.6011		0.84
	R-11-5	Welded Biax. Conv. 9%	3.6003		0.70
	R-18-5	Welded Biax. Expl. 4%	3.6017		0.98

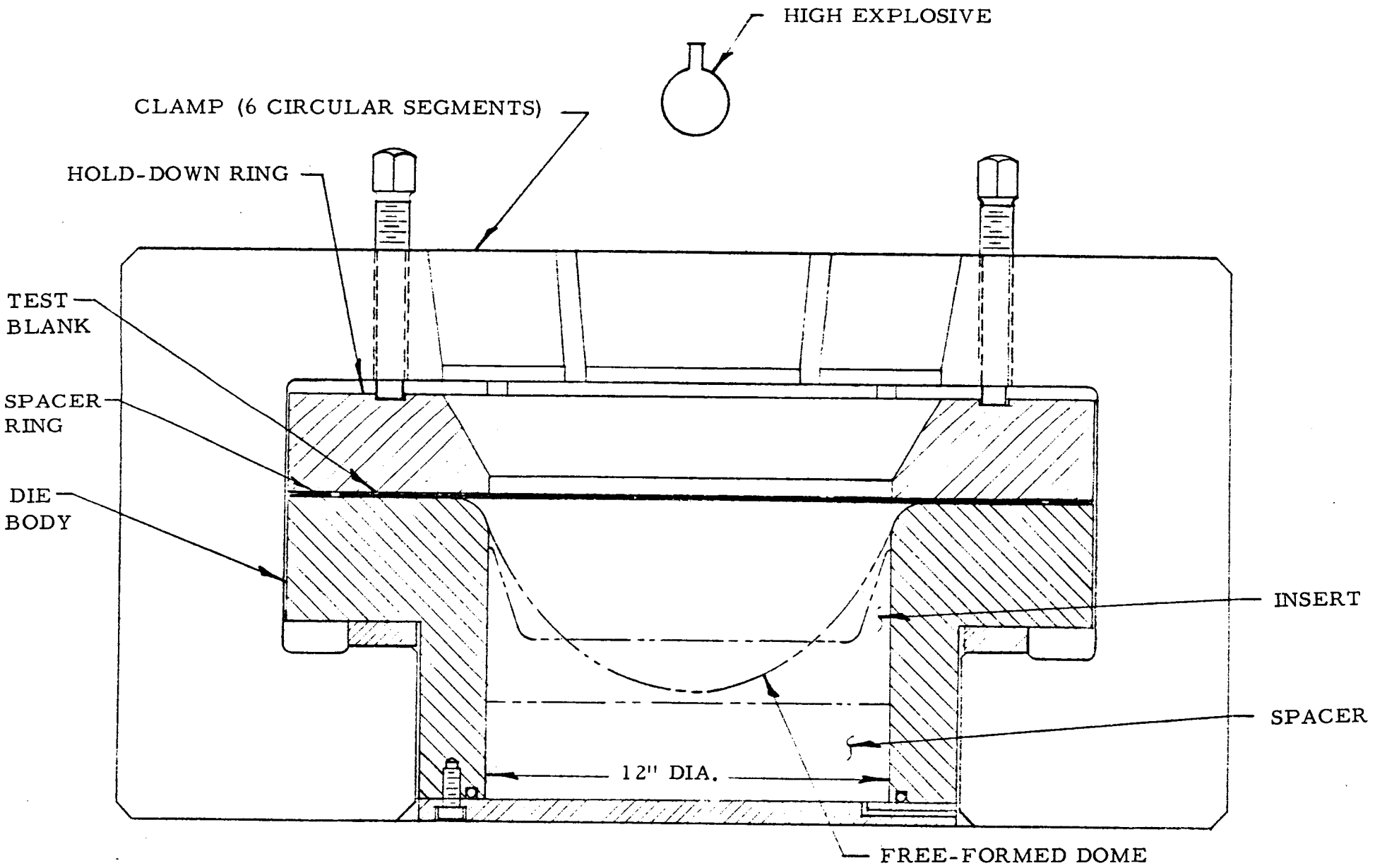

FIGURE 1. FORMING DIE - EXPLOSIVE FORMING

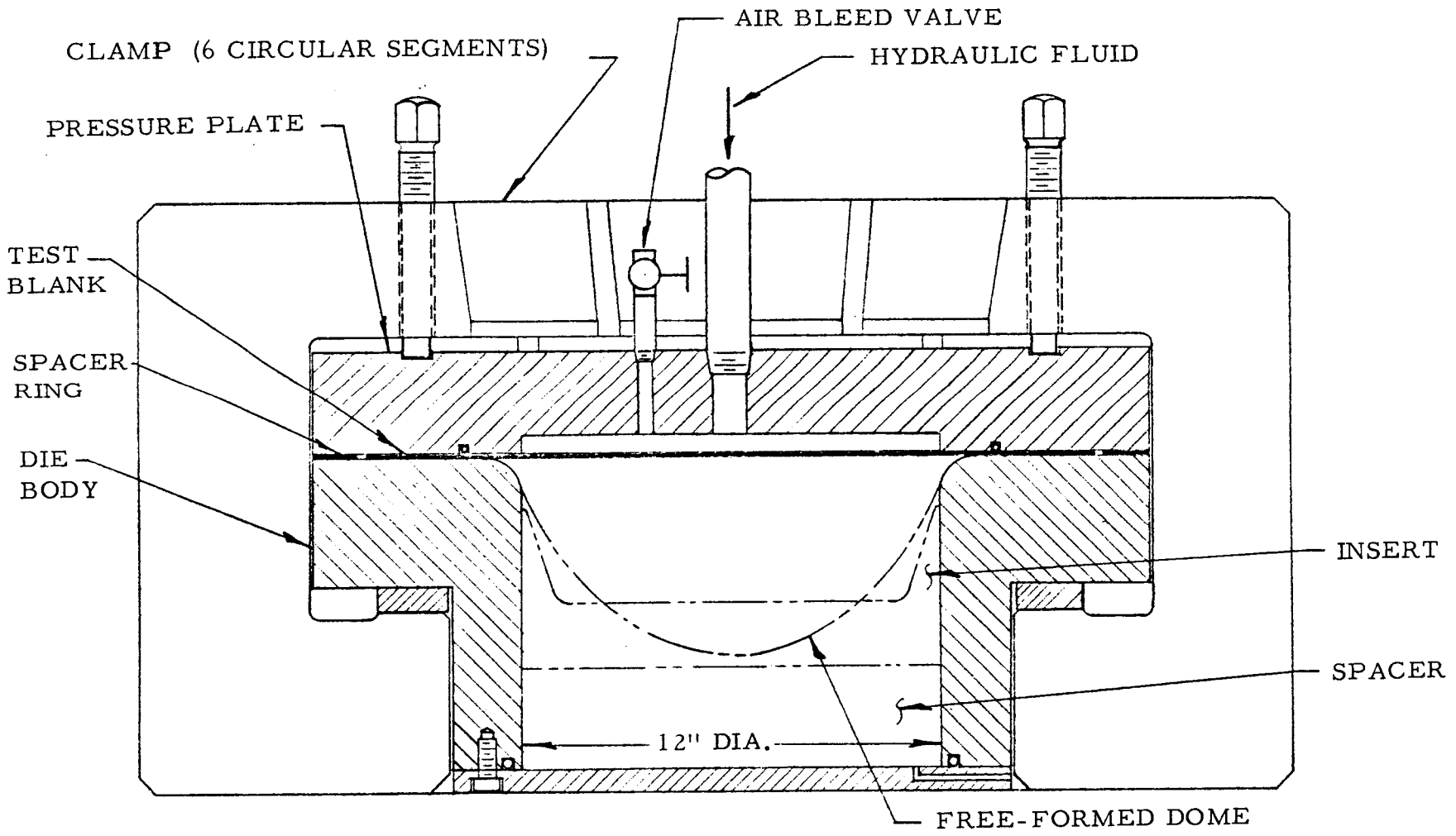

FIGURE 2. FORMING DIE - HYDRAULIC FORMING

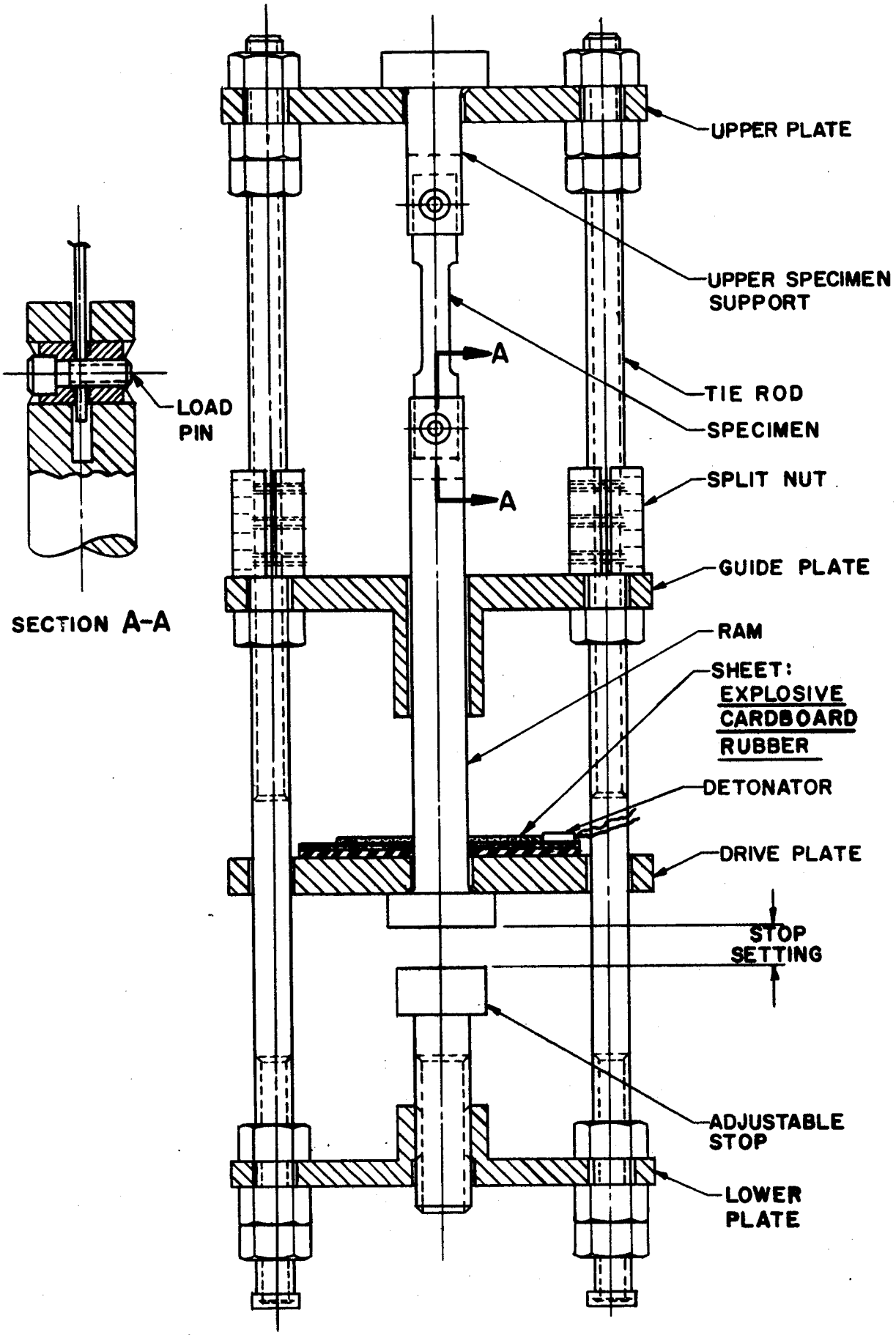

FIGURE 3. DYNAMIC TEST FIXTURE

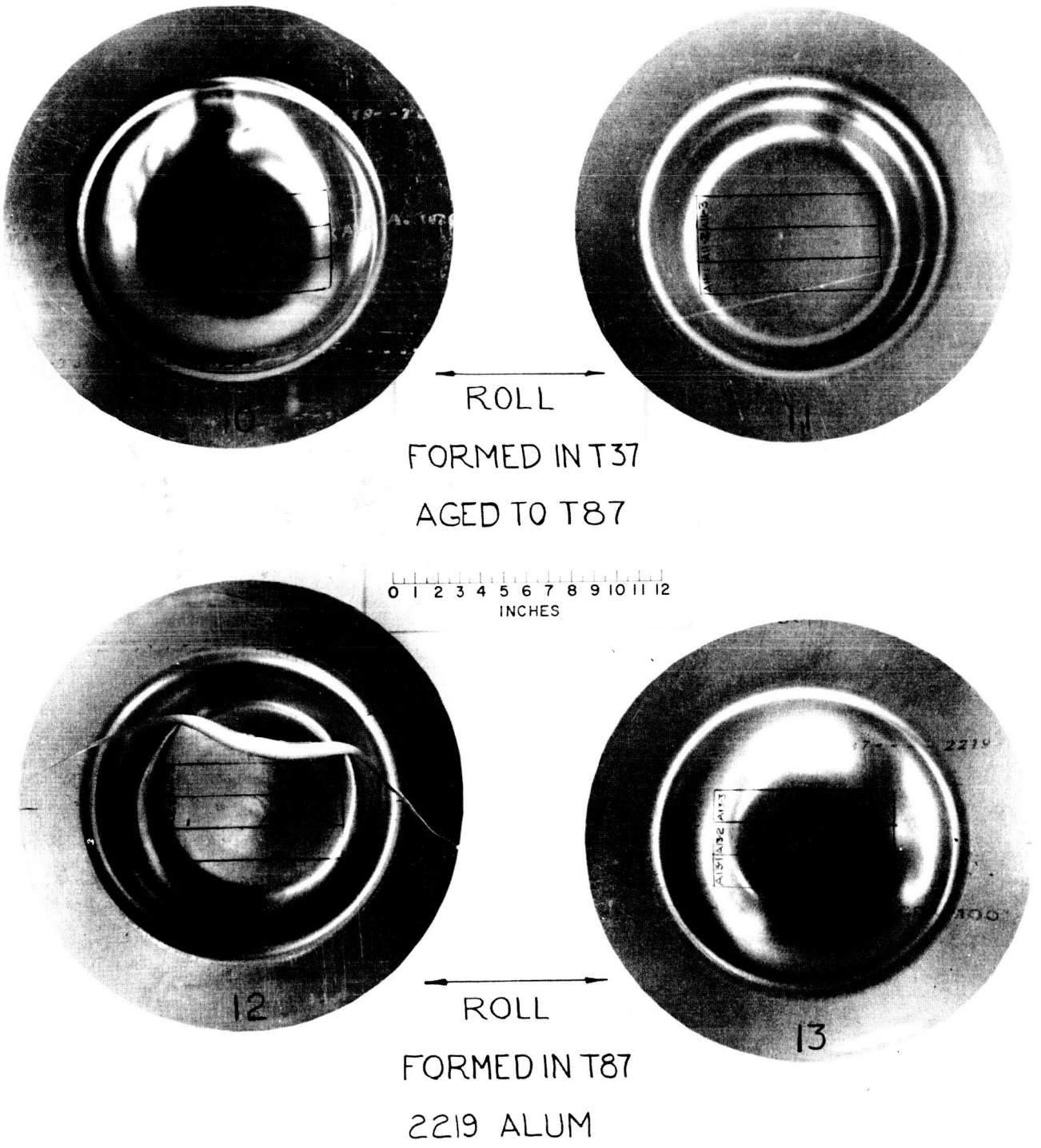

FIGURE 4. DOMES FOR PRELIMINARY EXPERIMENT

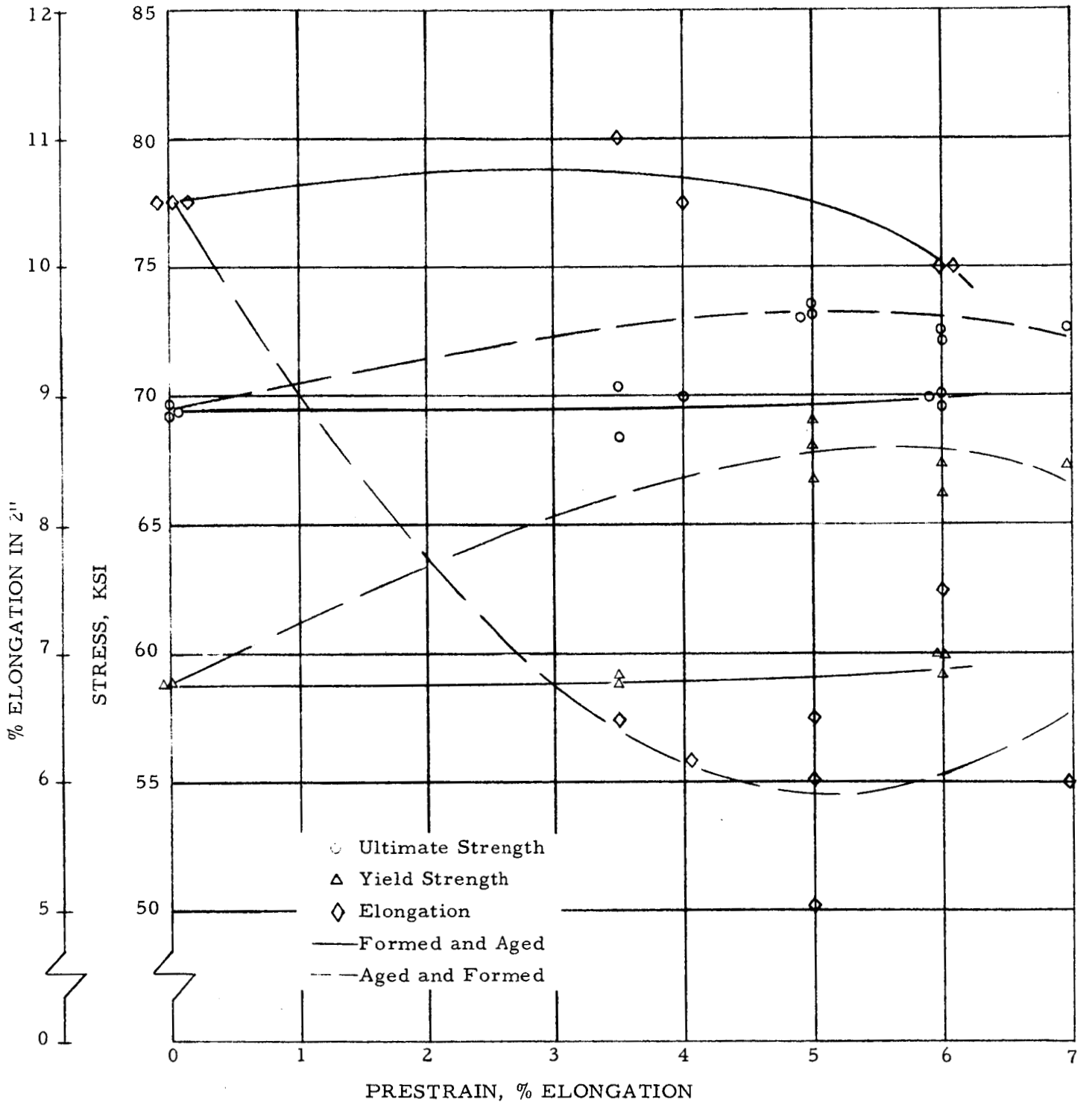

FIGURE 5. PLOT OF MECHANICAL PROPERTIES OF 2219-T37 ALUMINUM AGED TO T87

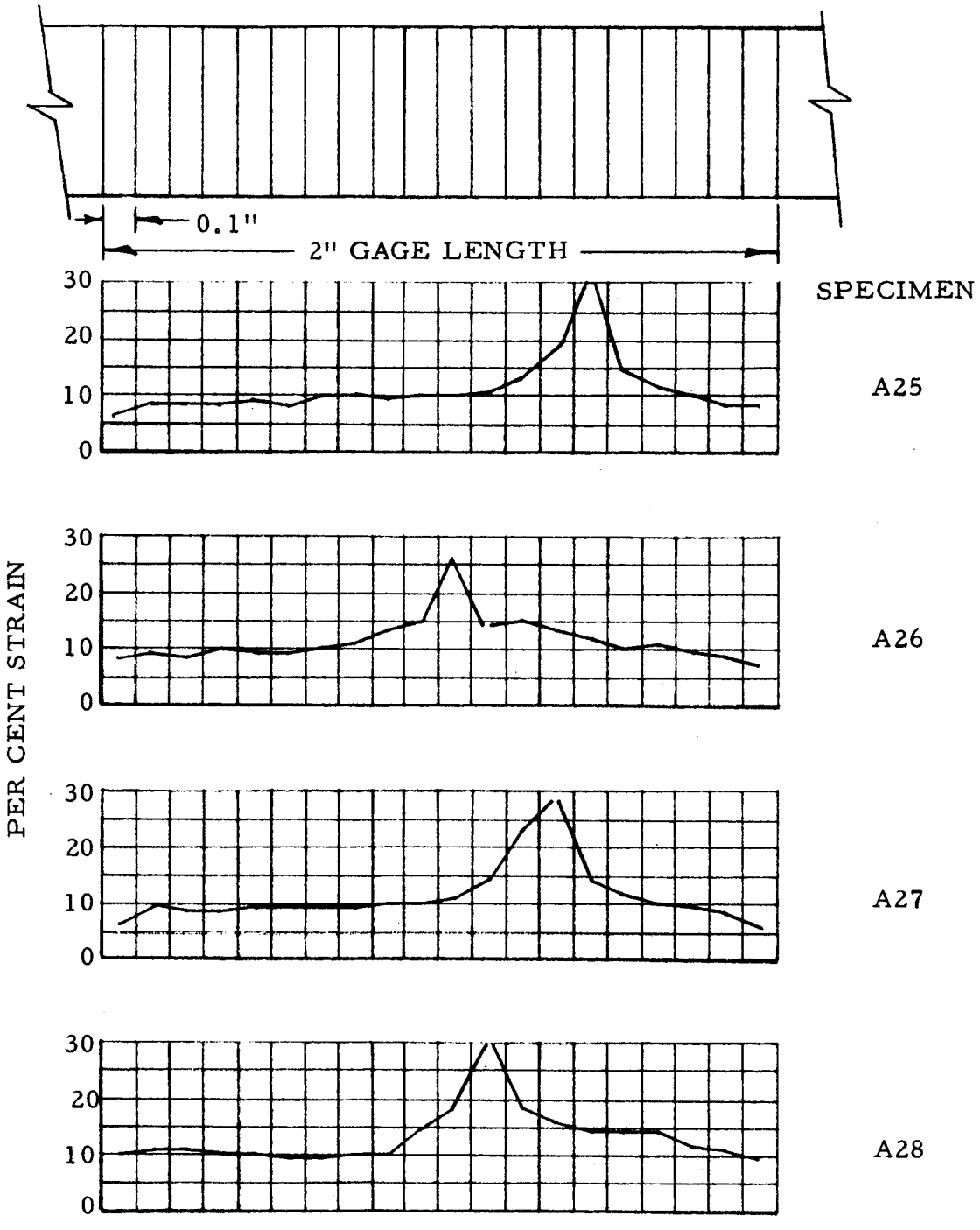

FIGURE 6. STRAIN DISTRIBUTION - UNWELDED EXPLOSIVELY STRAINED SPECIMENS, 2219-T87 ALUMINUM ALLOY

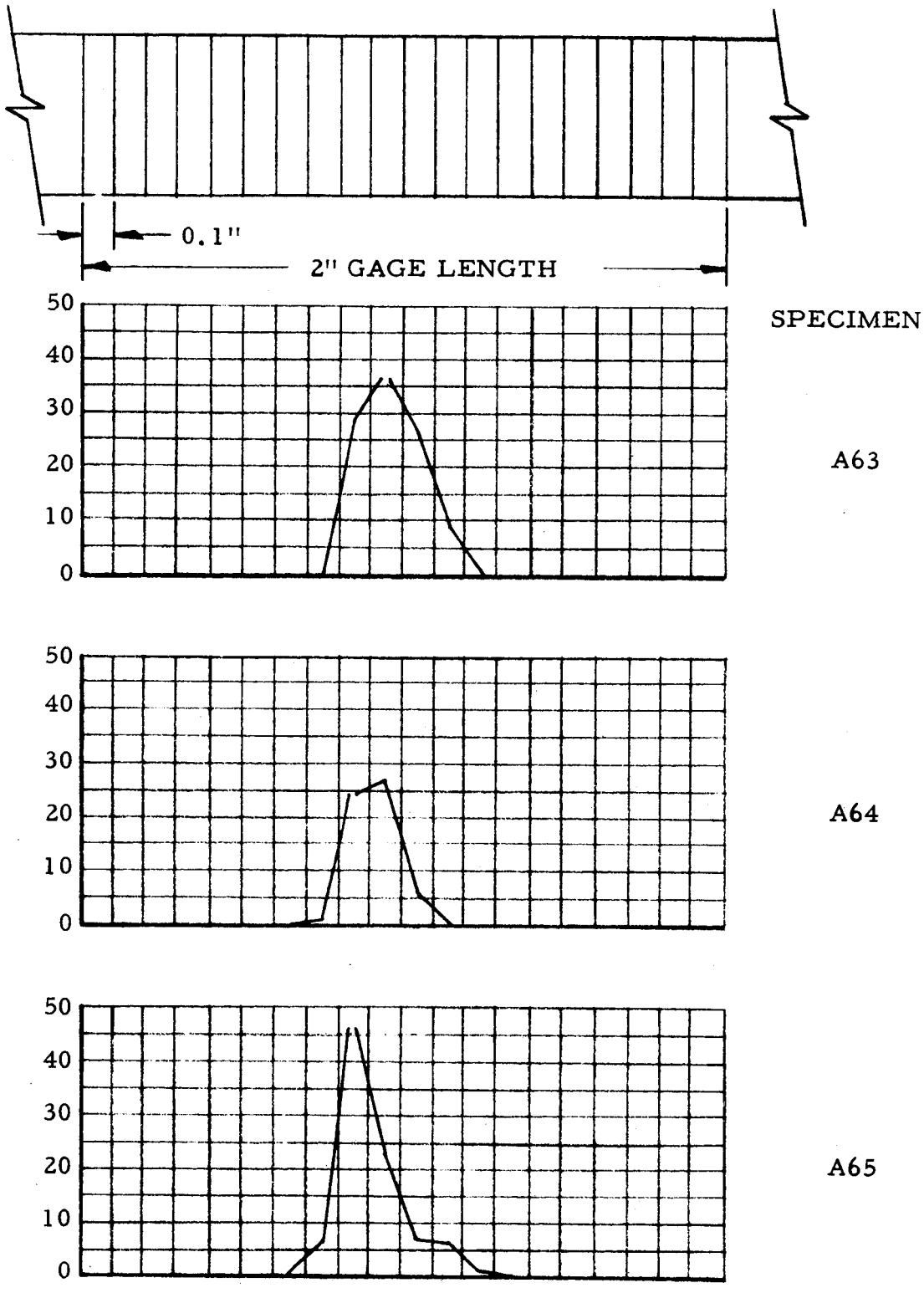

FIGURE 7. STRAIN DISTRIBUTION - WELDED EXPLOSIVELY STRAINED SPECIMENS, 2219-T87 ALUMINUM ALLOY

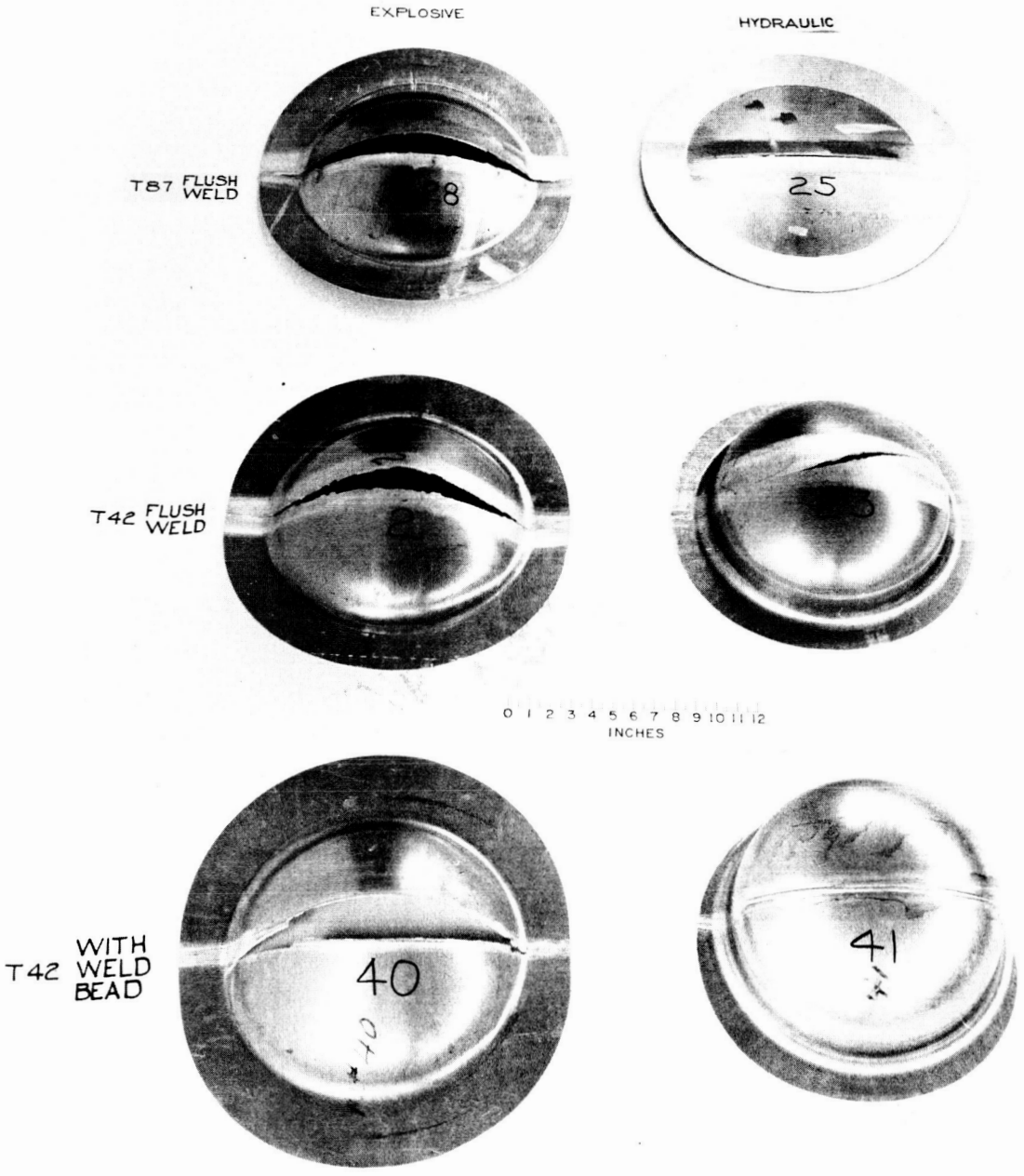

FIGURE 8. WELDED 2219 ALUMINUM DOMES

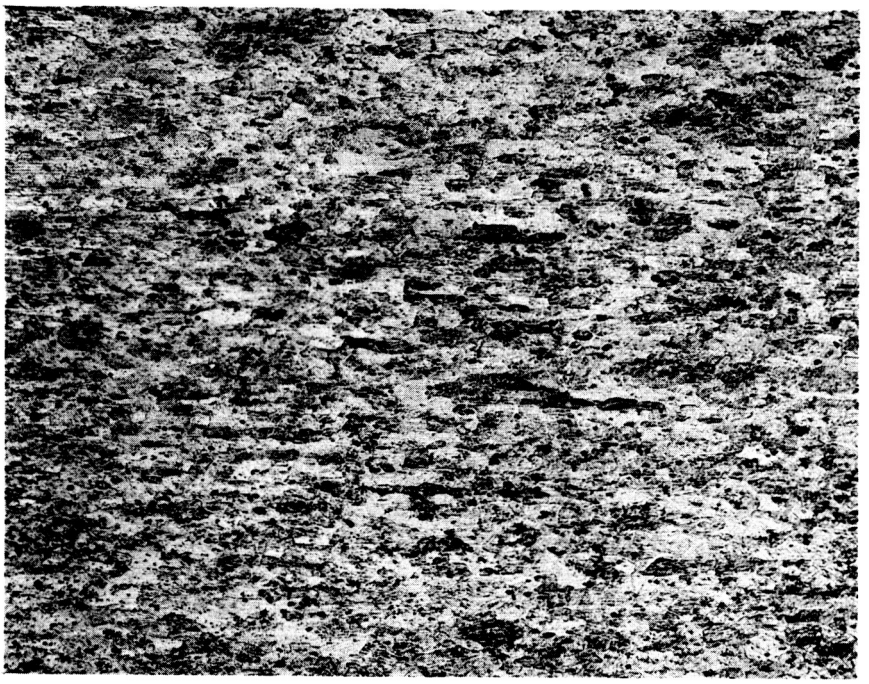

A

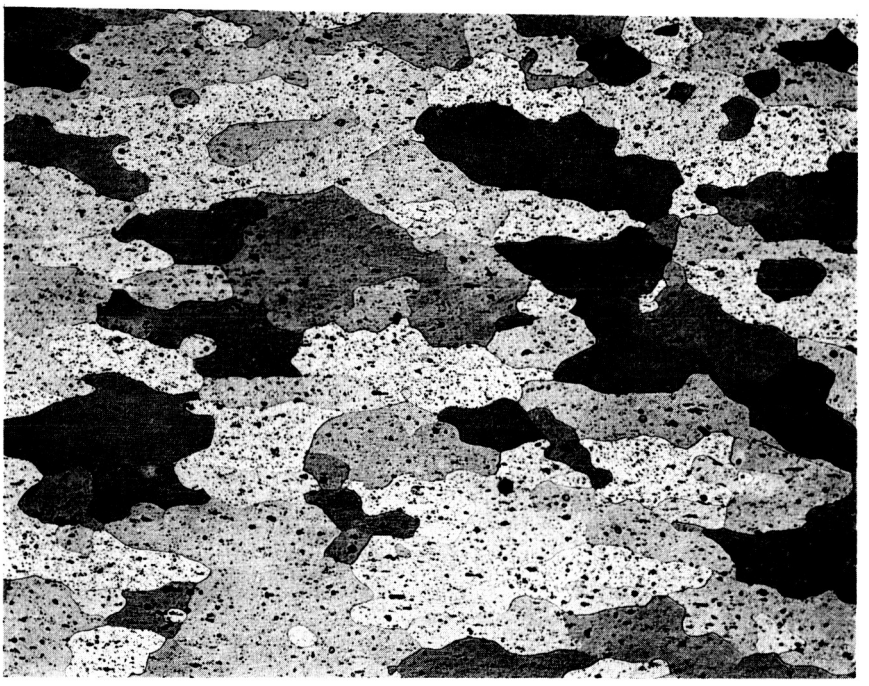

B

100X

FIGURE 9. 2219 ALUMINUM ALLOY PARENT MATERIAL EXPLOSIVELY FORMED

(A) T87 CONDITION (Dome 28)
(B) T42 CONDITION (Dome 2)

KELLER'S ETCH

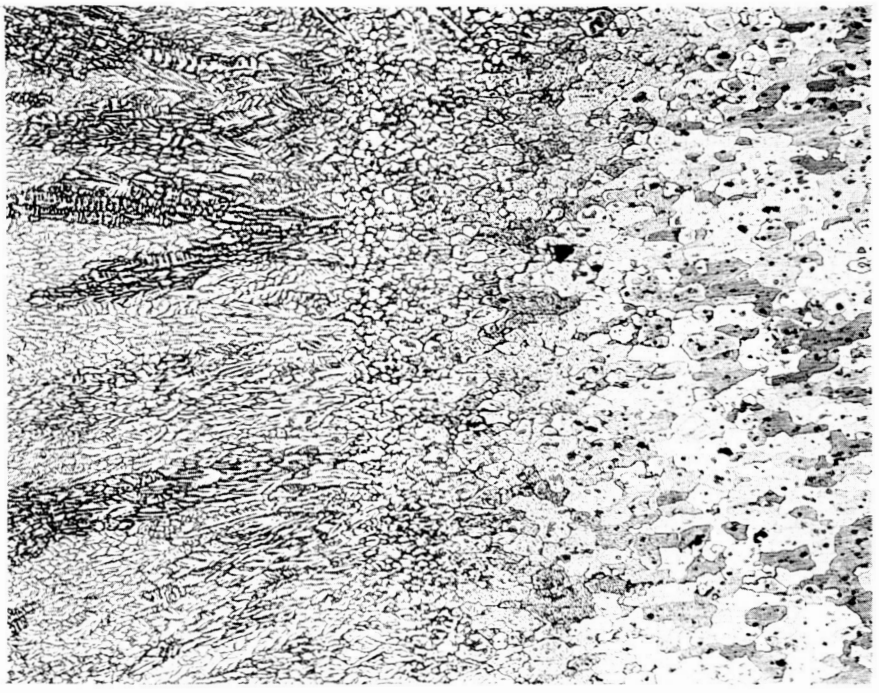

A

B

100X

FIGURE 10. 2219 ALUMINUM ALLOY HEAT-AFFECTED ZONE

(A) T87 CONDITION (Hydraulically Formed) (Dome 25)
(B) T42 CONDITION (Explosively Formed) (Dome 2)

KELLER'S ETCH

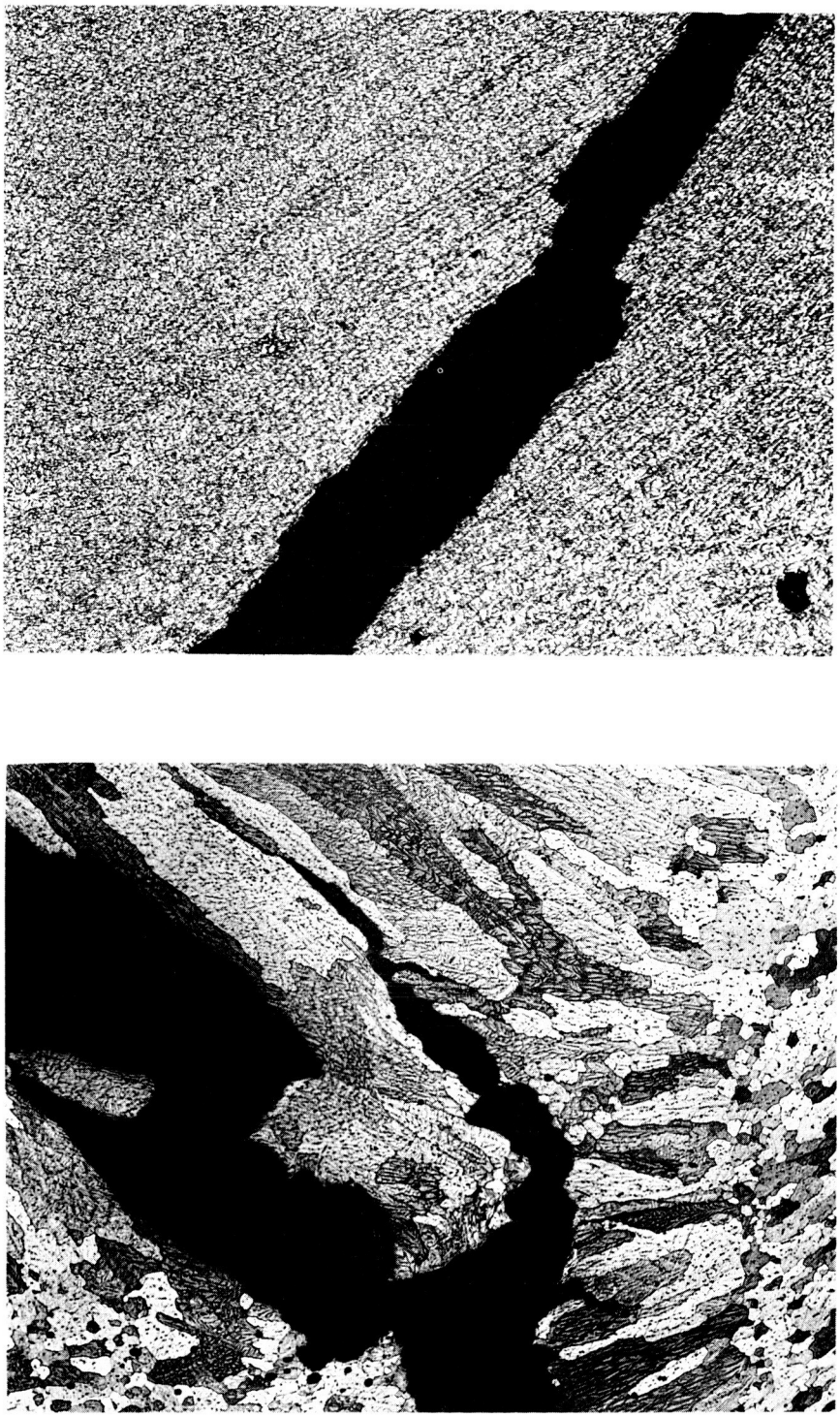

A

B

100X

FIGURE 11. 2219 ALUMINUM ALLOY AT FRACTURE EXPLOSIVELY FORMED

(A) T87 CONDITION (Dome 28)
(B) T42 CONDITION (Dome 40)

KELLER'S ETCH

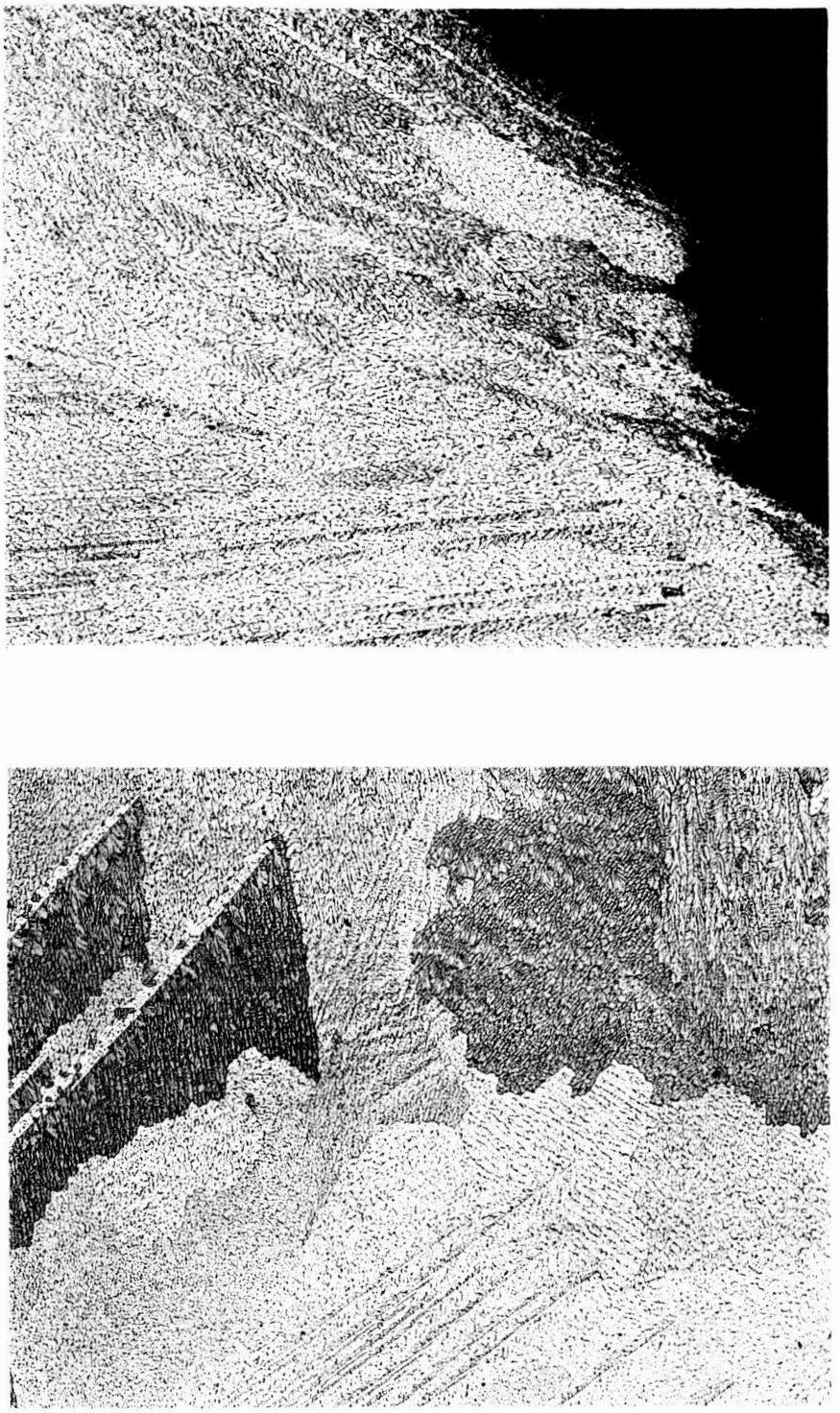

A

B

100X

FIGURE 12. 2219 ALUMINUM ALLOY - WELD MATERIAL HYDRAULICALLY FORMED

(A) T42 AT FRACTURE (Dome 23)
(B) T42 - NO FRACTURE (Dome 41)

KELLER'S ETCH

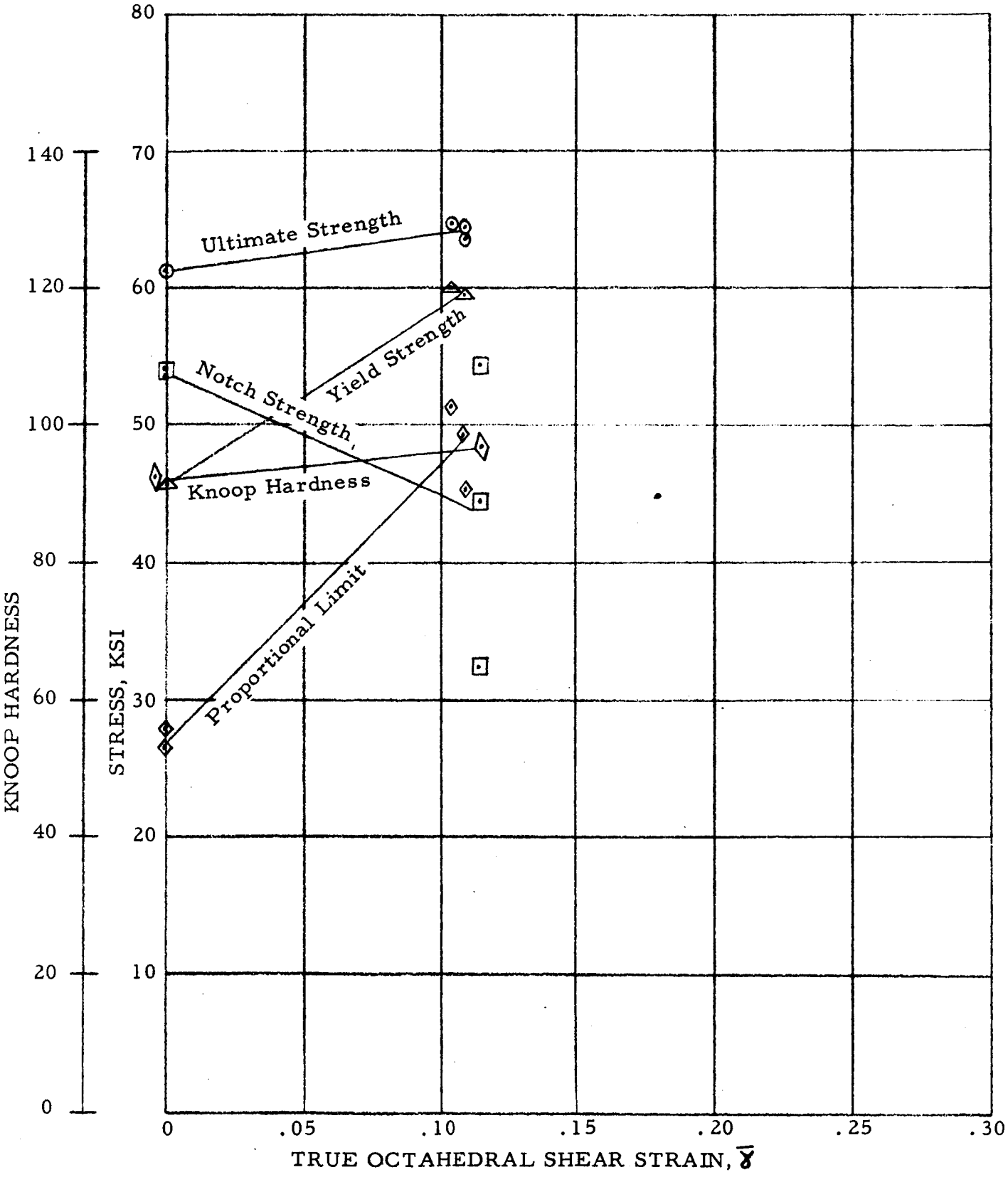

FIGURE 13. MECHANICAL PROPERTIES OF UNWELDED 2219-T37 ALUMINUM AFTER UNIAXIAL PRE-STRAINING AT CONVENTIONAL STRAIN RATE

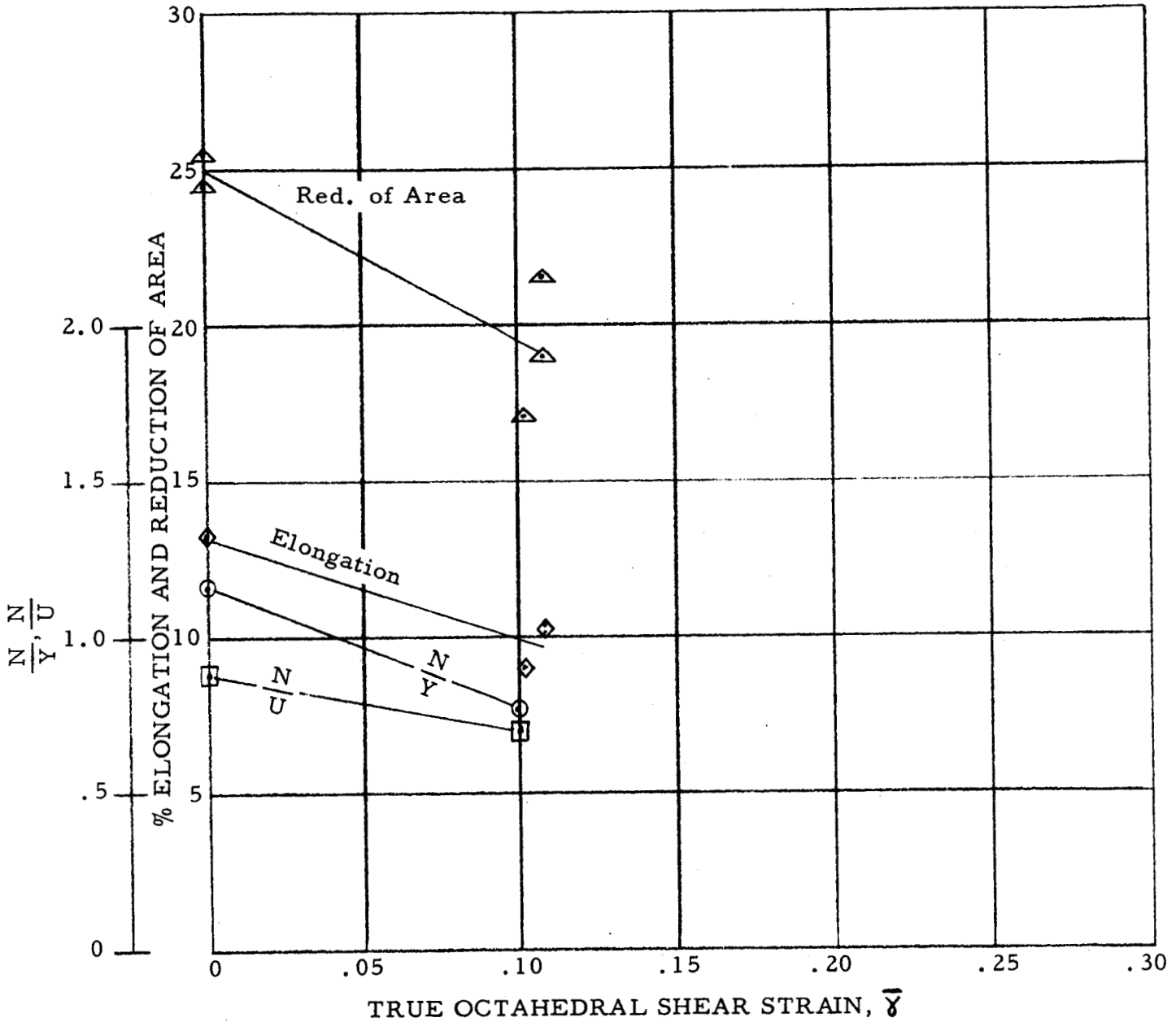

FIGURE 14. MECHANICAL PROPERTIES OF UNWELDED 2219-T37 ALUMINUM AFTER UNIAXIAL PRESTRAINING AT CONVENTIONAL STRAIN RATE

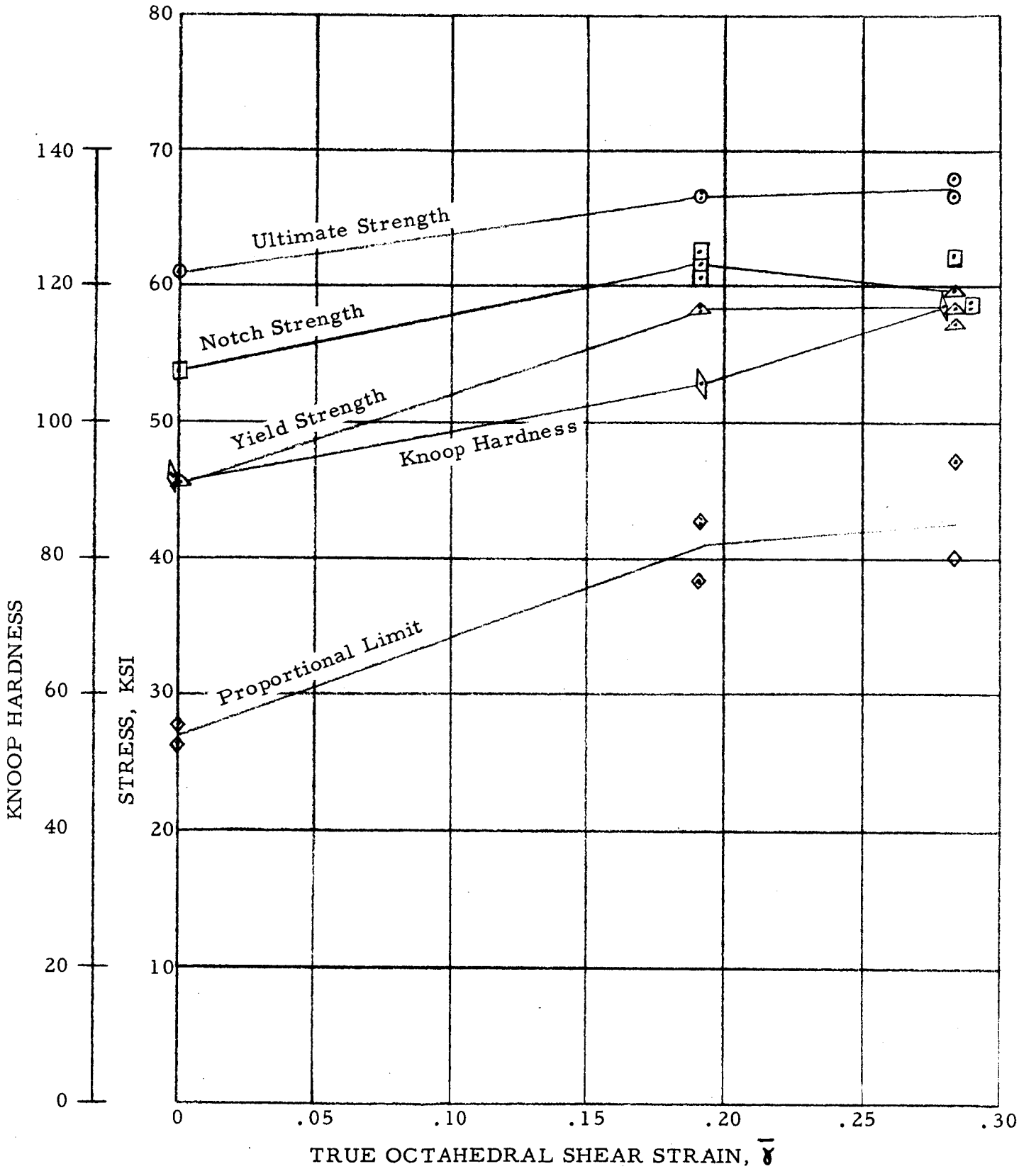

FIGURE 15. MECHANICAL PROPERTIES OF UNWELDED 2219-T37 ALUMINUM AFTER BIAXIAL PRESTRAINING AT CONVENTIONAL STRAIN RATE

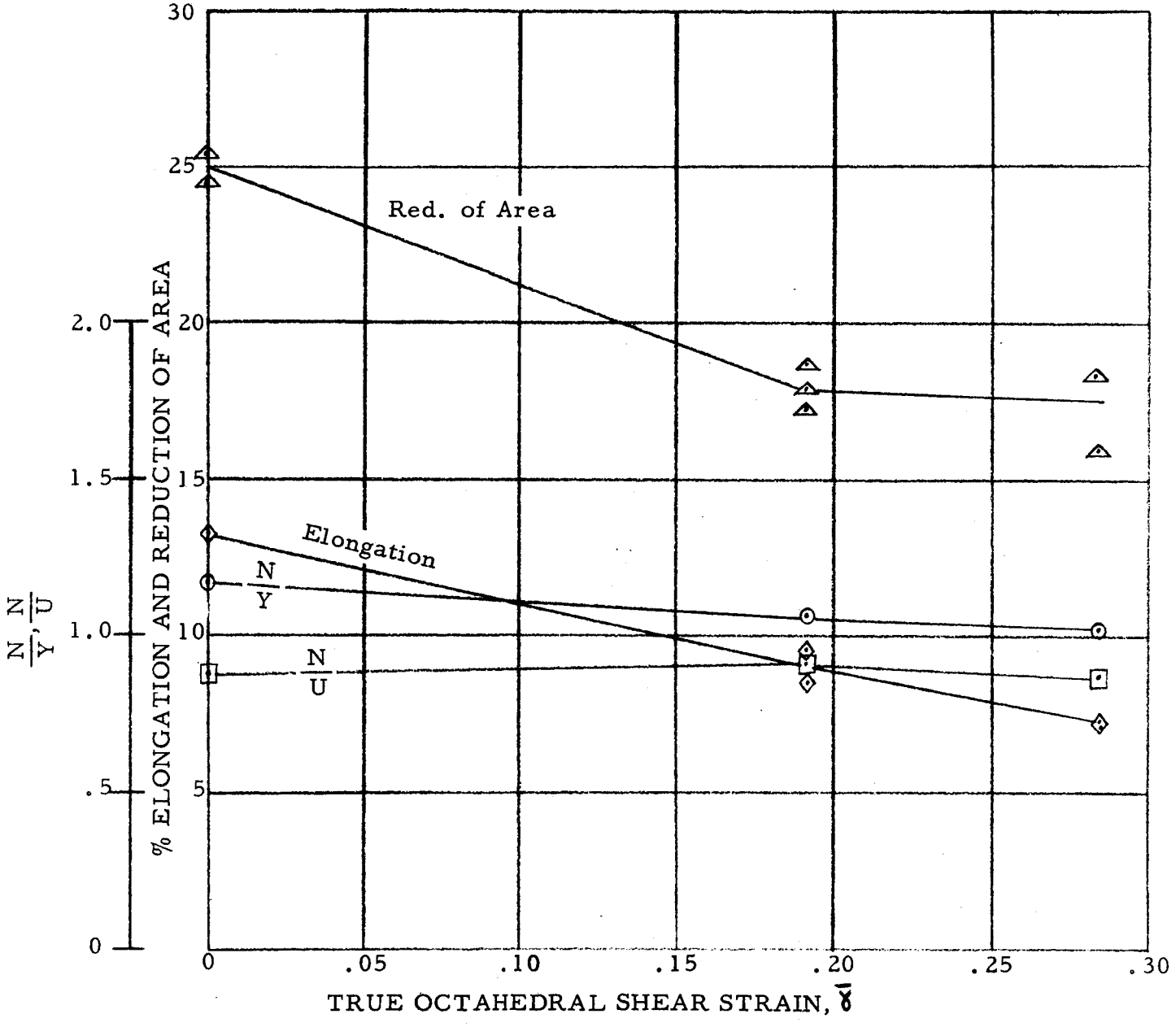

FIGURE 16. MECHANICAL PROPERTIES OF UNWELDED 2219-T37 ALUMINUM AFTER BIAXIAL PRESTRAINING AT CONVENTIONAL STRAIN RATE

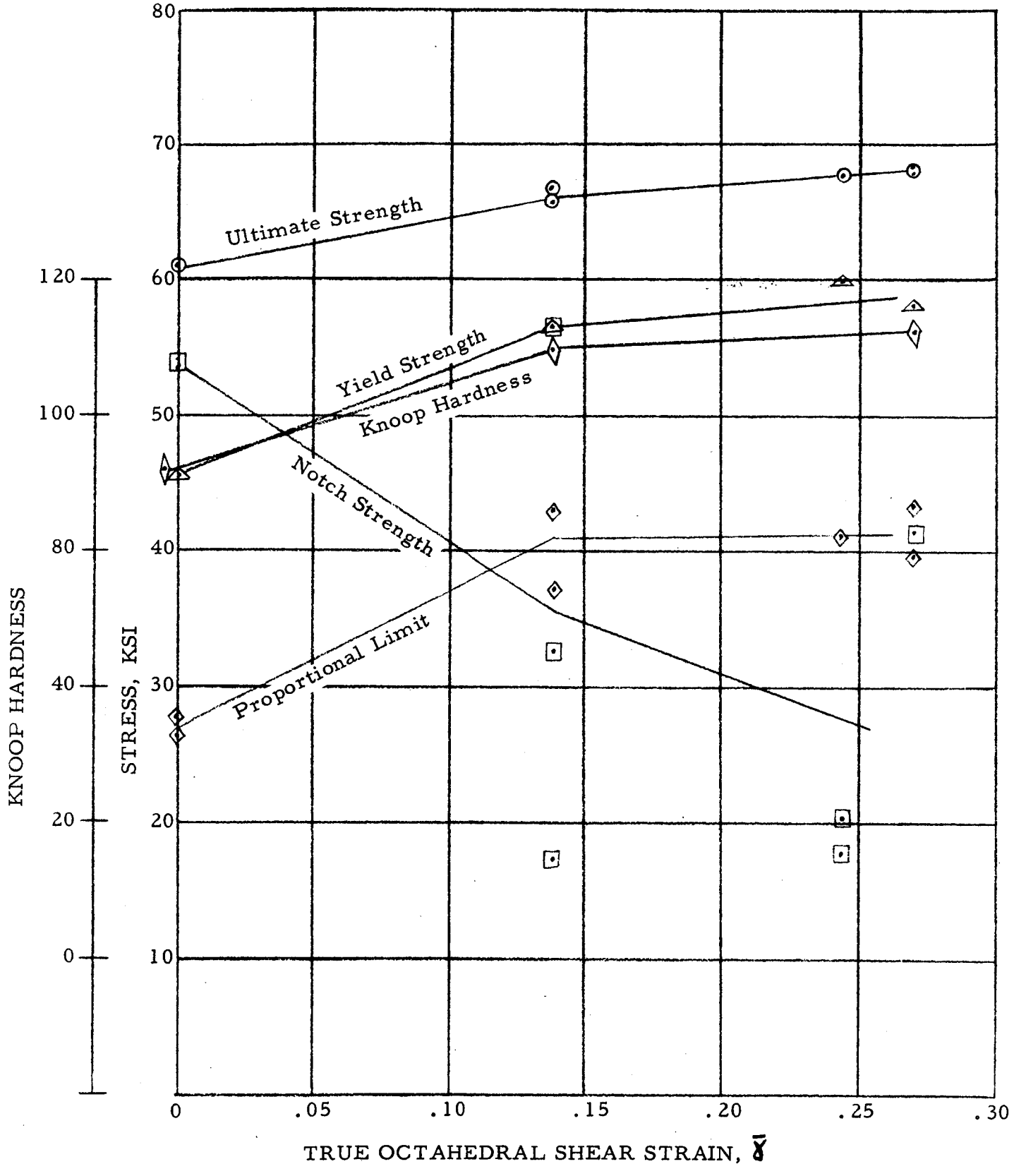

FIGURE 17. MECHANICAL PROPERTIES OF UNWELDED 2219-T37 ALUMINUM AFTER BIAXIAL PRESTRAINING AT EXPLOSIVE STRAIN RATE

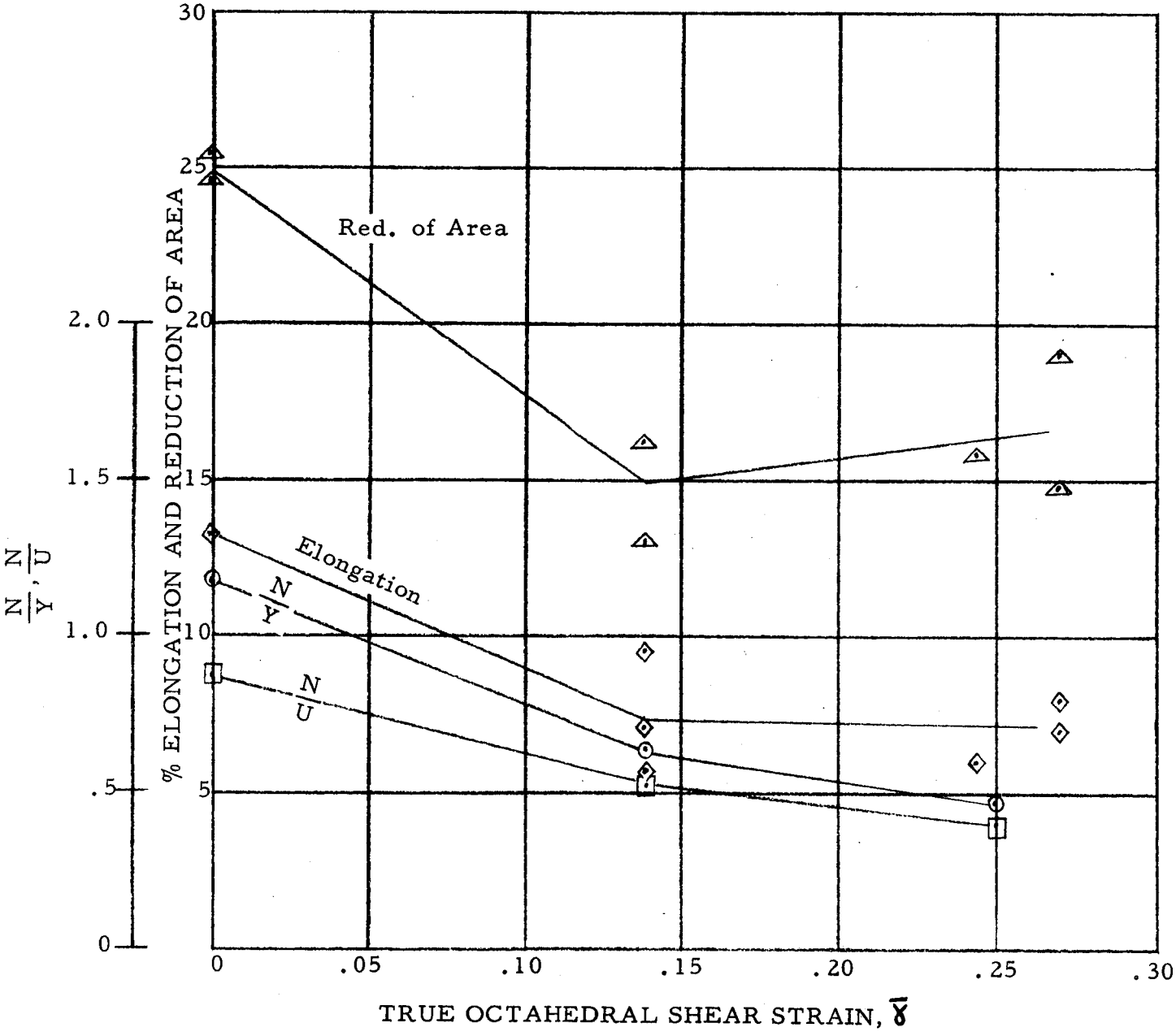

FIGURE 18. MECHANICAL PROPERTIES OF UNWELDED 2219-T37 ALUMINUM AFTER BIAXIAL PRESTRAINING AT EXPLOSIVE STRAIN RATE

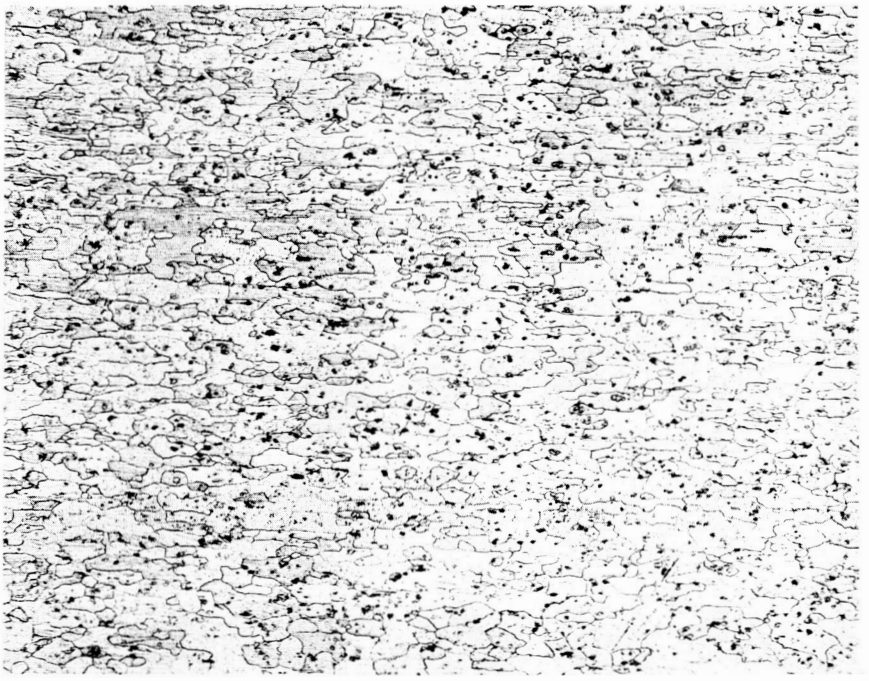

A

100X

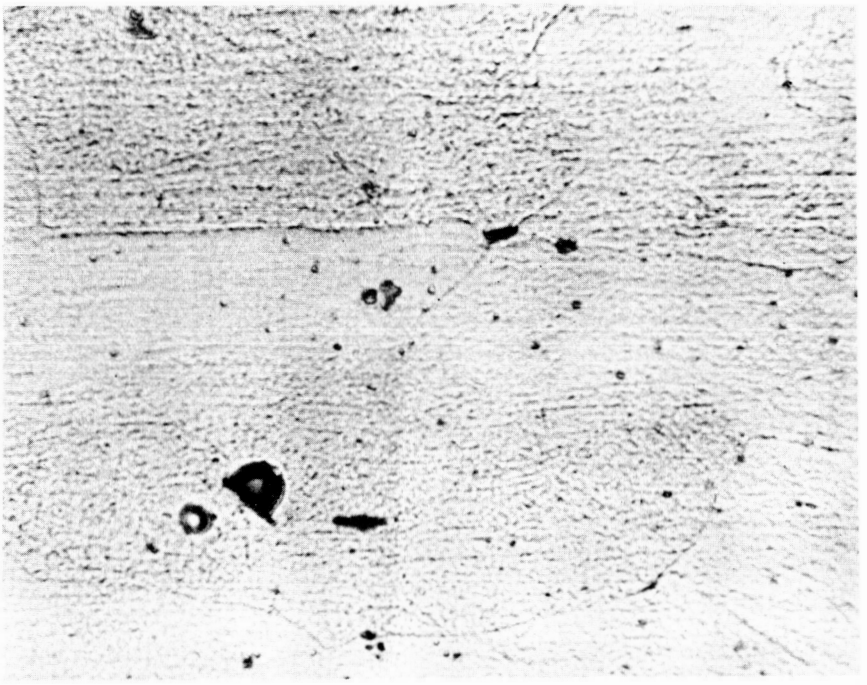

B

2000X

FIGURE 19. 2219-T37 ALUMINUM ALLOY UNSTRAINED
(Specimen A128)

KELLER'S ETCH

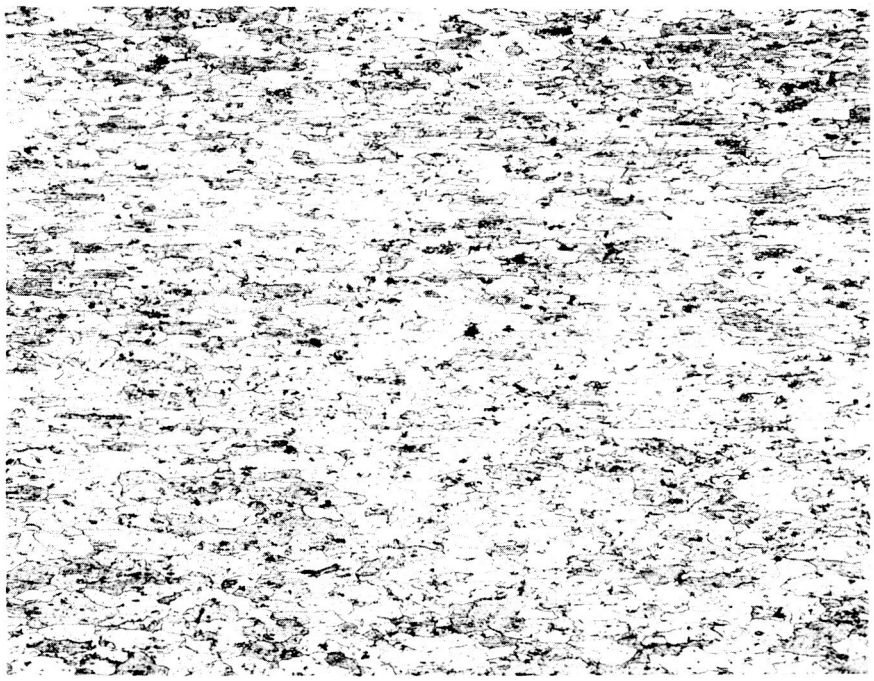

A

100X

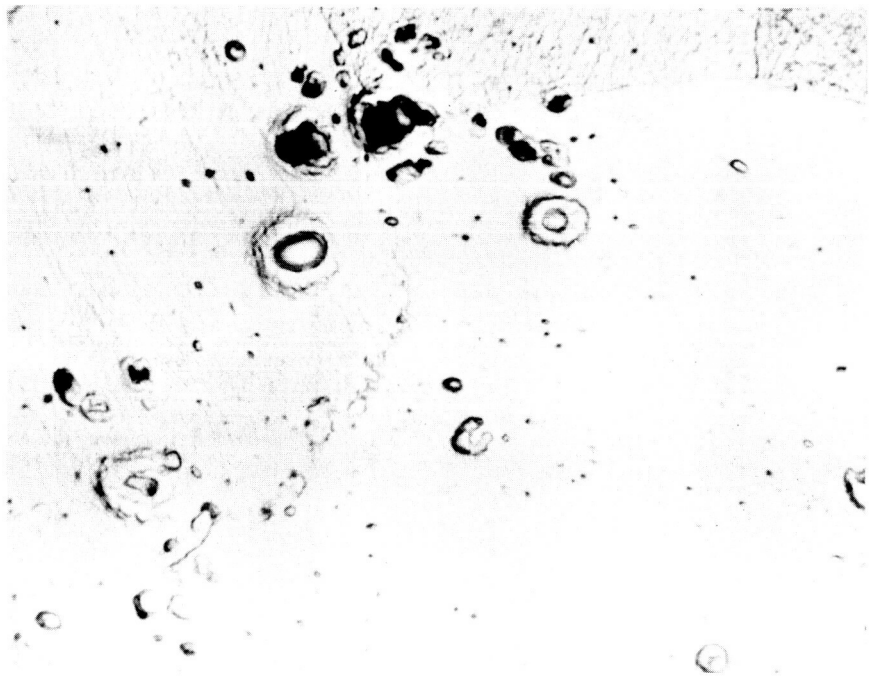

B

2000X

FIGURE 20. 2219-T37 ALUMINUM ALLOY BIAXIALLY STRAINED AT EXPLOSIVE STRAIN RATE TO 10% ELONGATION

(A) (Specimen 37-6-4)

(B) (Specimen 37-6-5) KELLER'S ETCH

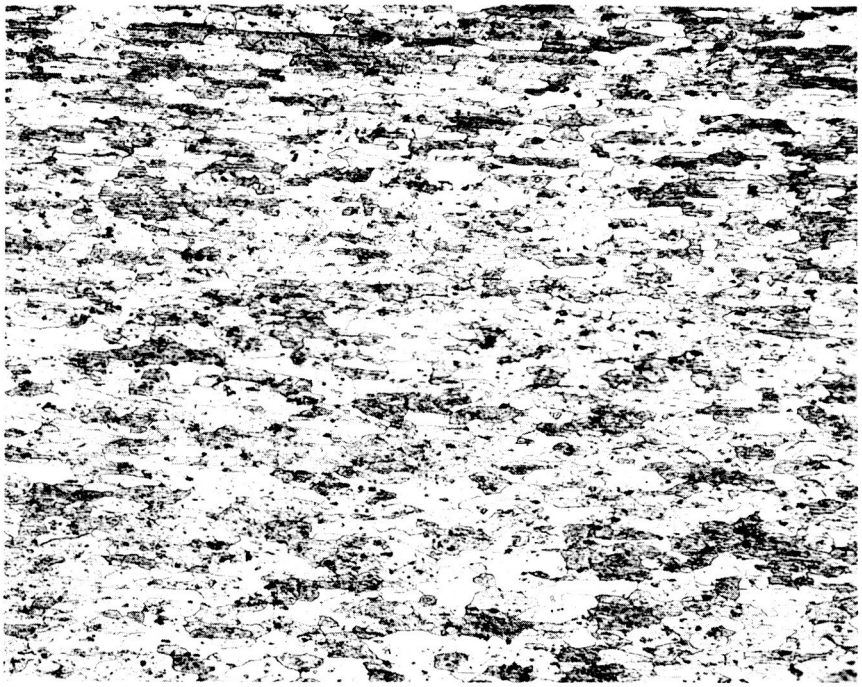

A

100X

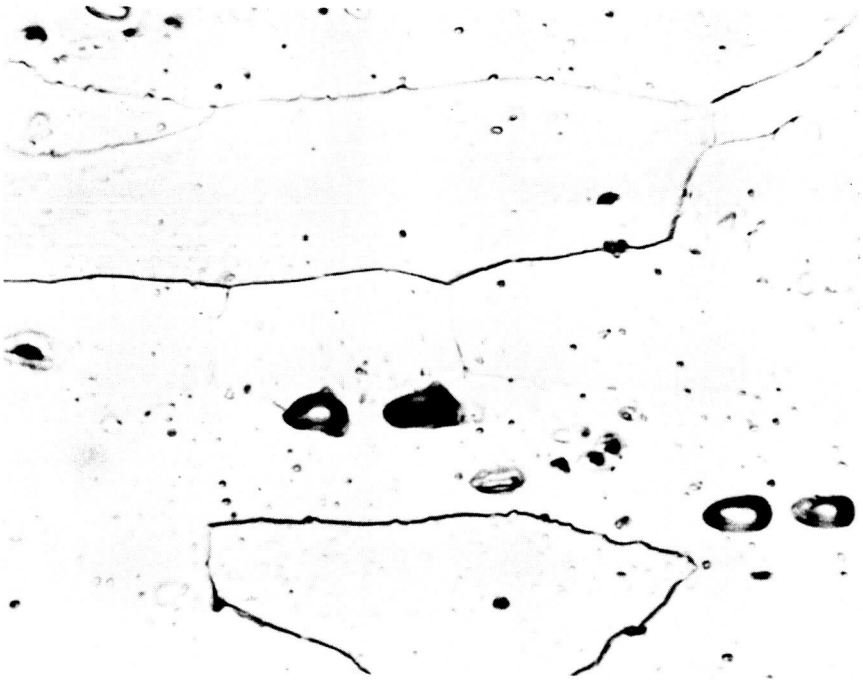

B

2000X

FIGURE 21. 2219-T37 ALUMINUM ALLOY BIAXIALLY STRAINED AT CONVENTIONAL STRAIN RATE TO 10.5% ELONGATION

(A) SPECIMEN NO. 37-11-4
(B) SPECIMEN NO. 37-11-5

KELLER'S ETCH

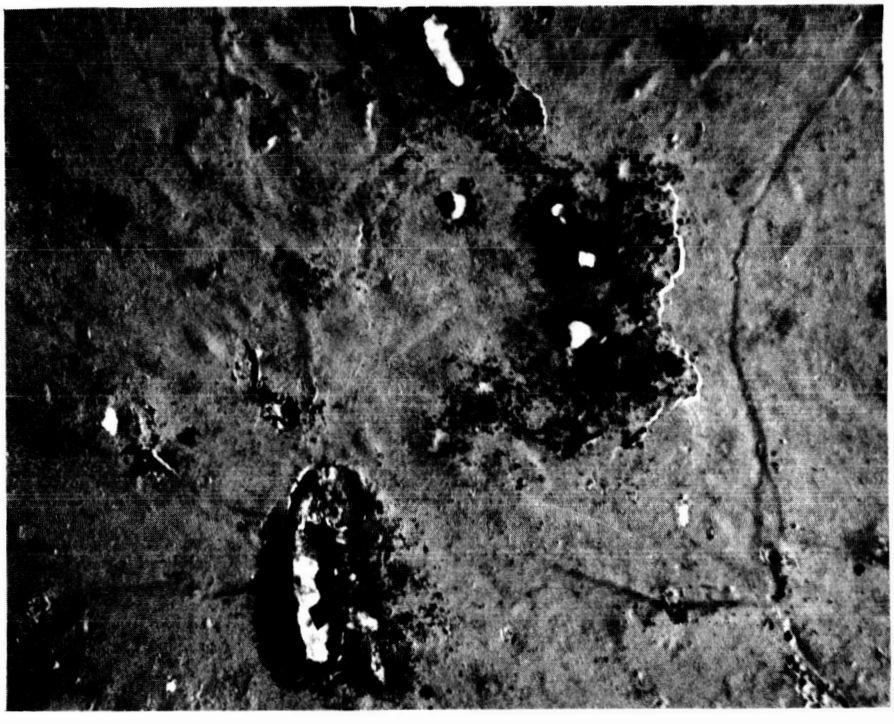

5000X

FIGURE 22. 2219-T37 ALUMINUM ALLOY BIAXIALLY STRAINED AT CONVENTIONAL STRAIN RATE TO 10.5% ELONGATION (Specimen 37-11-5)

KELLER'S ETCH

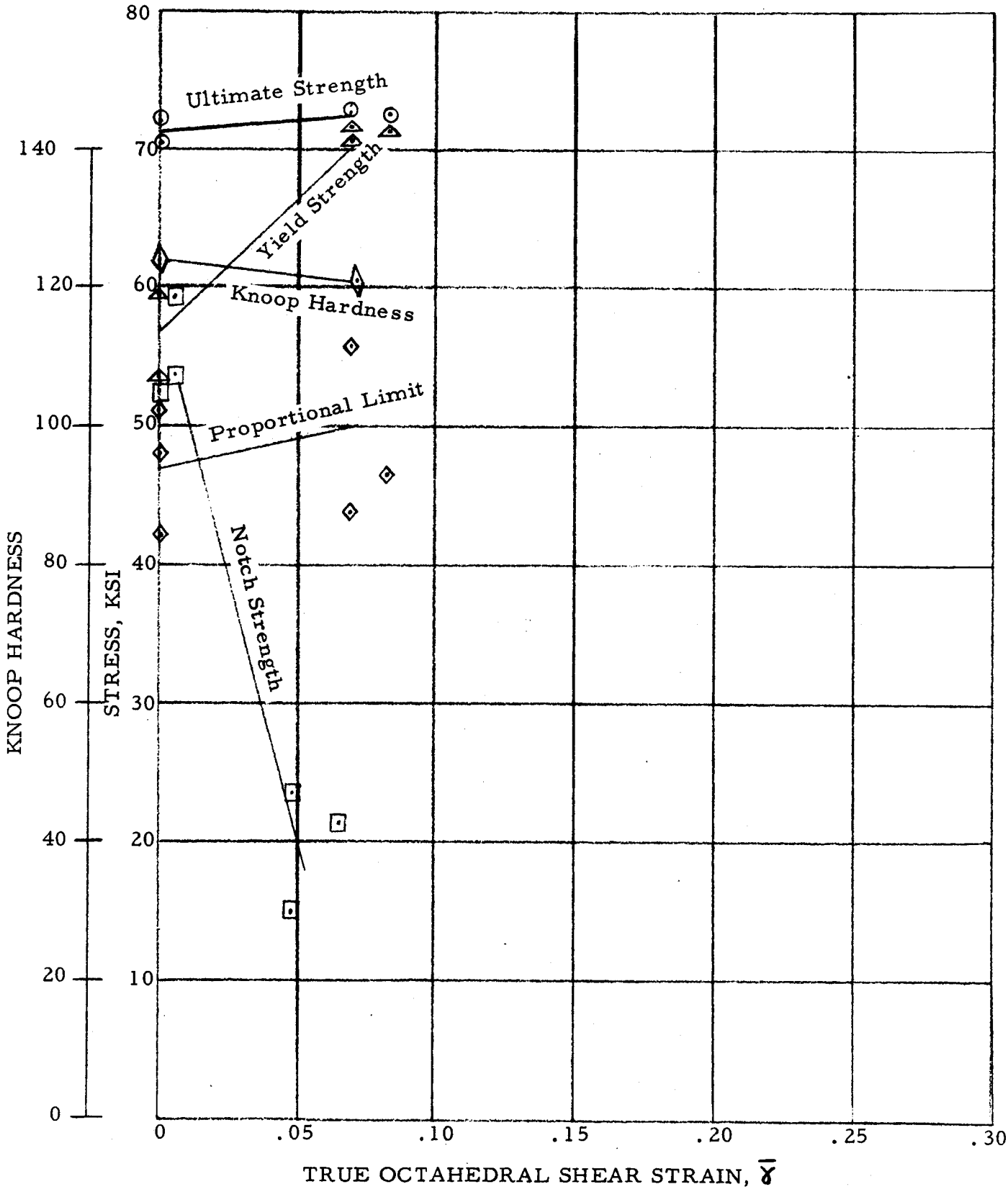

FIGURE 23. MECHANICAL PROPERTIES OF UNWELDED 2219-T87 ALUMINUM AFTER UNIAXIAL PRESTRAINING AT CONVENTIONAL STRAIN RATE

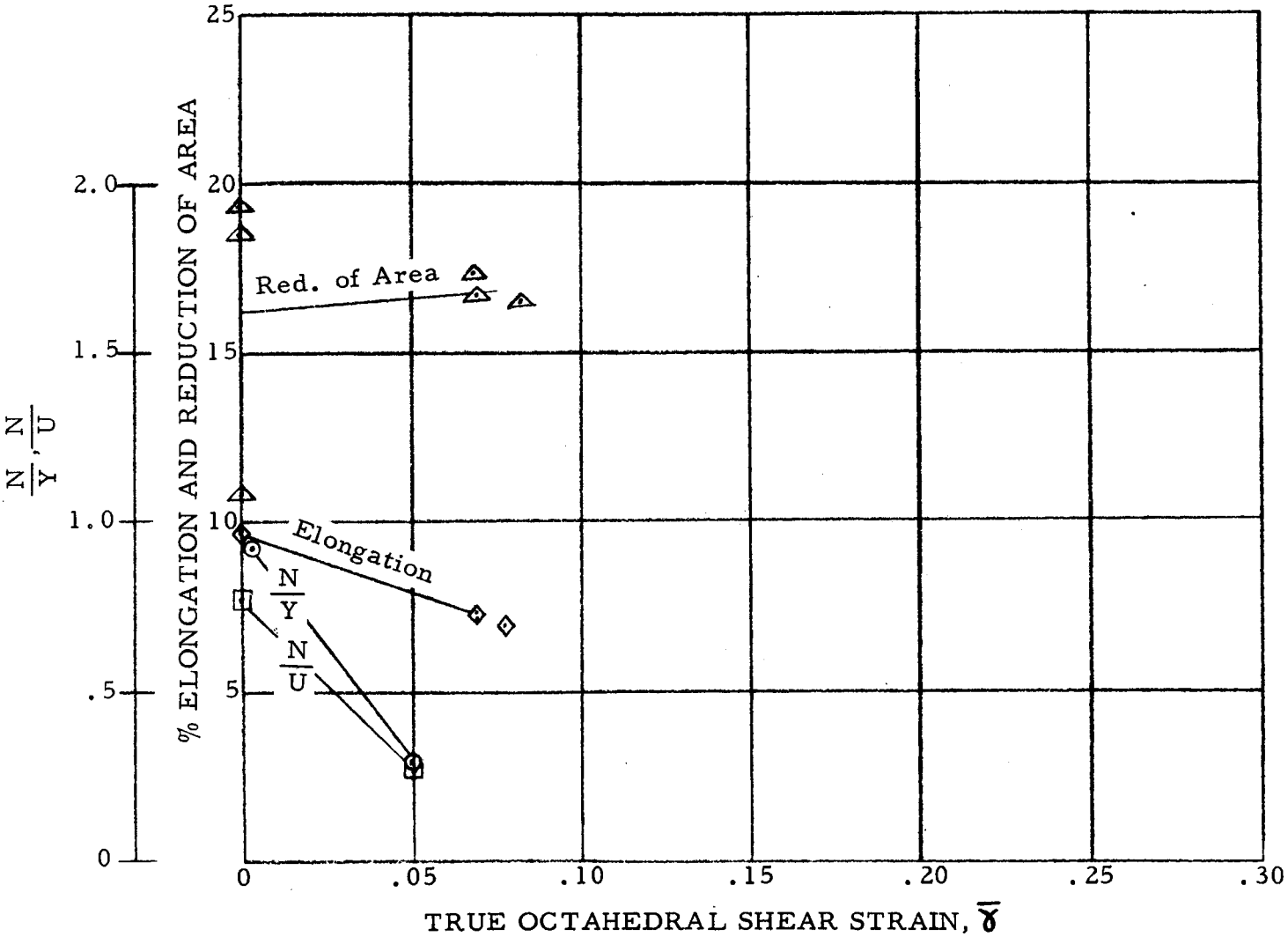

FIGURE 24. MECHANICAL PROPERTIES OF UNWELDED 2219-T87 ALUMINUM AFTER UNIAXIAL PRESTRAINING AT CONVENTIONAL STRAIN RATE

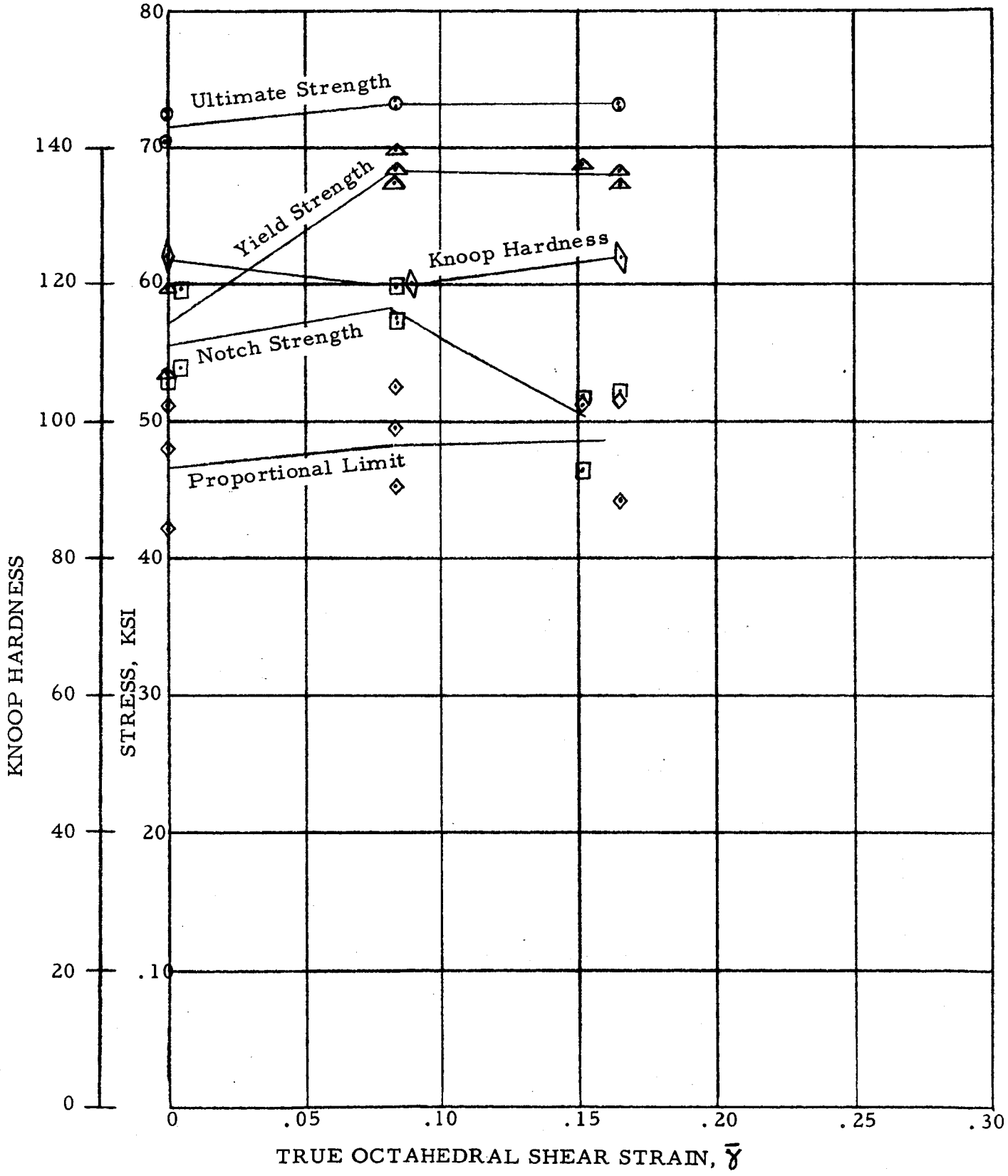

FIGURE 25. MECHANICAL PROPERTIES OF UNWELDED 2219-T87 ALUMINUM AFTER BIAXIAL PRESTRAINING AT CONVENTIONAL STRAIN RATE

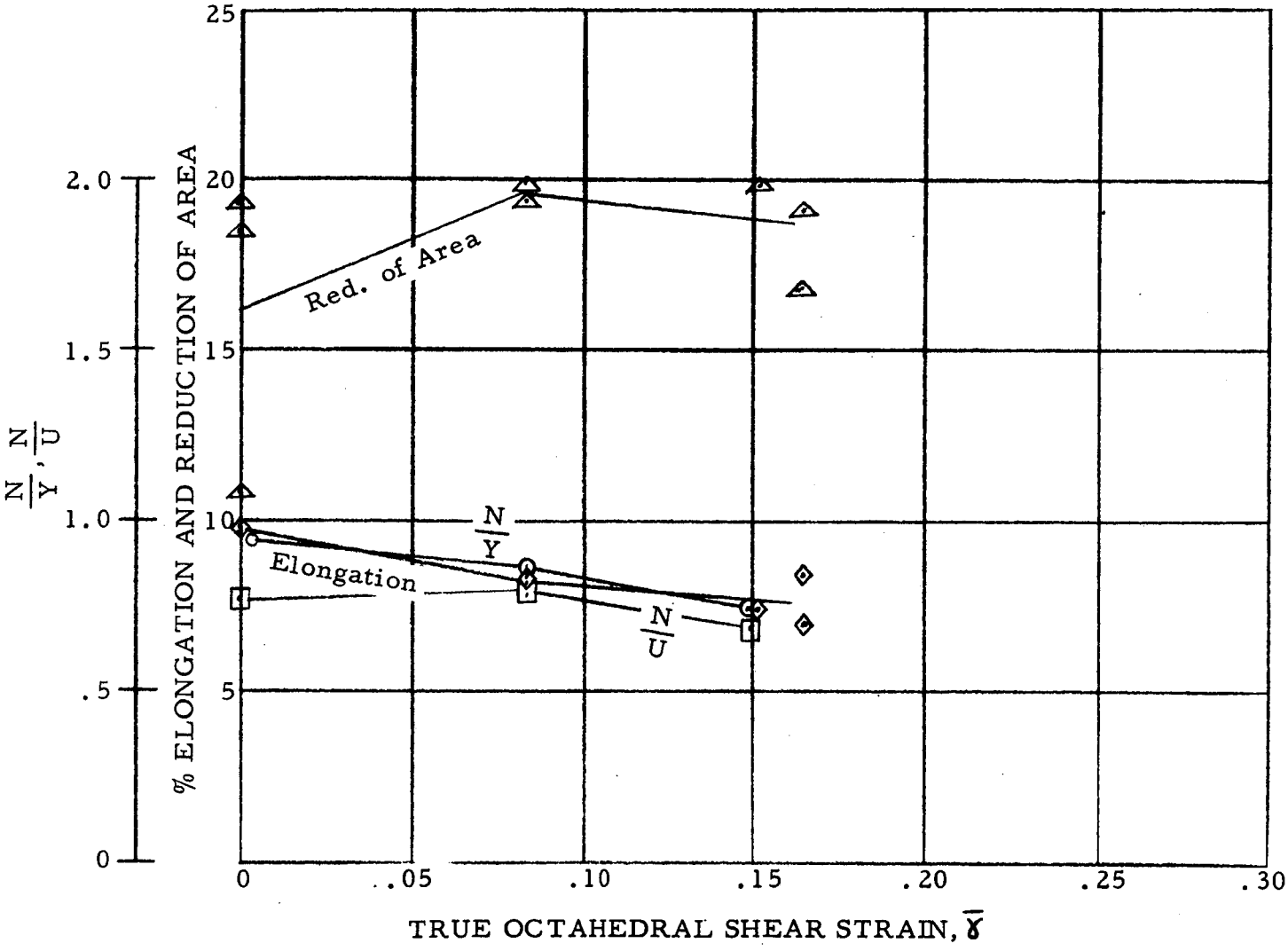

FIGURE 26. MECHANICAL PROPERTIES OF UNWELDED 2219-T87 ALUMINUM AFTER BIAXIAL PRESTRAINING AT CONVENTIONAL STRAIN RATE

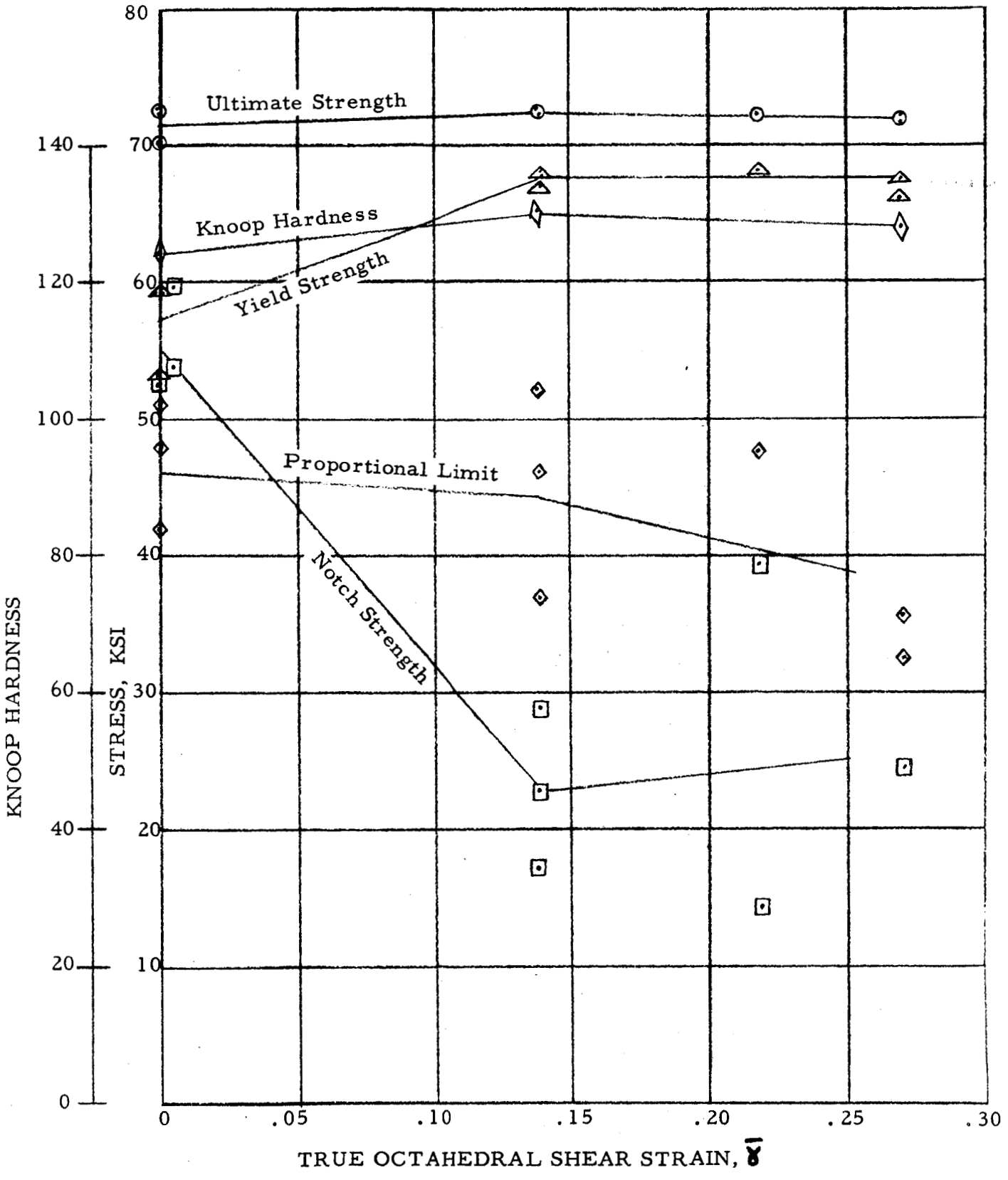

FIGURE 27. MECHANICAL PROPERTIES OF UNWELDED 2219-T87 ALUMINUM AFTER BIAXIAL PRESTRAINING AT EXPLOSIVE STRAIN RATE

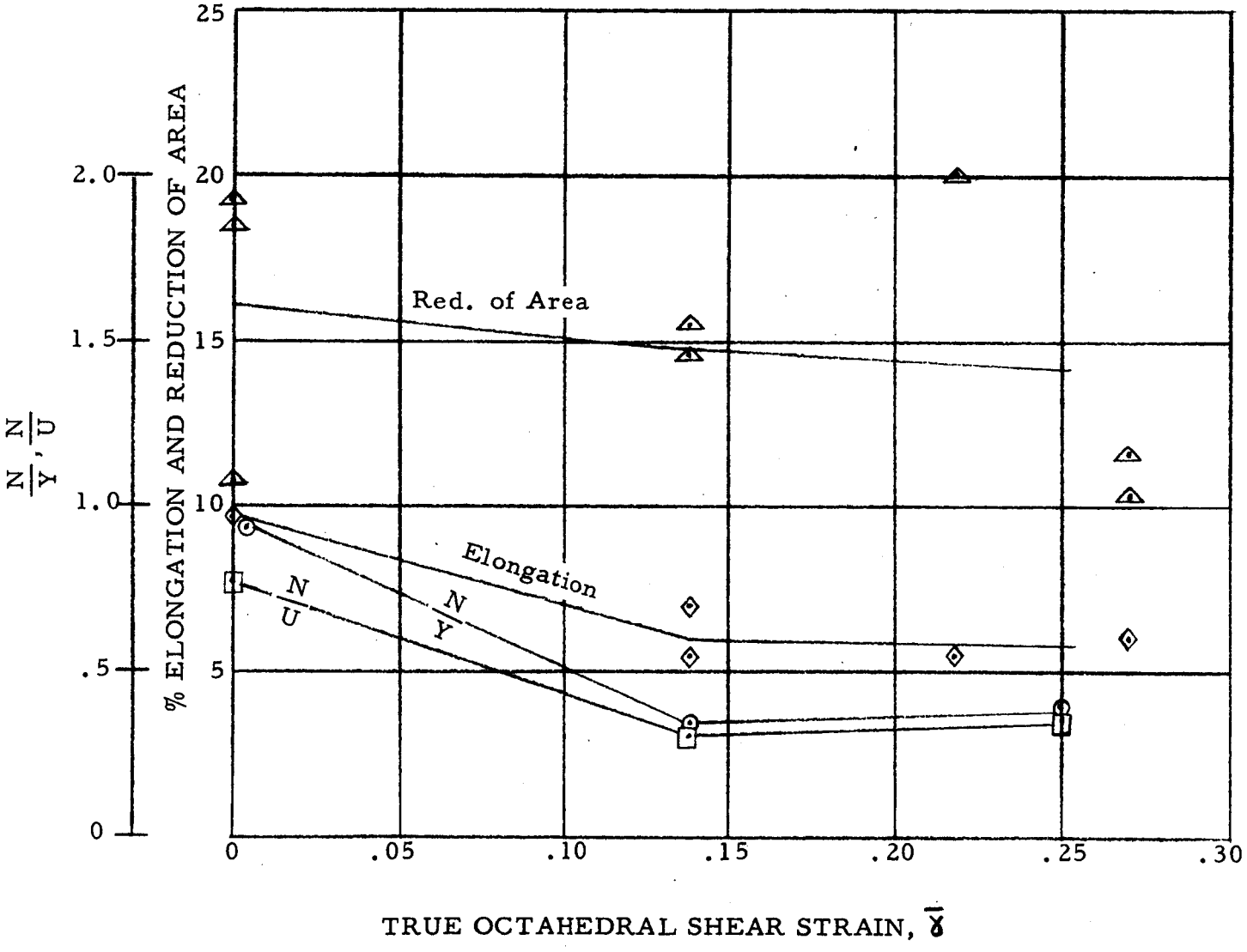

FIGURE 28. MECHANICAL PROPERTIES OF UNWELDED 2219-T87 ALUMINUM AFTER BIAXIAL PRESTRAINING AT EXPLOSIVE STRAIN RATE

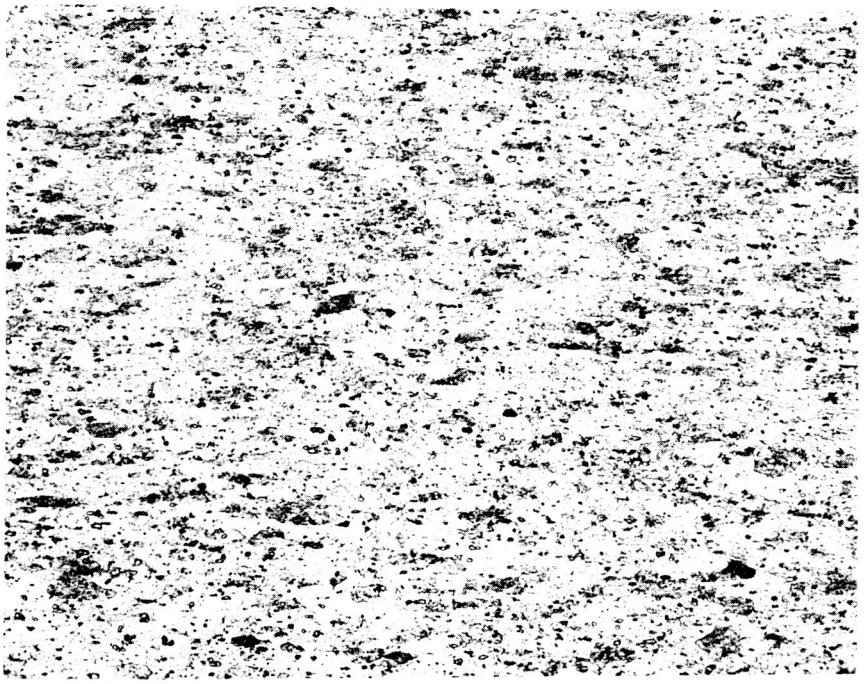

A

100X

B

2000X

FIGURE 29. 2219-T87 ALUMINUM ALLOY UNSTRAINED PARENT METAL (Specimen A85)

KELLER'S ETCH

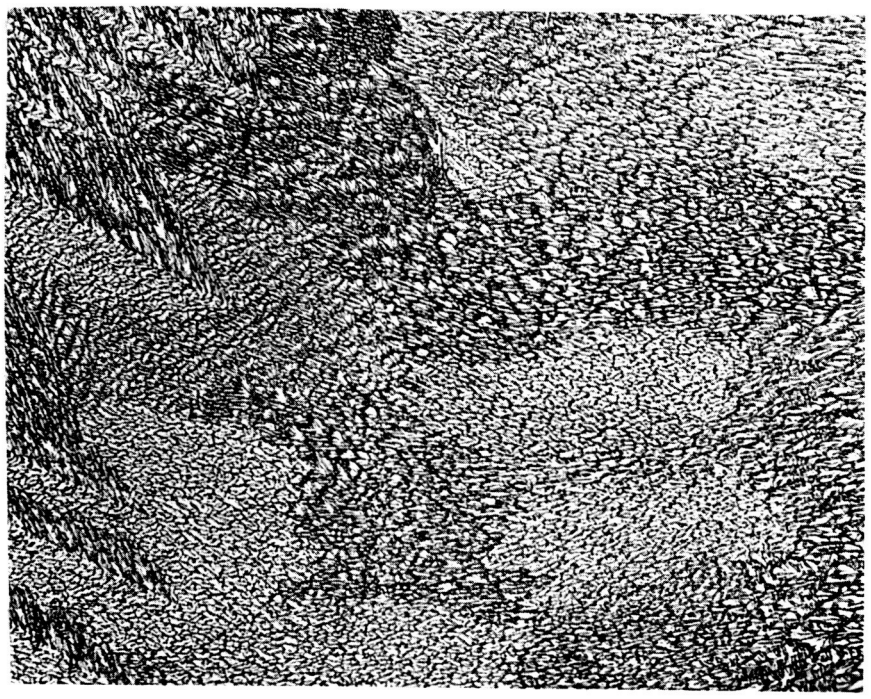

A

100X

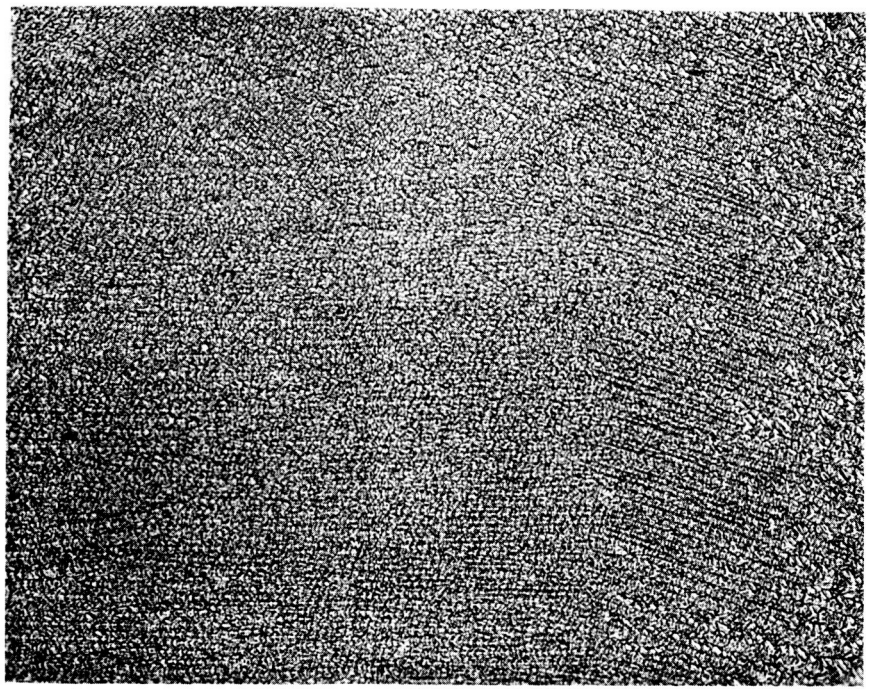

B

100X

FIGURE 30. 2219-T87 ALUMINUM ALLOY WELDED AND UNSTRAINED (Specimen A85)

(A) HEAT-AFFECTED ZONE
(B) WELD METAL

KELLER'S ETCH

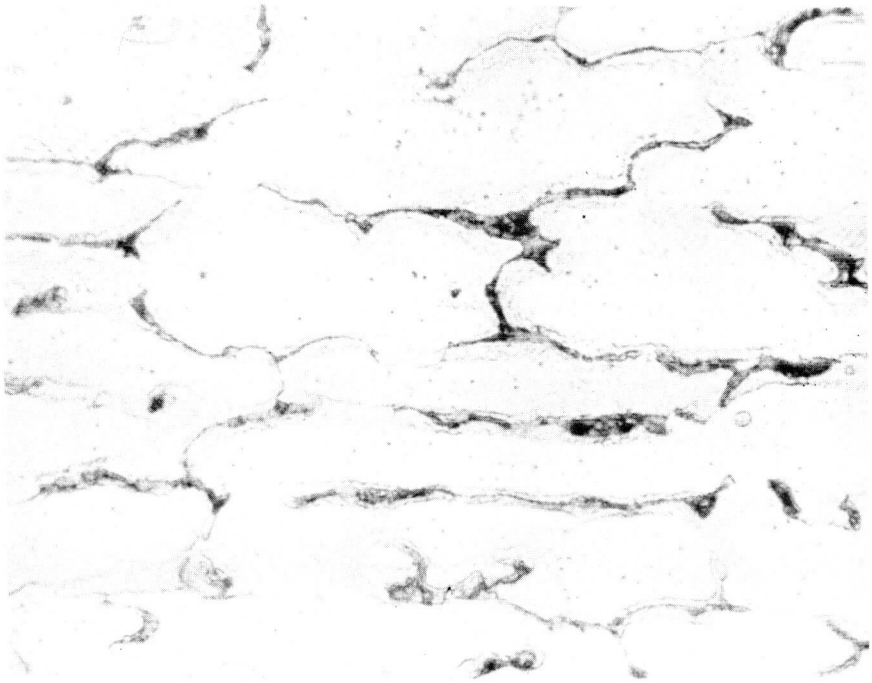

A

2000X

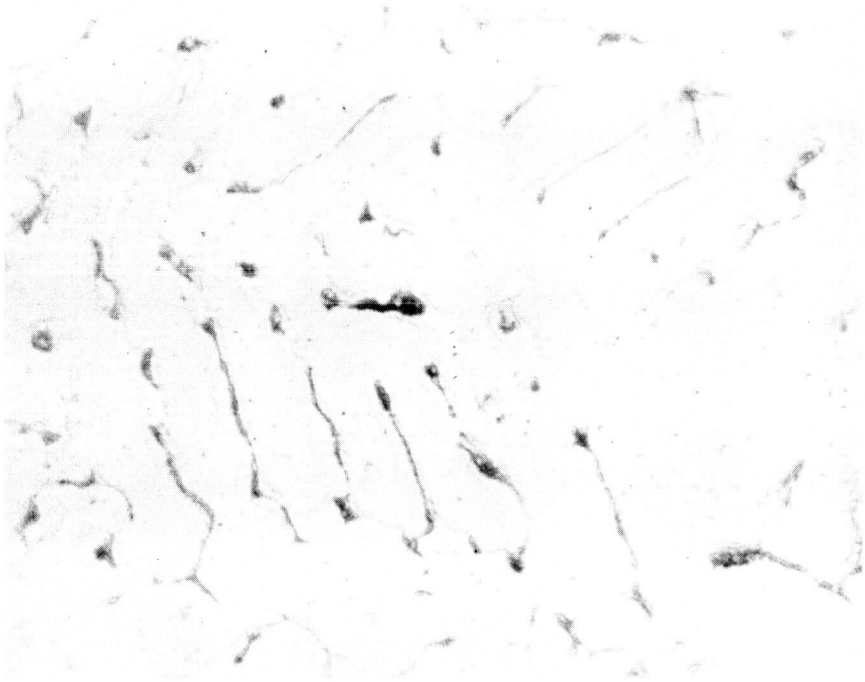

B

2000X

FIGURE 31. 2219-T87 ALUMINUM ALLOY WELDED AND UNSTRAINED (Specimen A85)

(A) HEAT-AFFECTED ZONE
(B) WELD METAL

KELLER'S ETCH

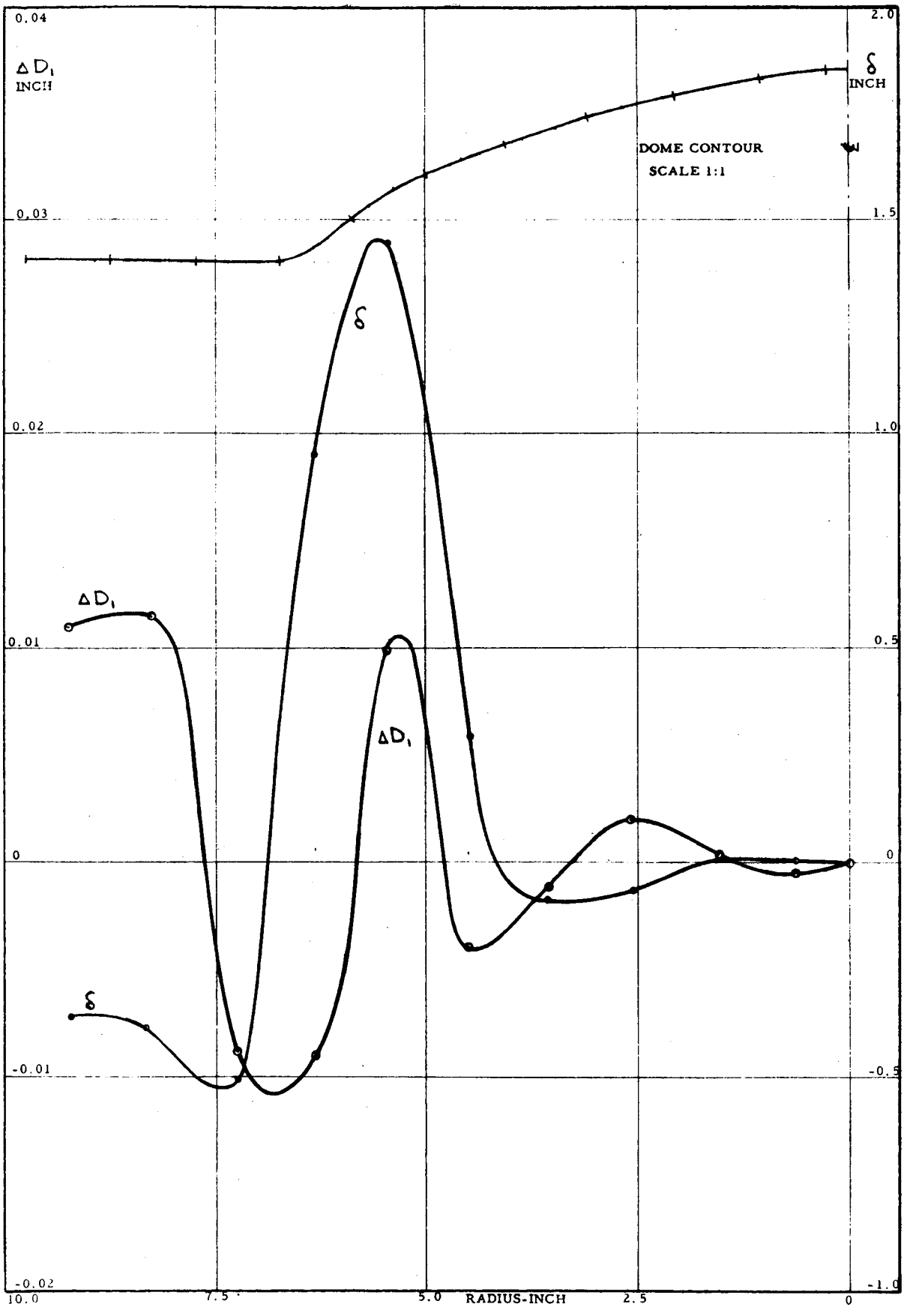

FIGURE 32. MEASURED DEFORMATIONS ΔD_1 AND δ FOR DOME NO. 87-16, EXPLOSIVELY FORMED

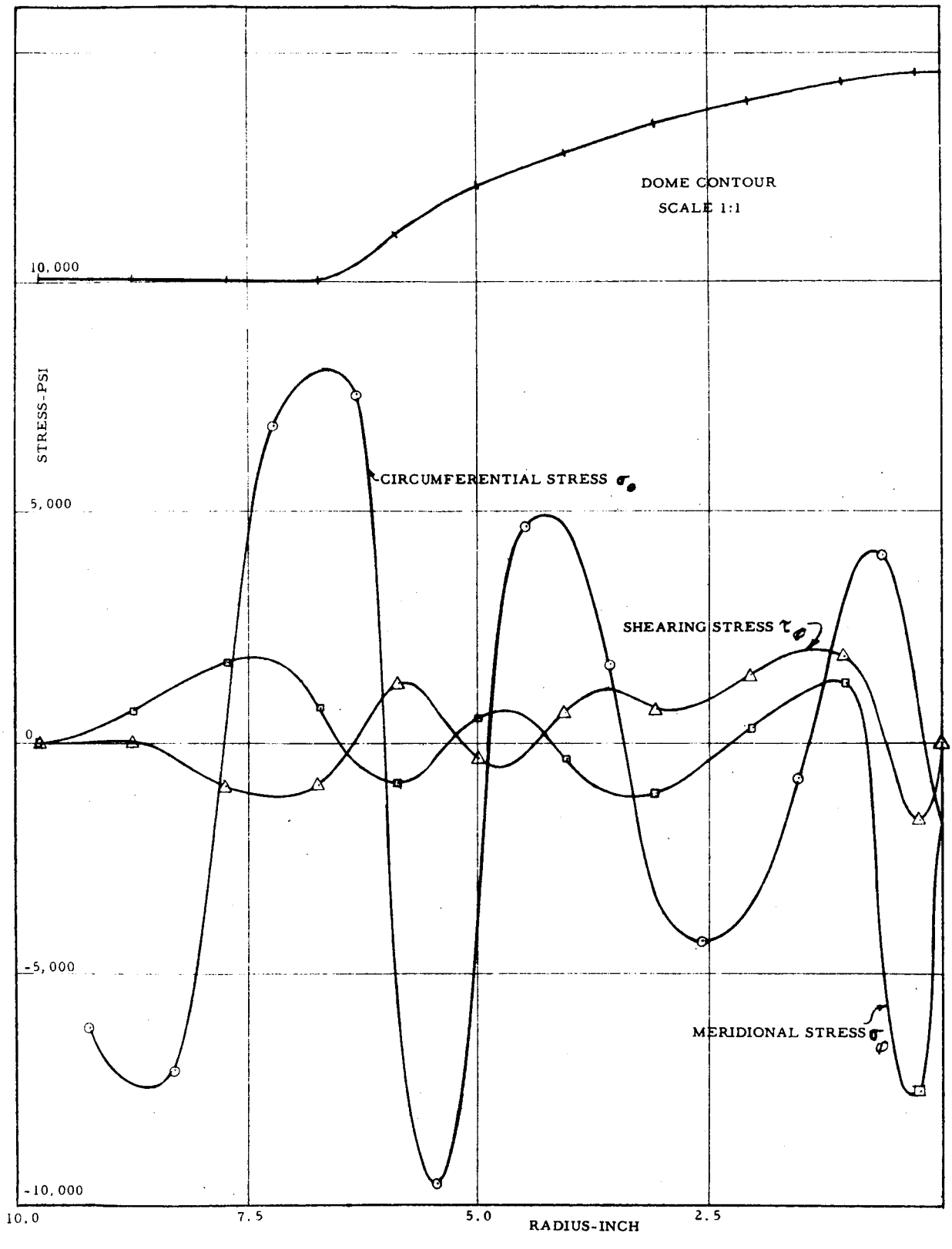

FIGURE 33. CALCULATED NORMAL STRESSES σ_θ AND σ_ϕ AND SHEARING STRESS τ_ϕ IN DOME NO. 87-16, EXPLOSIVELY FORMED

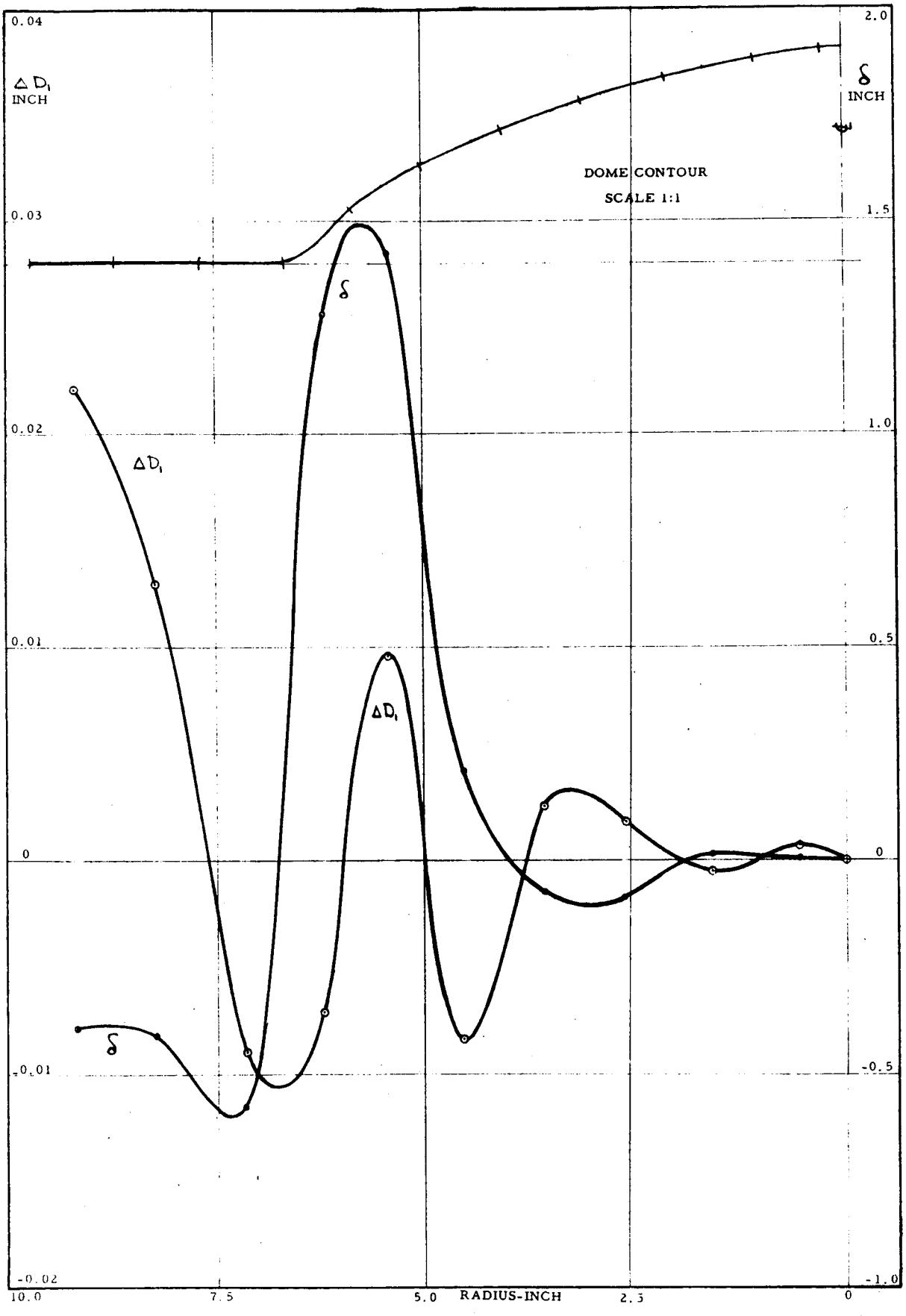

FIGURE 34. MEASURED DEFORMATIONS ΔD_1 AND δ FOR DOME NO. 87-17, EXPLOSIVELY FORMED

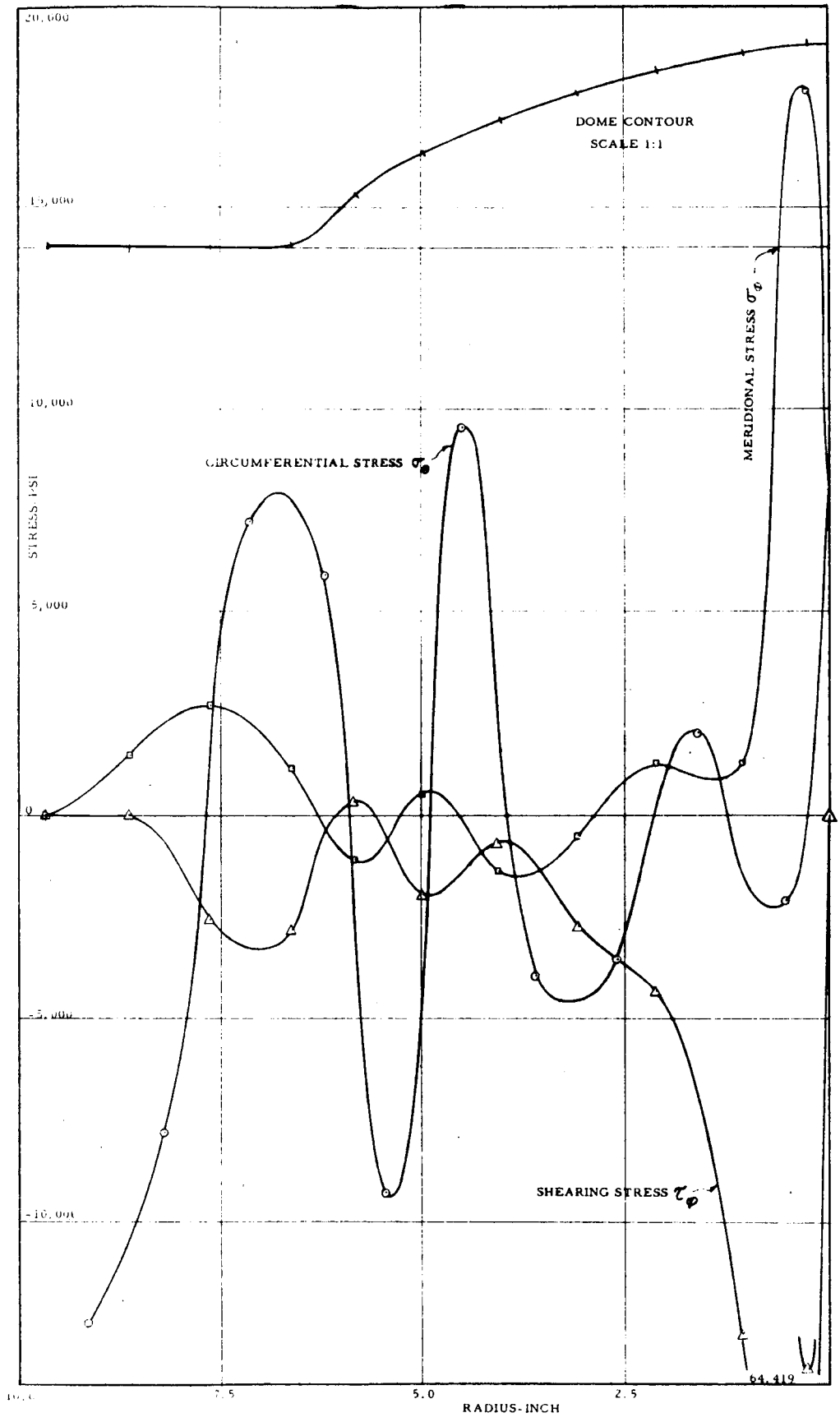

FIGURE 35. CALCULATED NORMAL STRESSES σ_φ AND σ_θ AND SHEARING STRESS $\tau_{\varphi\theta}$ IN DOME NO. 87-17, EXPLOSIVELY FORMED

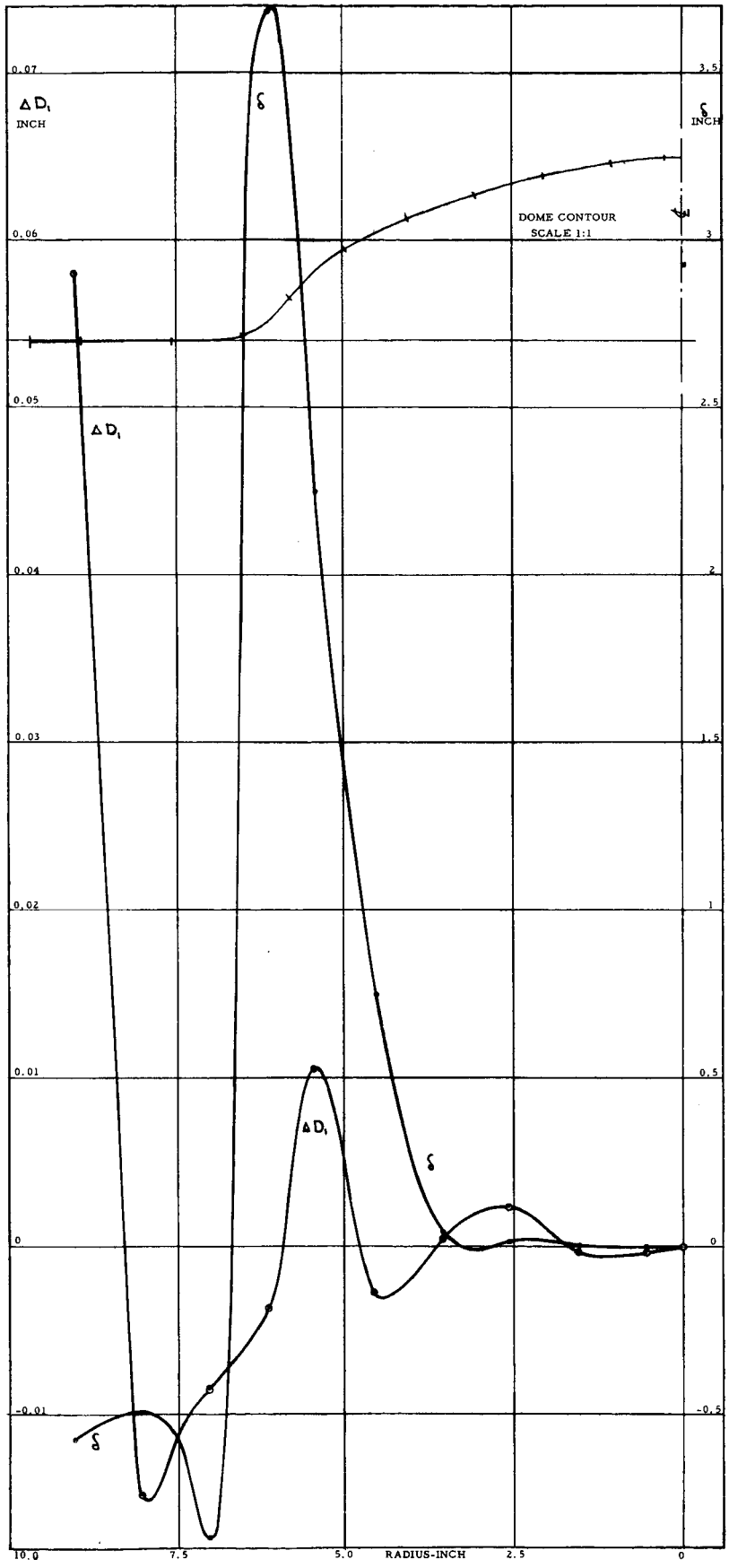

FIGURE 36. MEASURED DEFORMATIONS ΔD_i AND δ FOR DOME NO. 87-13, HYDRAULICALLY FORMED

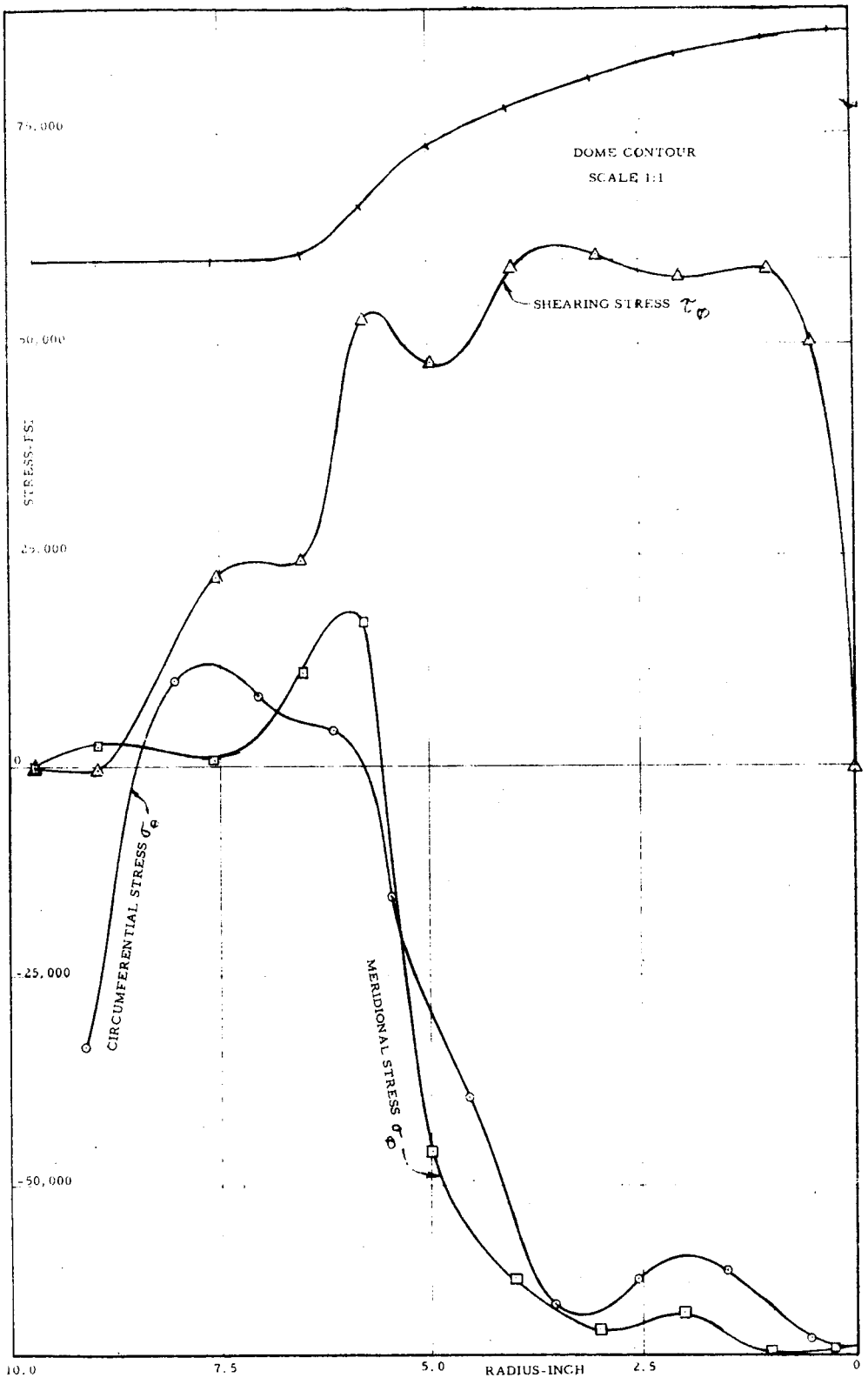

FIGURE 37. CALCULATED NORMAL STRESSES σ_θ AND σ_ϕ AND SHEARING STRESS τ_ϕ IN DOME NO. 87-13, HYDRAULICALLY FORMED

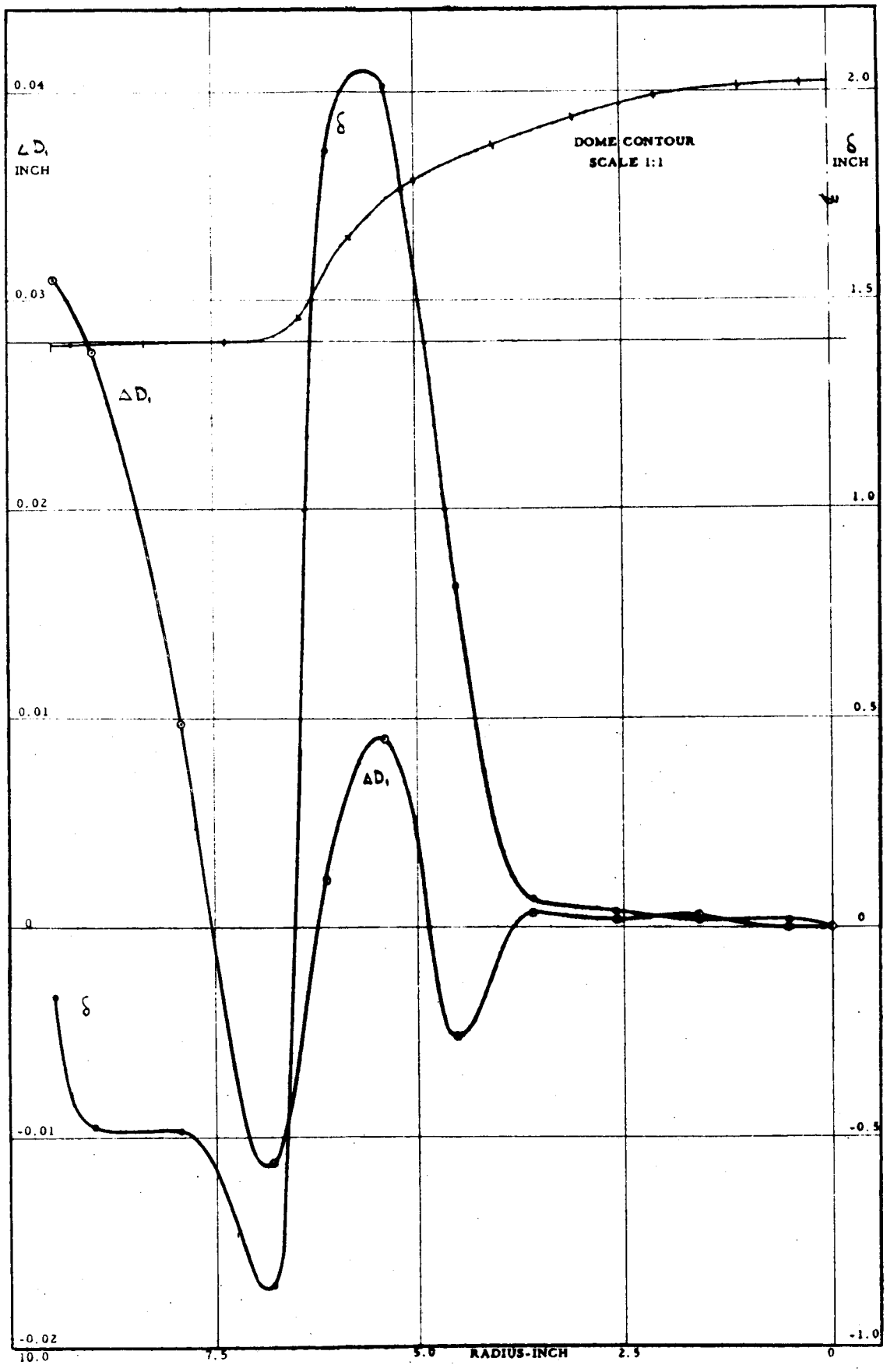

FIGURE 38. MEASURED DEFORMATIONS ΔD_1 AND δ FOR DOME NO. 87-15, HYDRAULICALLY FORMED

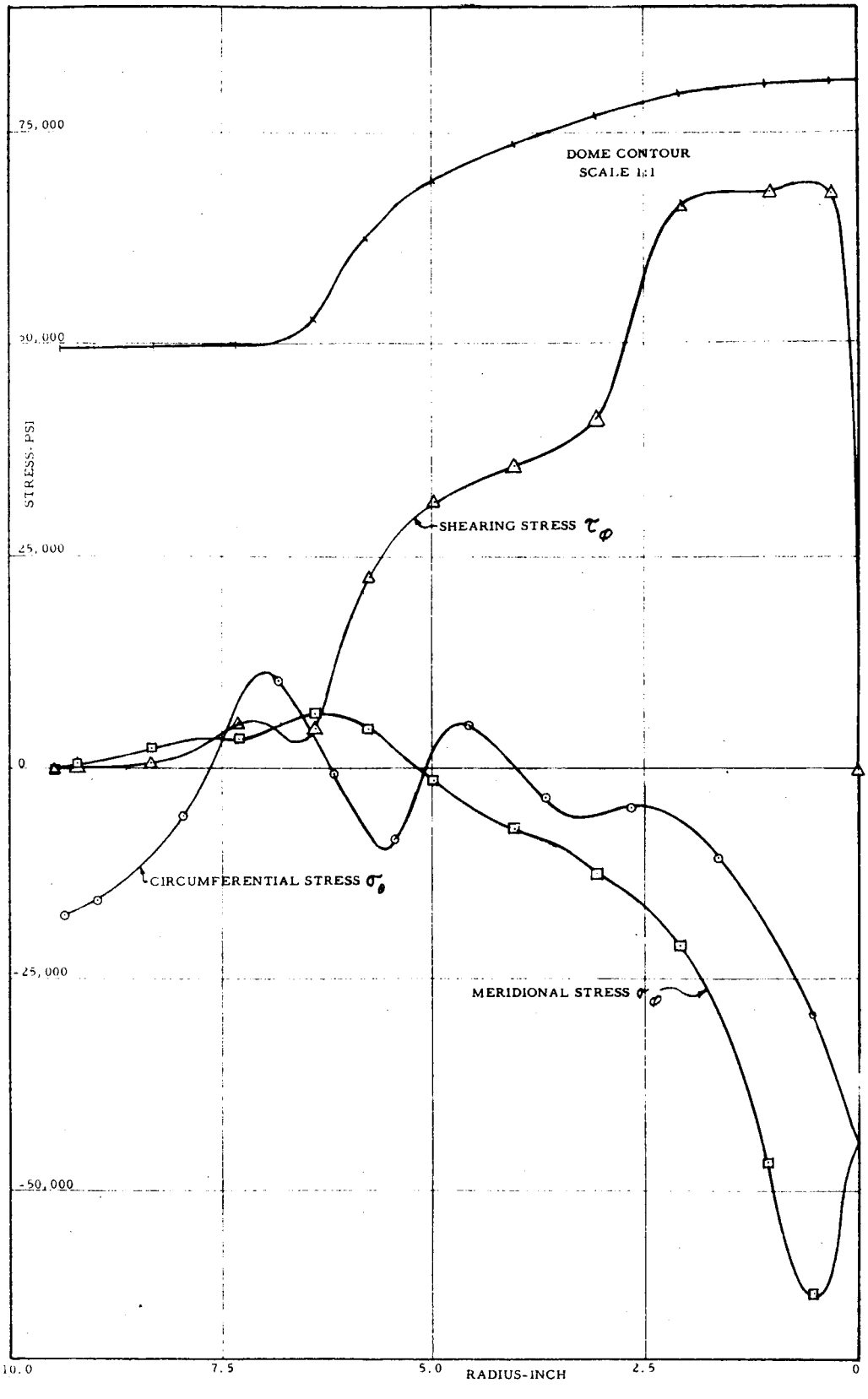

FIGURE 39. CALCULATED NORMAL STRESSES σ_θ AND σ_φ AND SHEARING STRESS τ_φ IN DOME NO. 87-15, HYDRAULICALLY FORMED

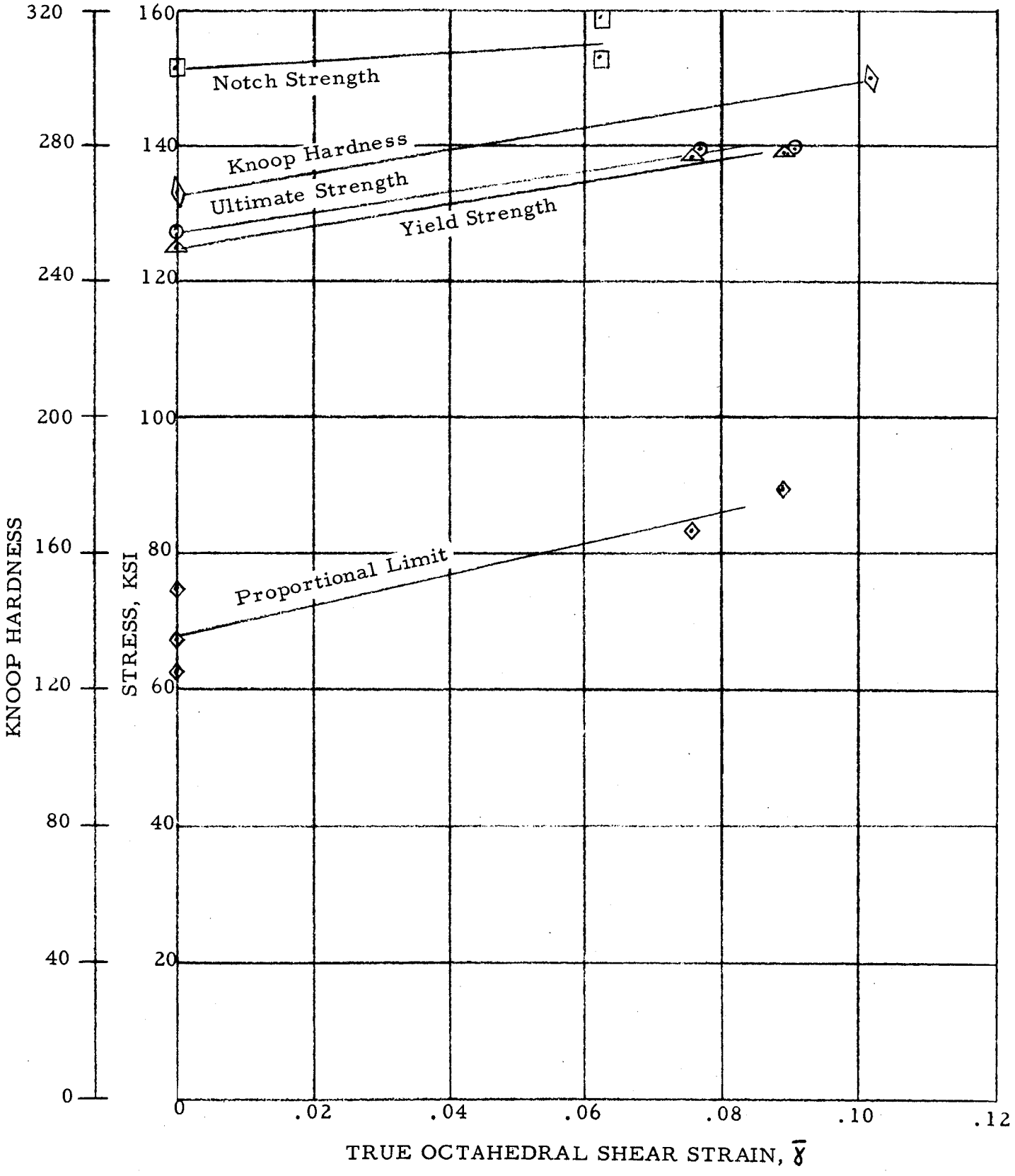

FIGURE 40. MECHANICAL PROPERTIES OF UNWELDED 5Al-2.5Sn TITANIUM AFTER UNIAXIAL PRESTRAINING AT CONVENTIONAL STRAIN RATE

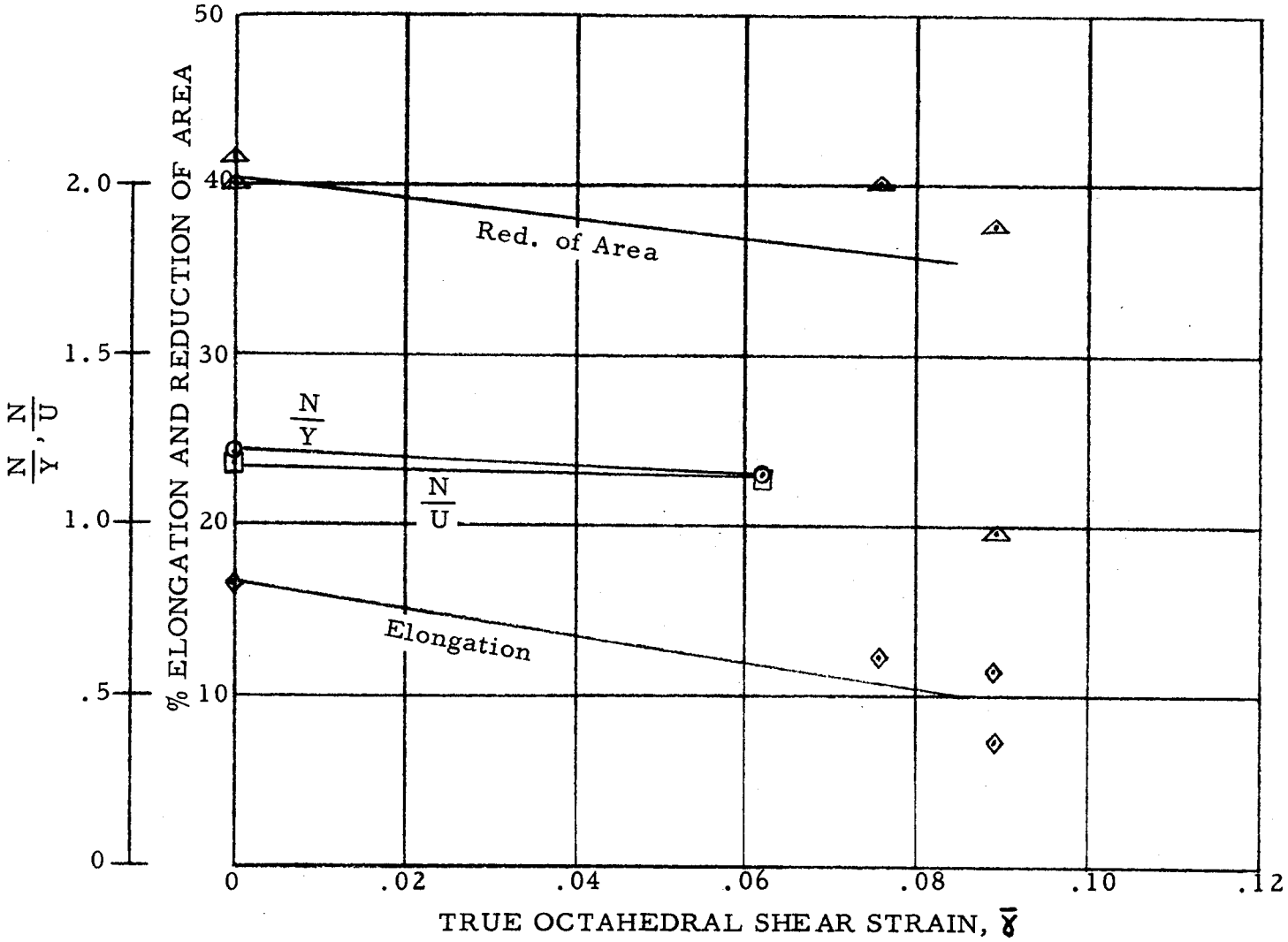

FIGURE 41. MECHANICAL PROPERTIES OF UNWELDED 5Al-2.5Sn TITANIUM AFTER UNIAXIAL PRESTRAINING AT CONVENTIONAL STRAIN RATE

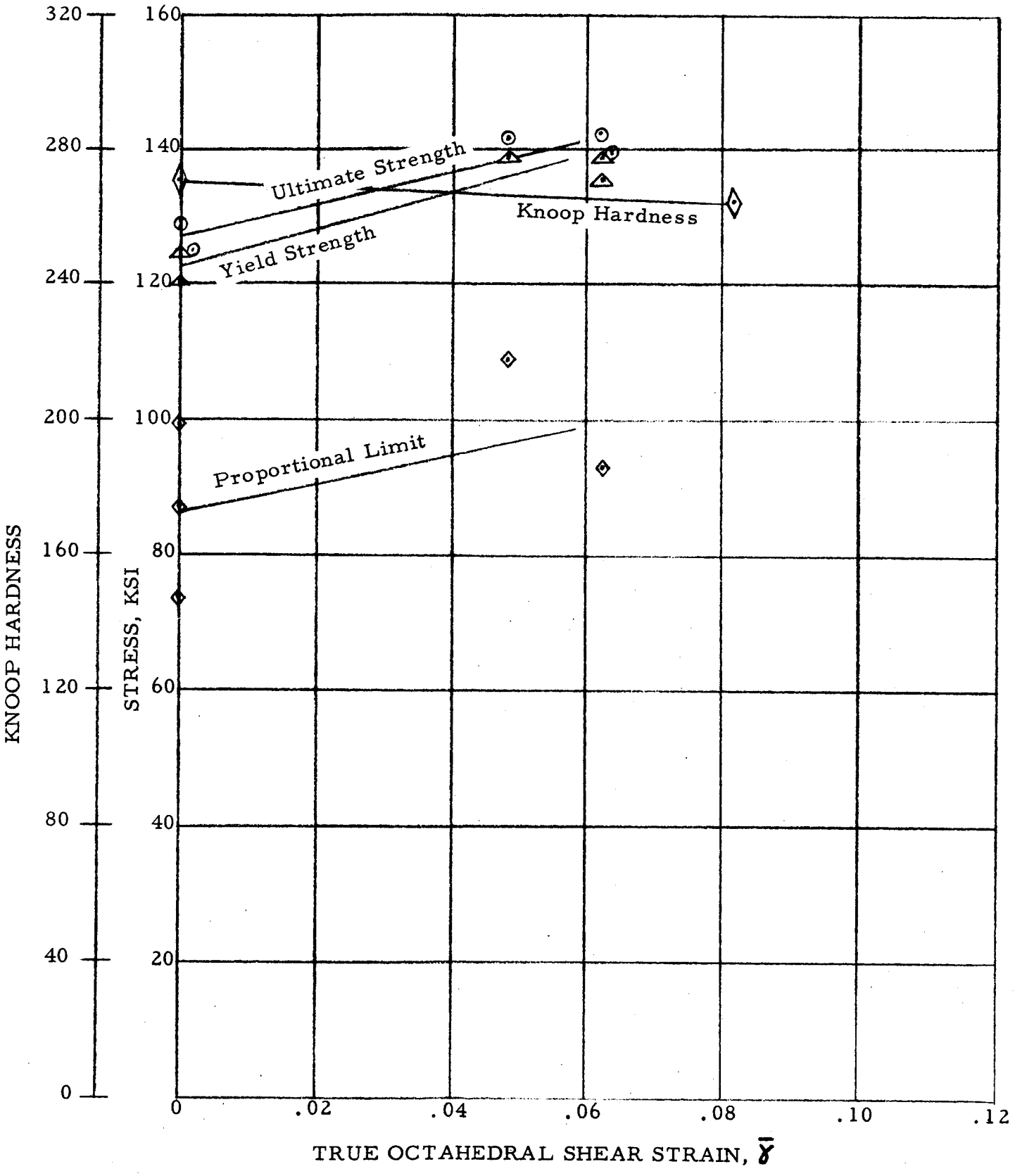

FIGURE 42. MECHANICAL PROPERTIES OF WELDED 5Al-2.5Sn TITANIUM AFTER UNIAXIAL PRESTRAINING AT CONVENTIONAL STRAIN RATE

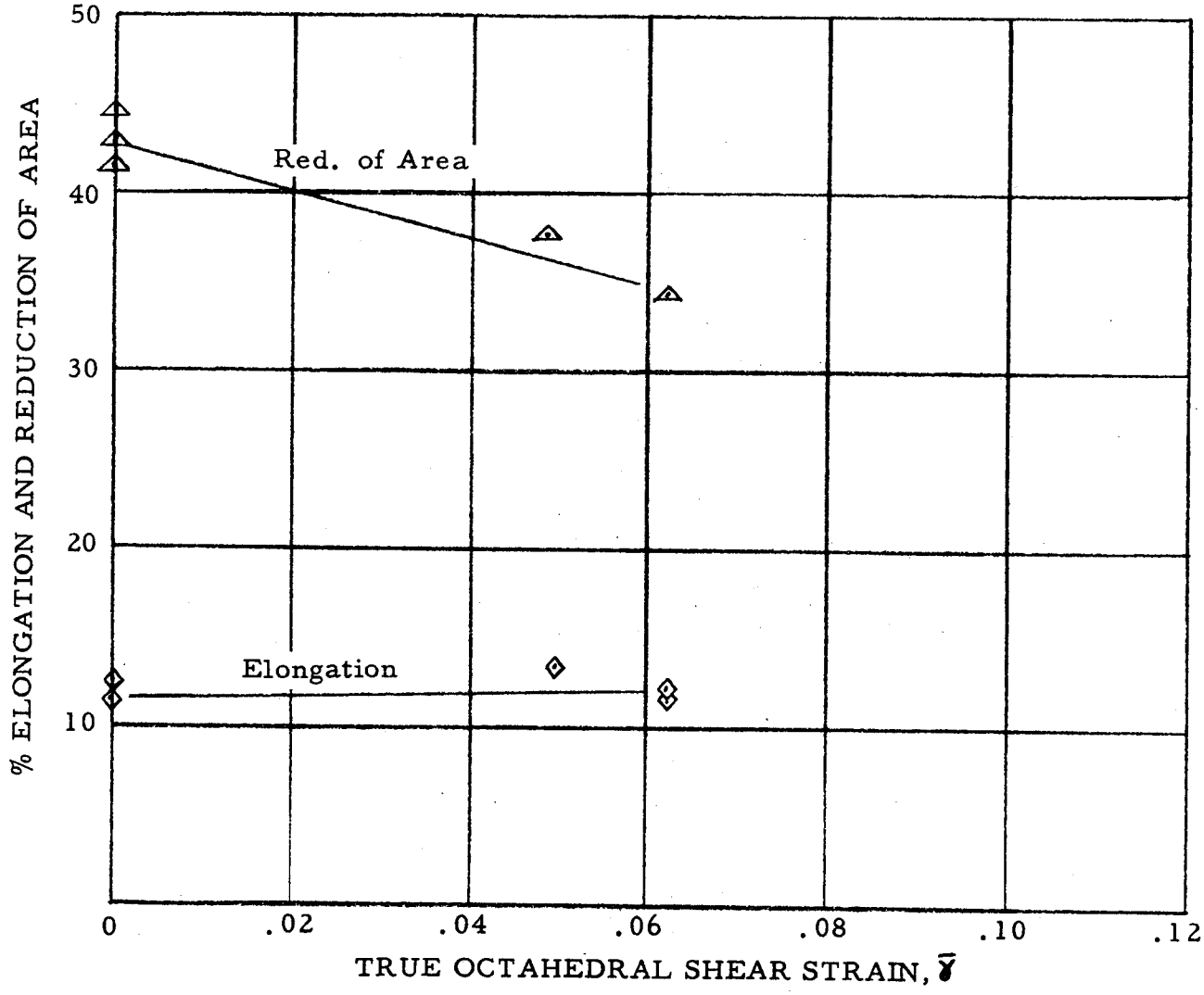

FIGURE 43. MECHANICAL PROPERTIES OF WELDED 5Al-2.5Sn TITANIUM AFTER UNIAXIAL PRESTRAINING AT CONVENTIONAL STRAIN RATE

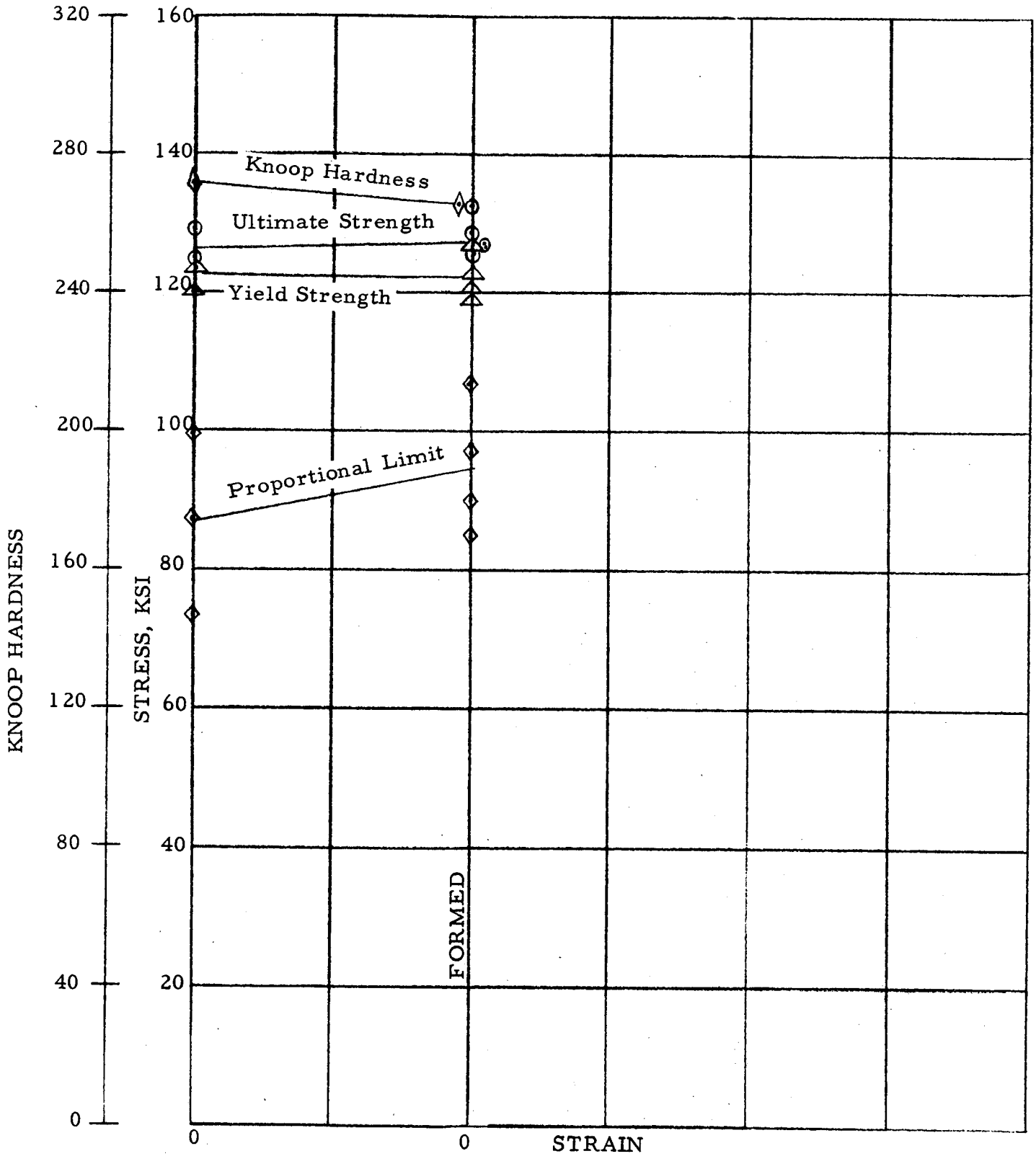

FIGURE 44. MECHANICAL PROPERTIES OF WELDED 5Al-2.5Sn TITANIUM AFTER BIAXIAL FORMING AT CONVENTIONAL RATE

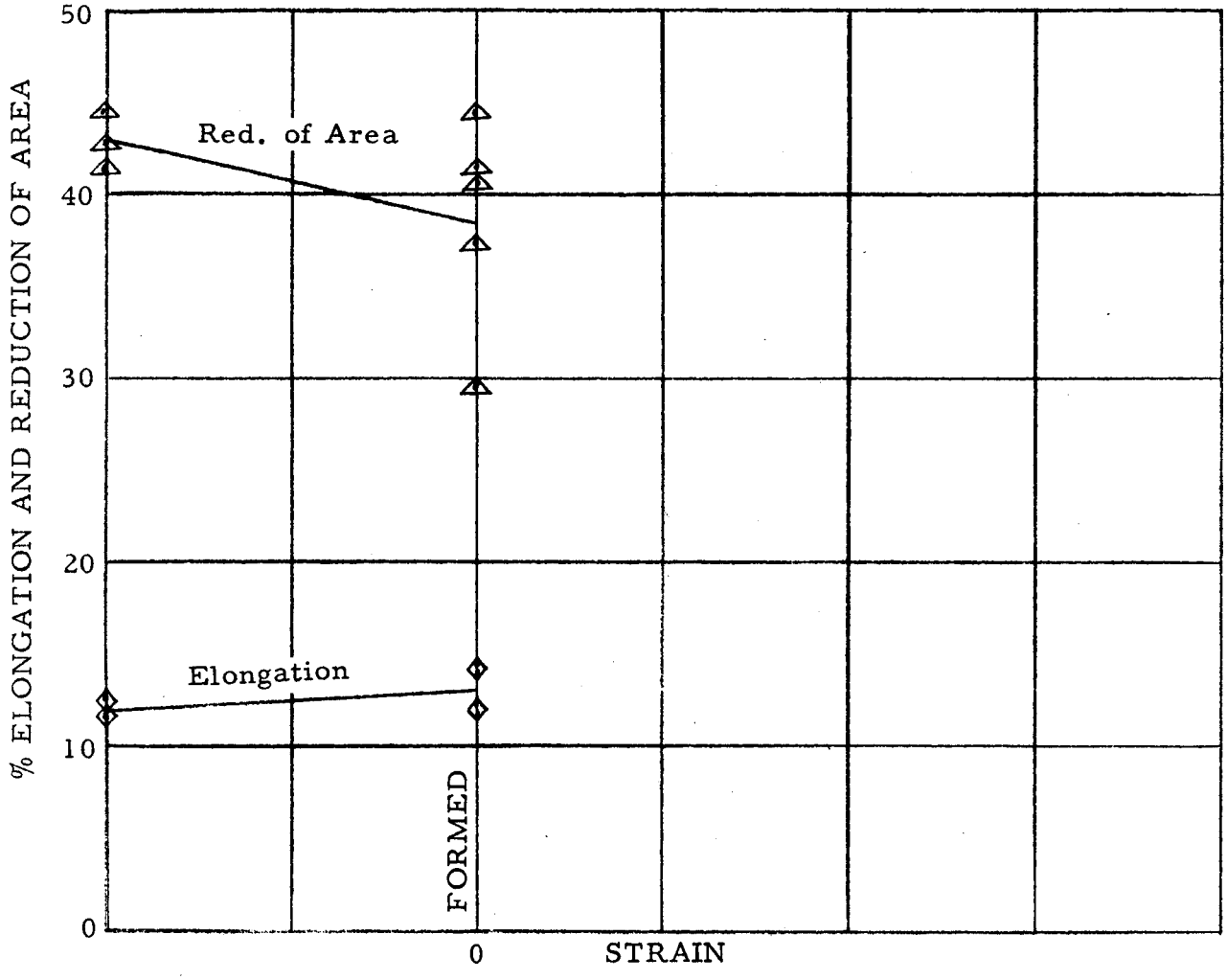

FIGURE 45. MECHANICAL PROPERTIES OF WELDED 5Al-2.5Sn TITANIUM AFTER BIAXIAL FORMING AT CONVENTIONAL RATE

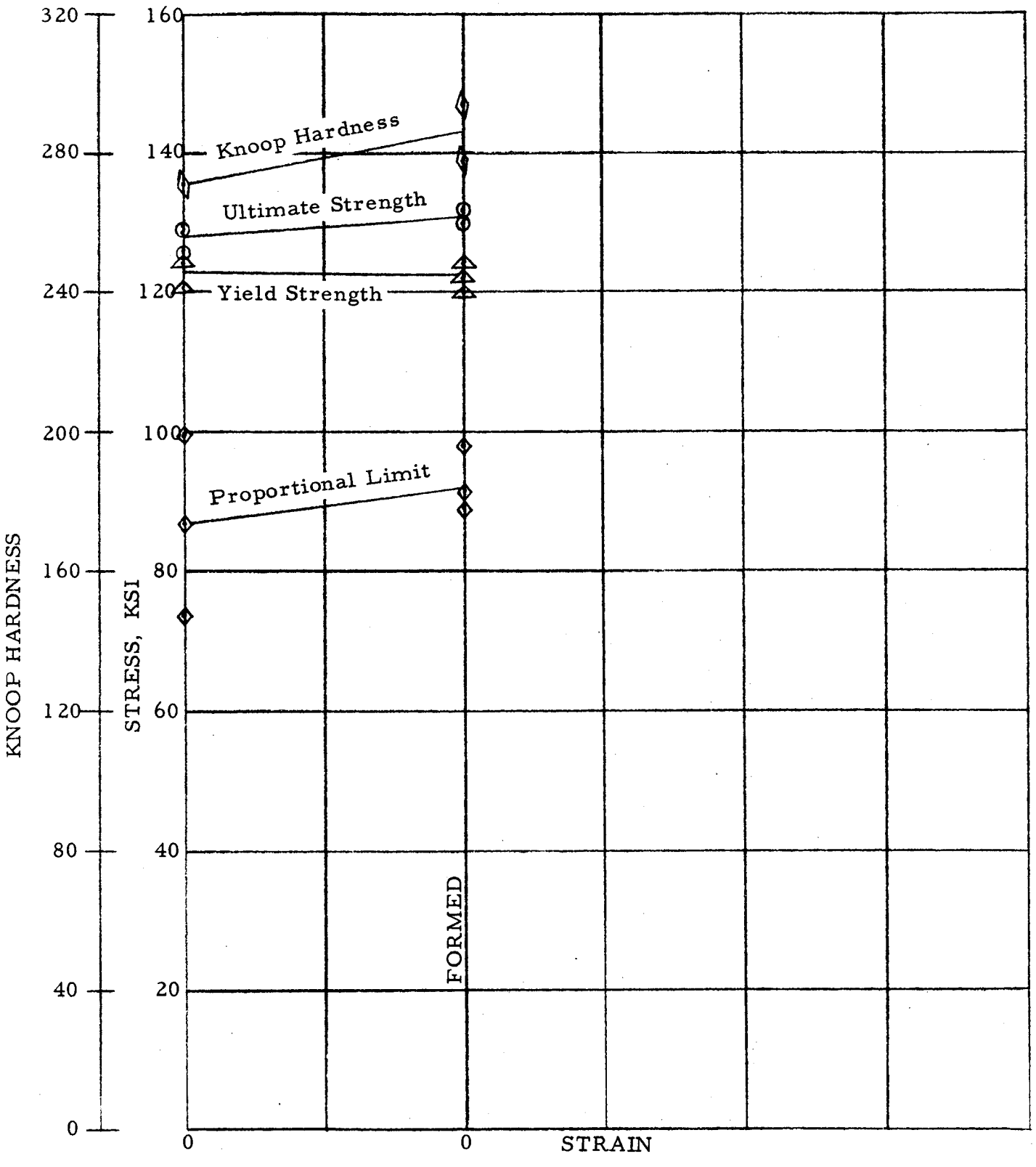

FIGURE 46. MECHANICAL PROPERTIES OF WELDED 5Al-2.5Sn TITANIUM AFTER BIAXIAL FORMING AT EXPLOSIVE RATE

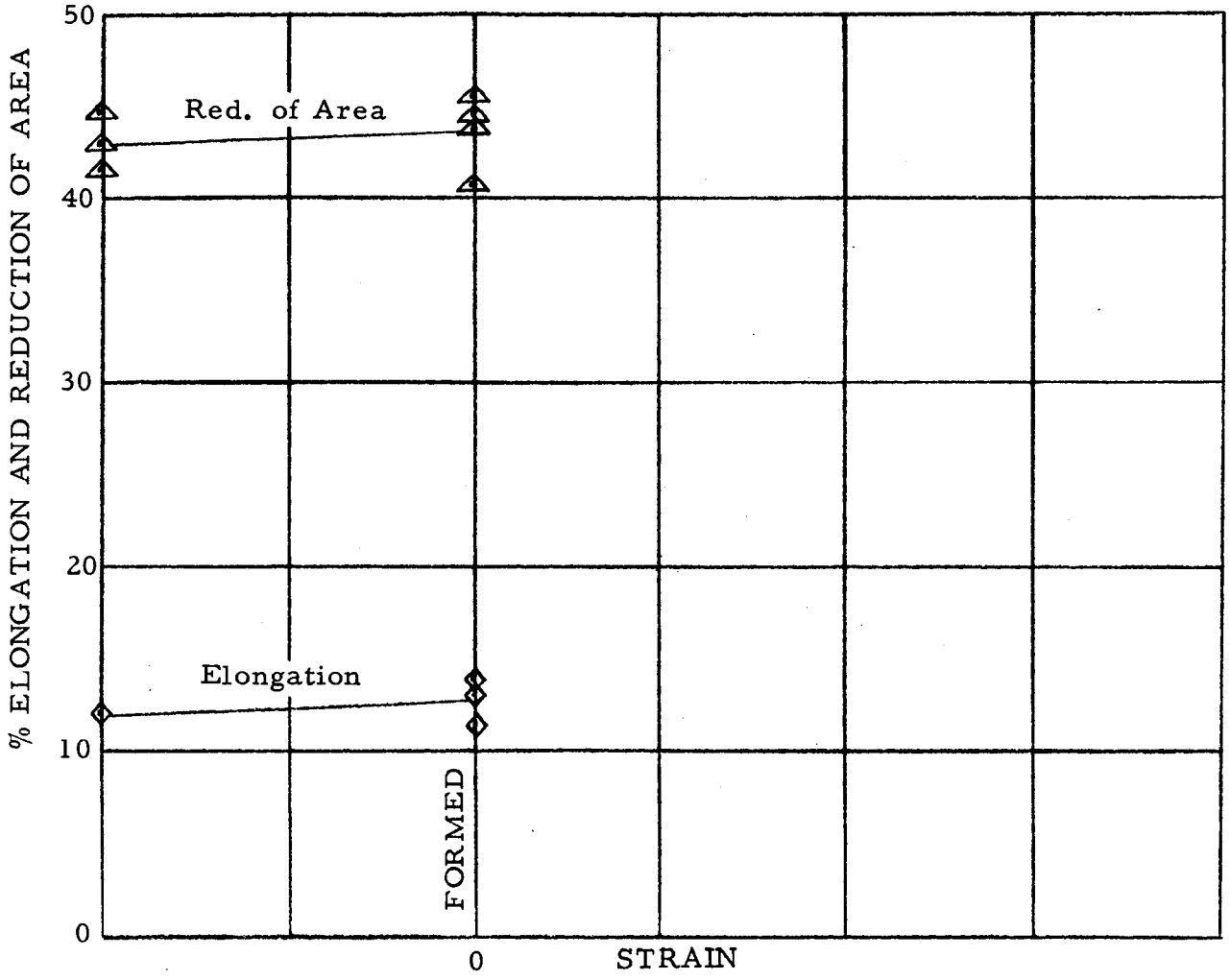

FIGURE 47. MECHANICAL PROPERTIES OF WELDED 5Al-2.5Sn TITANIUM AFTER BIAXIAL FORMING AT EXPLOSIVE RATE

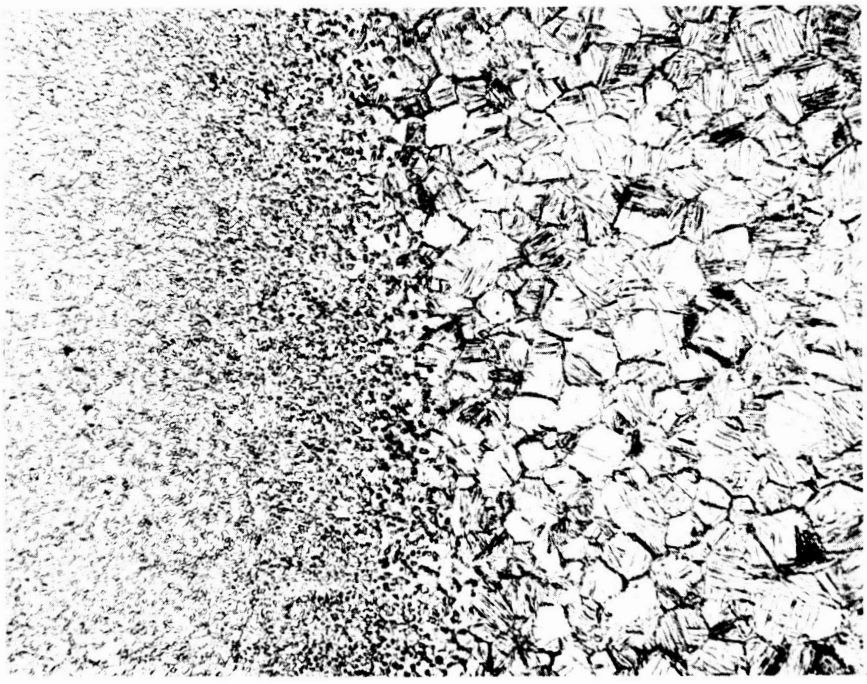

A

100X

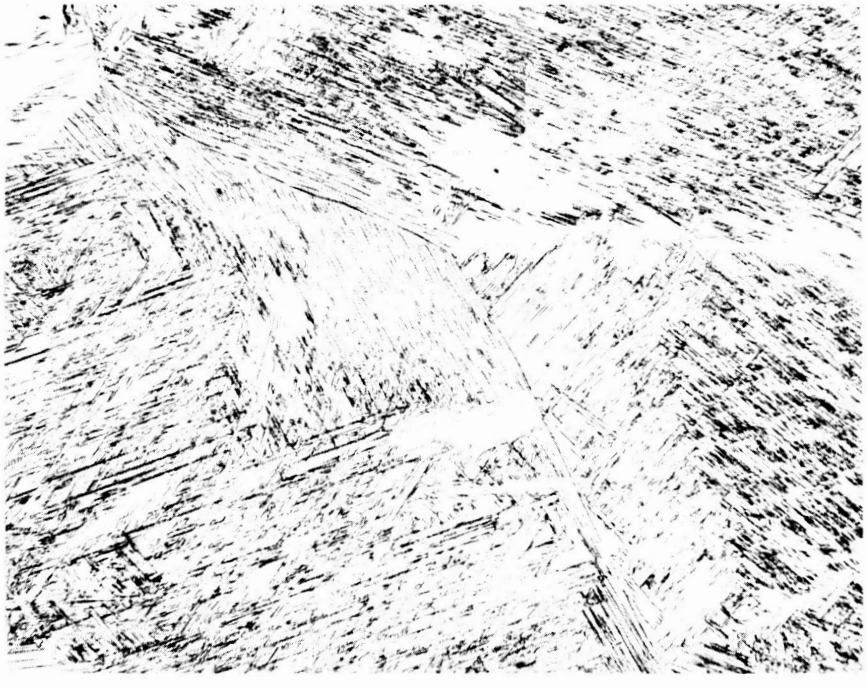

B

100X

FIGURE 48. 5Al-2.5Sn TITANIUM ALLOY UNSTRAINED
(Specimen T55)

(A) PARENT METAL (LEFT) AND HEAT-AFFECTED ZONE
(B) WELD METAL

KROLL'S ETCH

A

2000X

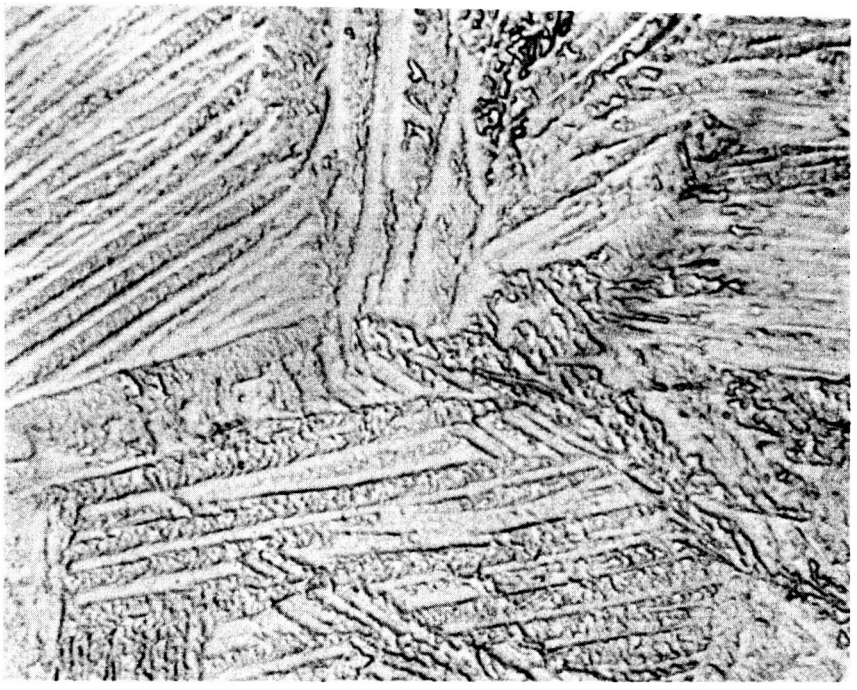

B

2000X

FIGURE 49. 5Al-2.5Sn TITANIUM ALLOY UNSTRAINED
(Specimen T55)

(A) PARENT METAL
(B) WELD METAL

KROLL'S ETCH

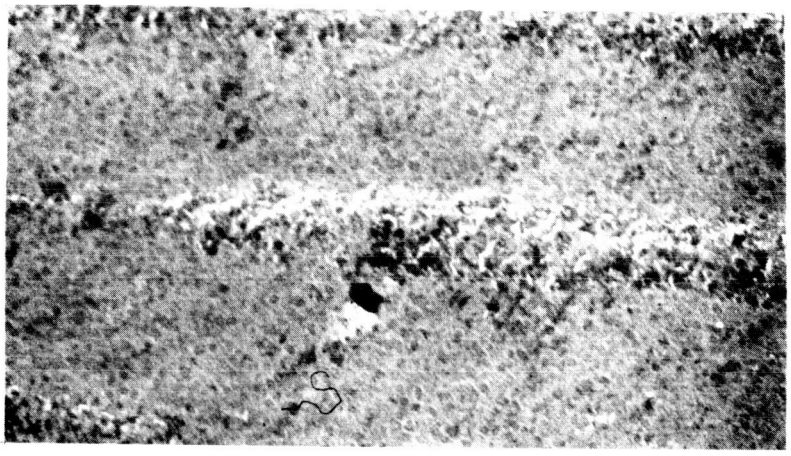

A

24, 000X

B

24, 000X

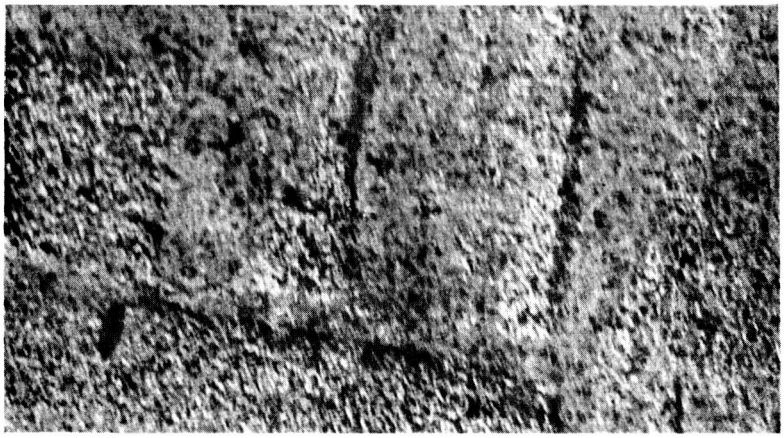

C

24, 000X

FIGURE 50. 5Al-2.5Sn TITANIUM ALLOY UNSTRAINED
(Specimen T55)

(A) PARENT METAL
(B) HEAT-AFFECTED ZONE
(C) WELD METAL

KROLL'S ETCH

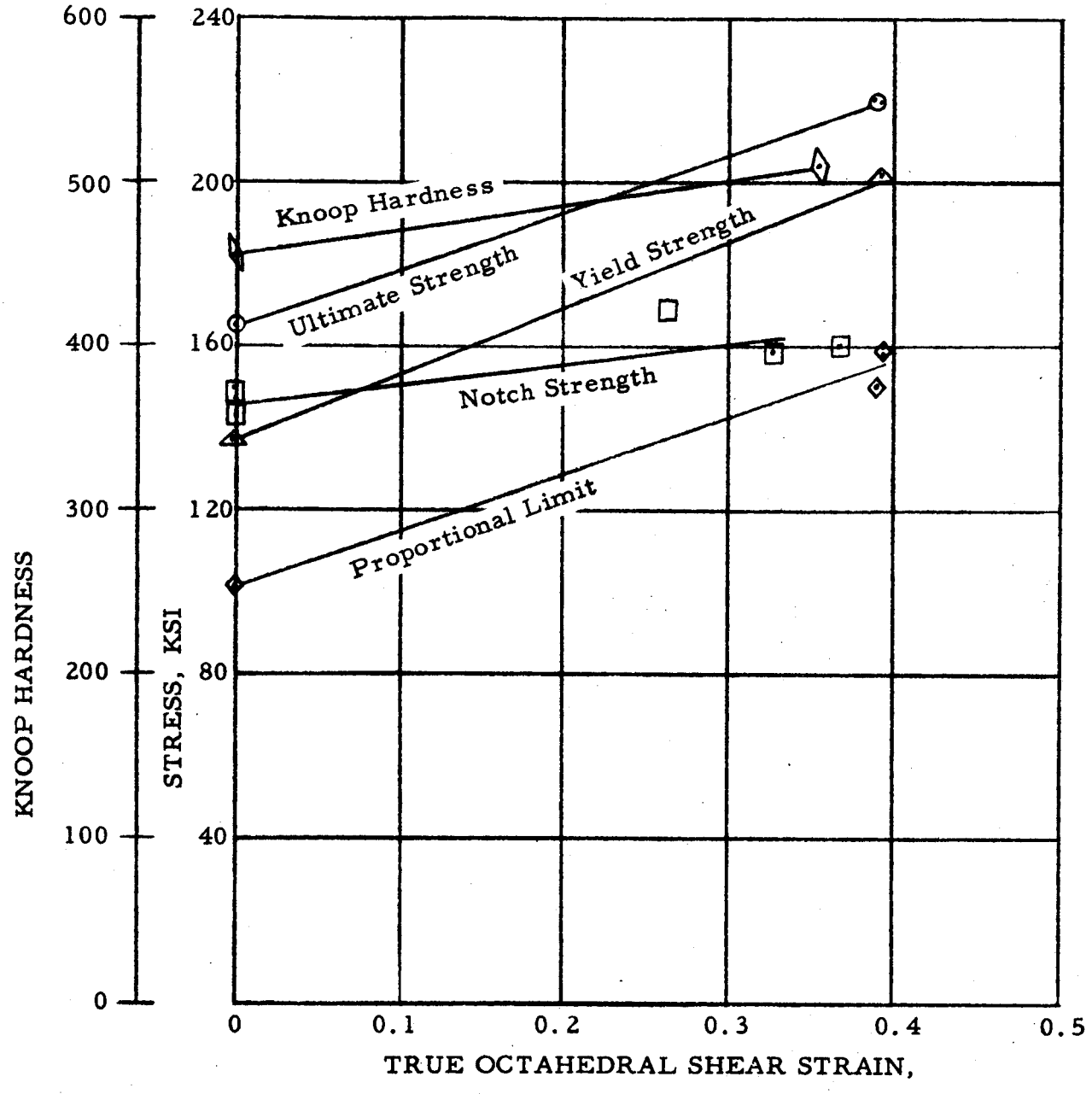

FIGURE 51. MECHANICAL PROPERTIES OF UNWELDED RENÉ 41 AFTER UNIAXIAL PRESTRAINING AT CONVENTIONAL STRAIN RATE

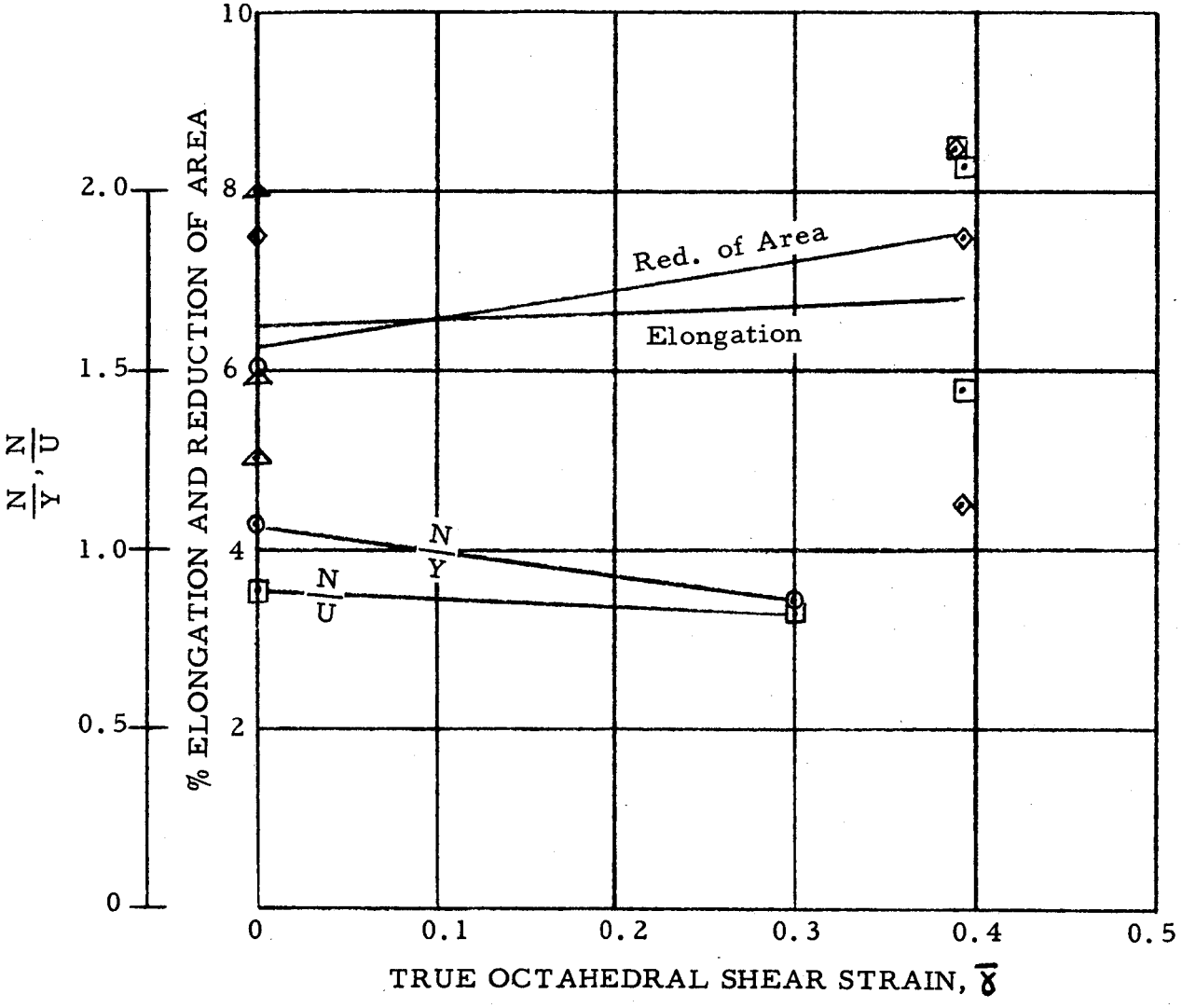

FIGURE 52. MECHANICAL PROPERTIES OF UNWELDED RENÉ 41 AFTER UNIAXIAL PRESTRAINING AT CONVENTIONAL STRAIN RATE

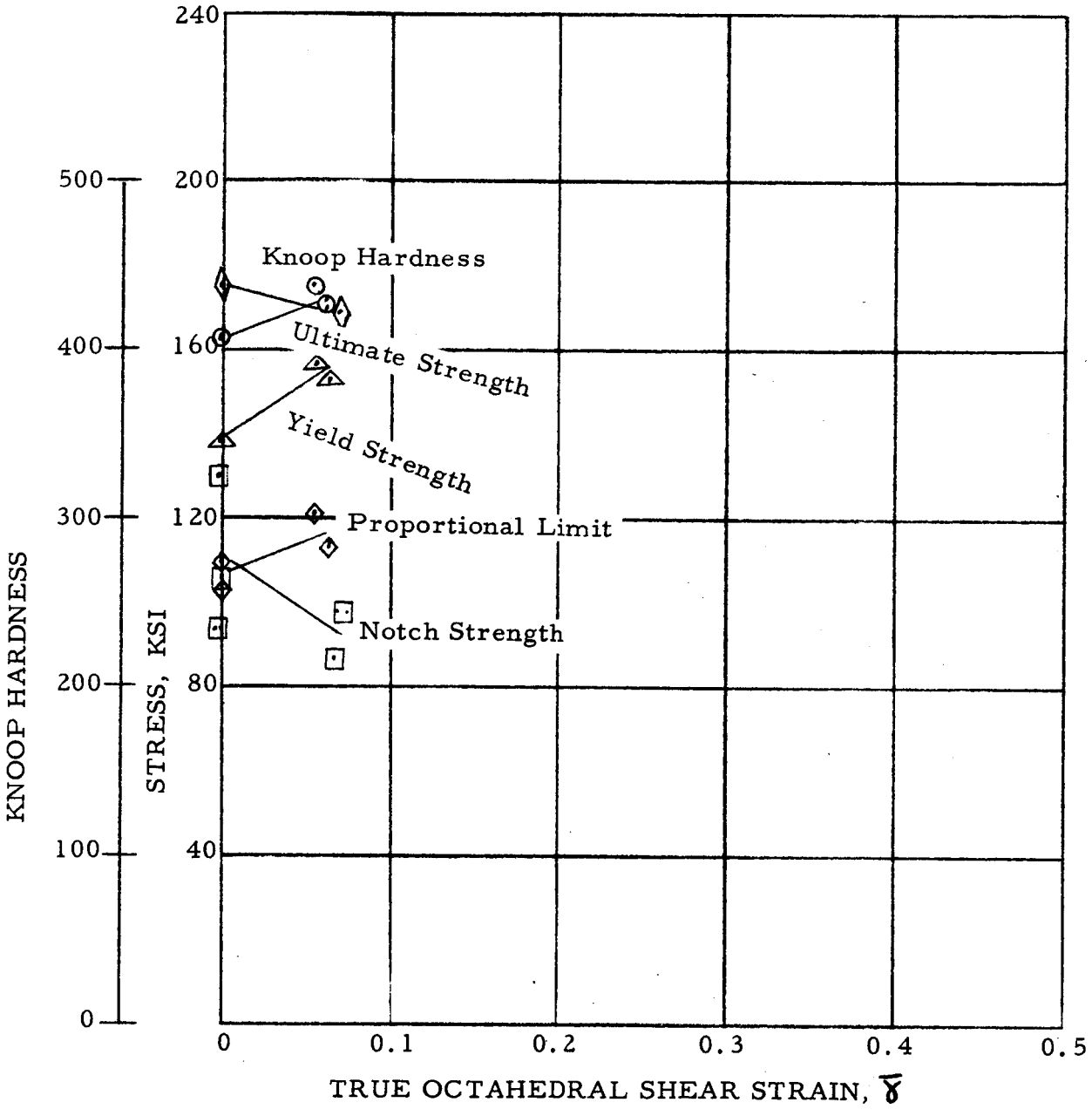

FIGURE 53. MECHANICAL PROPERTIES OF WELDED RENÉ 41 AFTER UNIAXIAL PRESTRAINING AT CONVENTIONAL STRAIN RATE

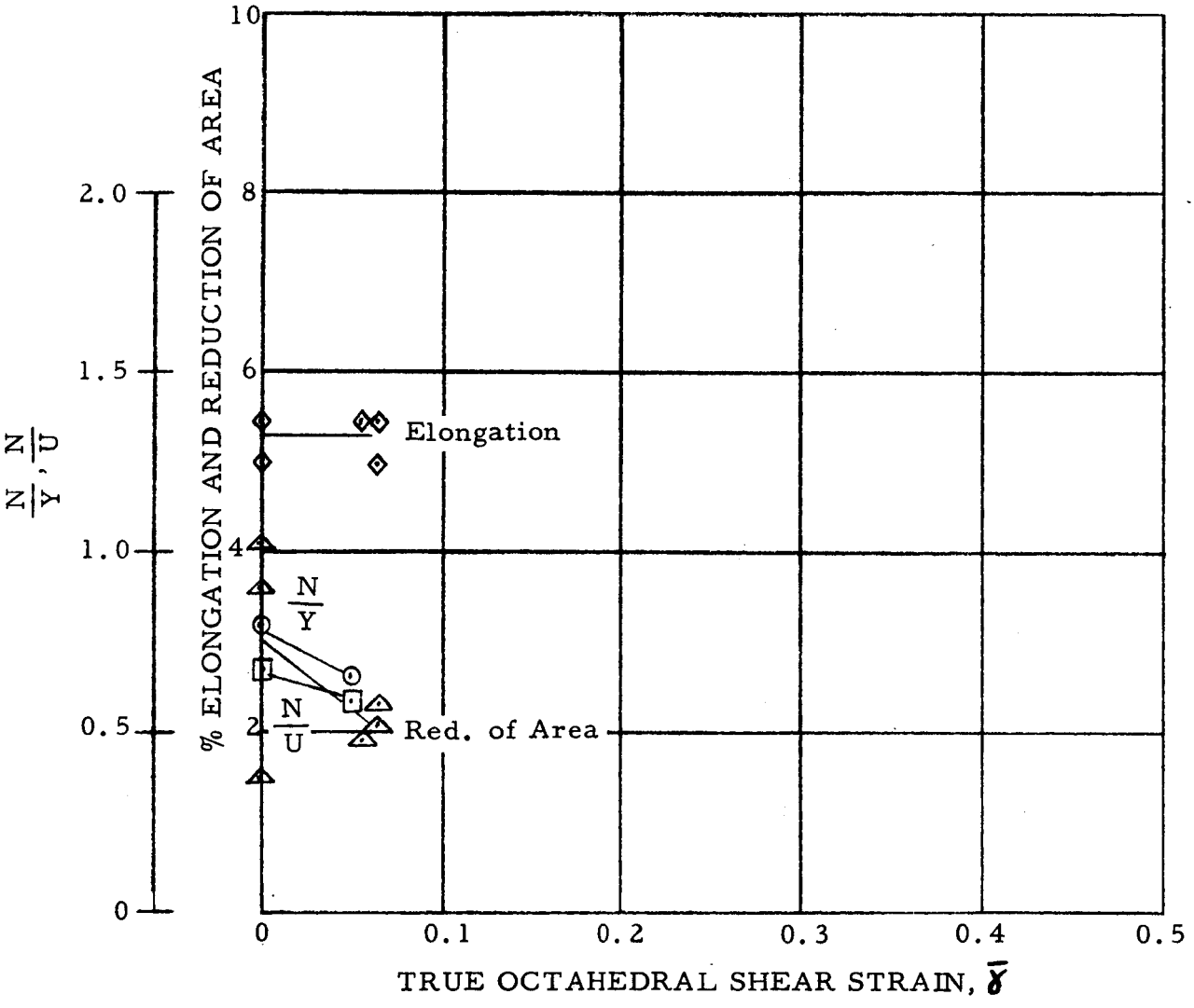

FIGURE 54. MECHANICAL PROPERTIES OF WELDED RENÉ 41 AFTER UNIAXIAL PRESTRAINING AT CONVENTIONAL STRAIN RATE

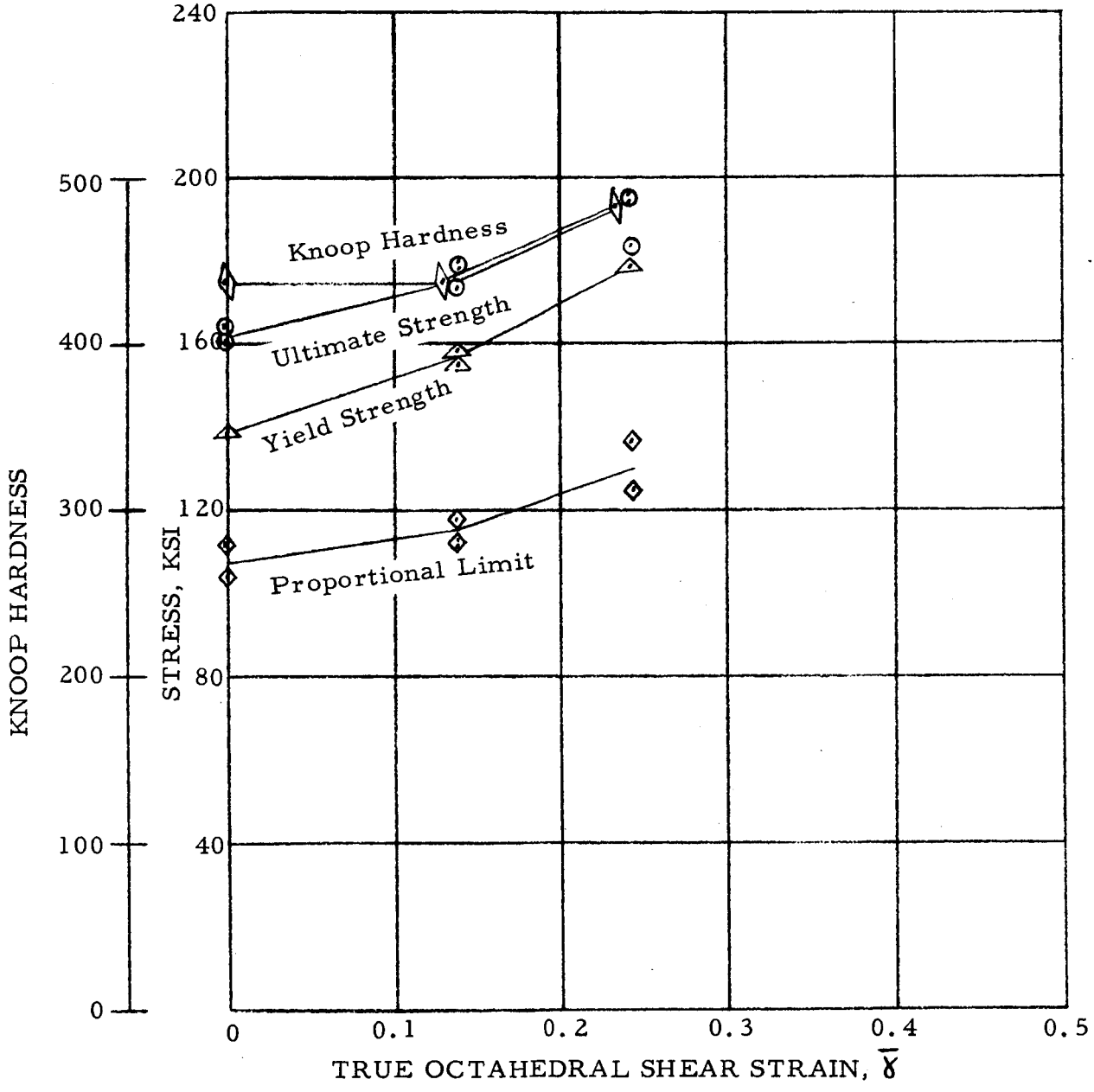

FIGURE 55. MECHANICAL PROPERTIES OF WELDED RENÉ 41 AFTER BIAXIAL PRESTRAINING AT CONVENTIONAL STRAIN RATE

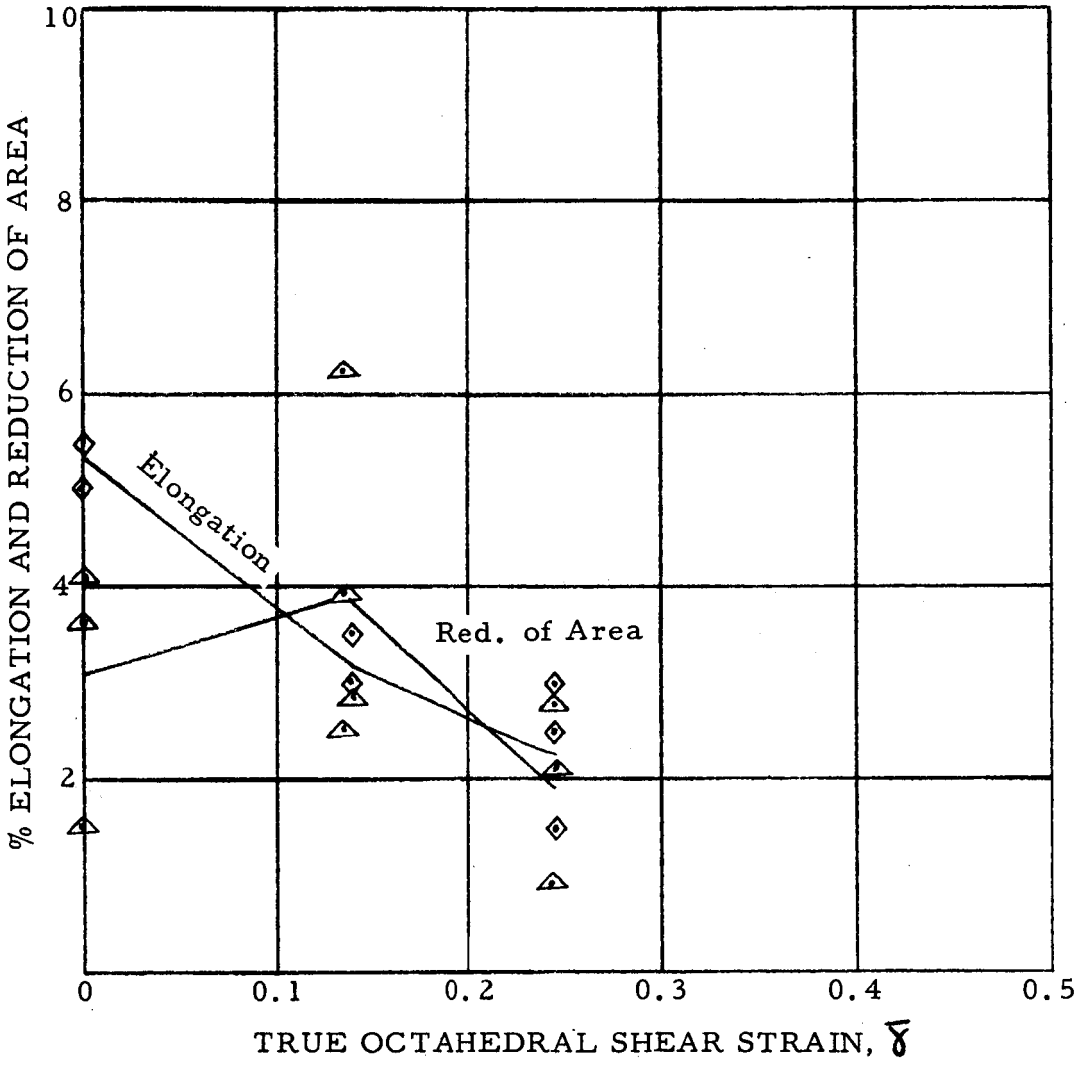

FIGURE 56. MECHANICAL PROPERTIES OF WELDED RENÉ 41 AFTER BIAXIAL PRESTRAINING AT CONVENTIONAL STRAIN RATE

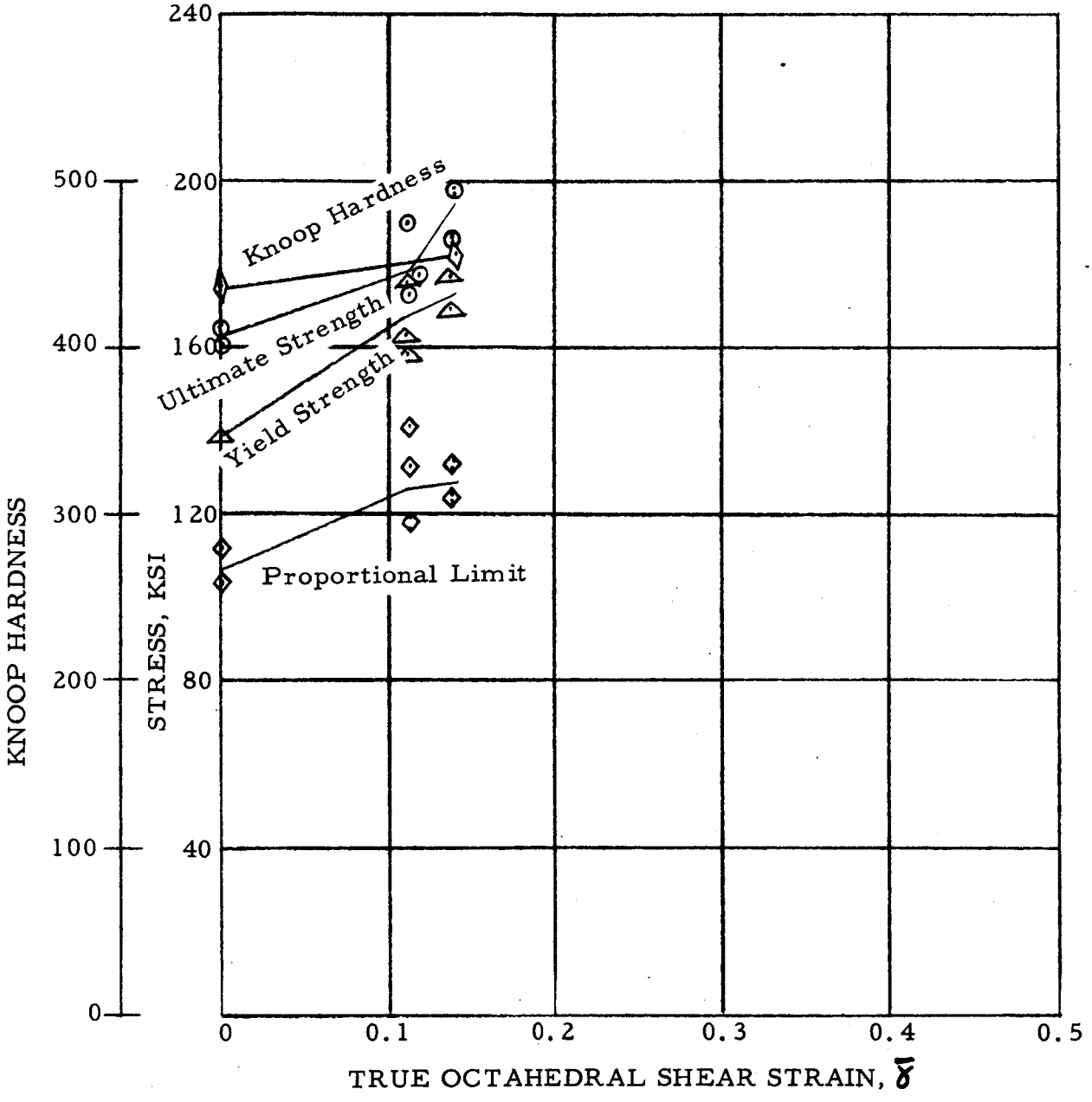

FIGURE 57. MECHANICAL PROPERTIES OF RENÉ 41 AFTER BIAXIAL PRESTRAINING AT EXPLOSIVE STRAIN RATE

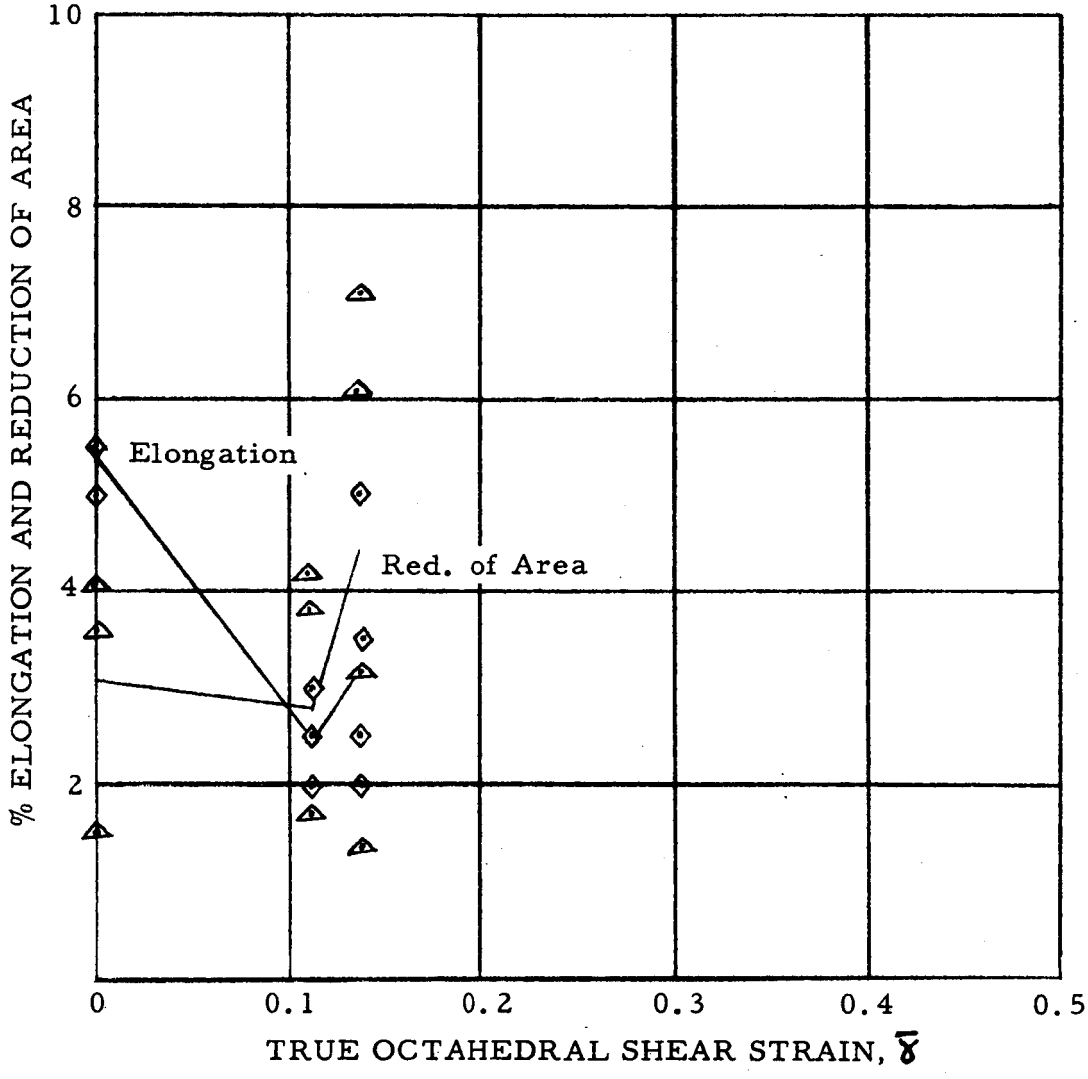

FIGURE 58. MECHANICAL PROPERTIES OF RENÉ 41 AFTER BIAXIAL PRESTRAINING AT EXPLOSIVE STRAIN RATE

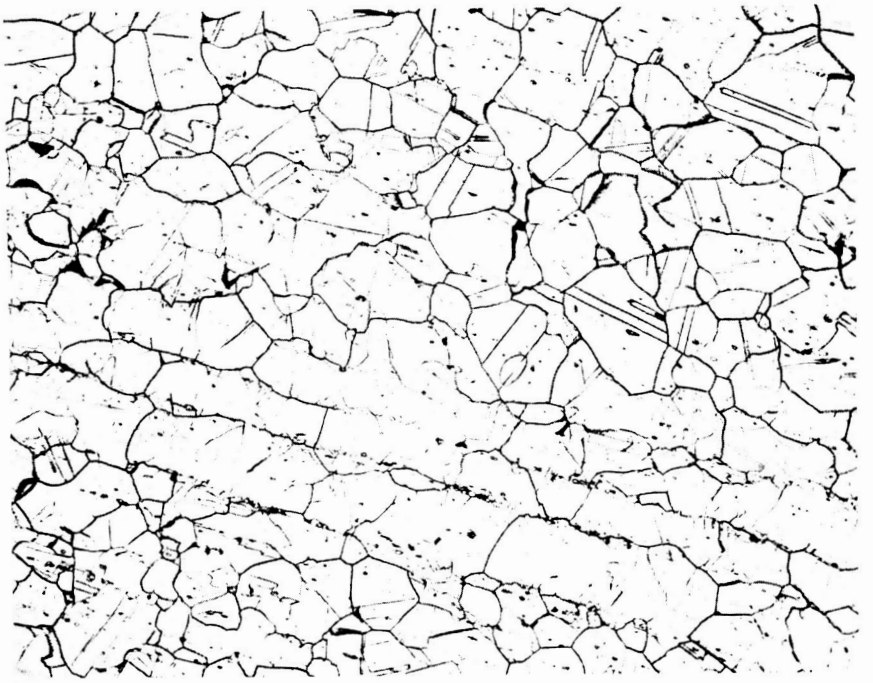

A

100X

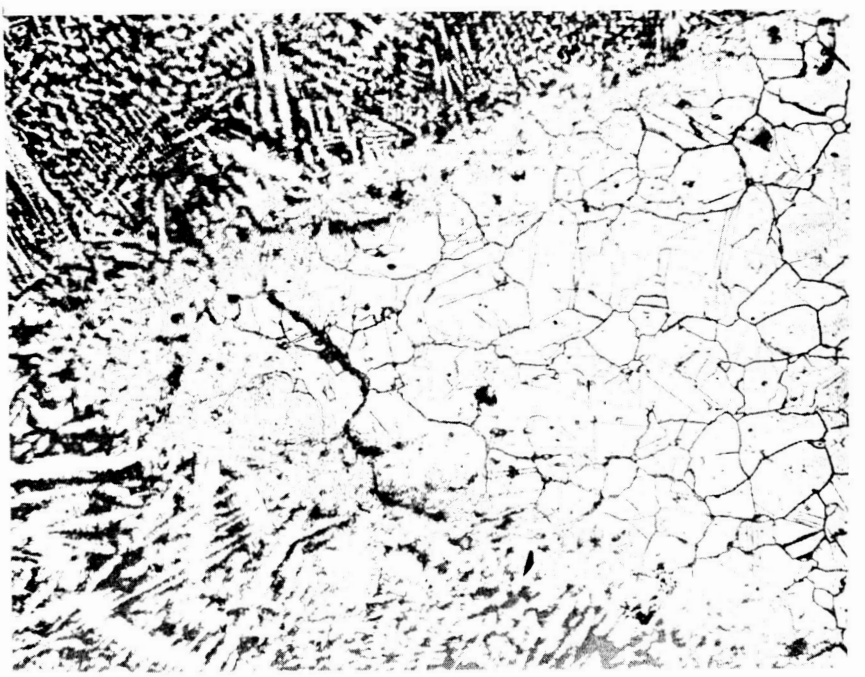

B

100X

FIGURE 59. RENÉ 41 UNSTRAINED

(A) PARENT METAL (Specimen R50)
(B) PARENT METAL, HEAT-AFFECTED ZONE, AND WELD DEPOSIT OF HASTALLOY W. (Specimen R51)

$HCl + HNO_3 + H_2O$ ETCH

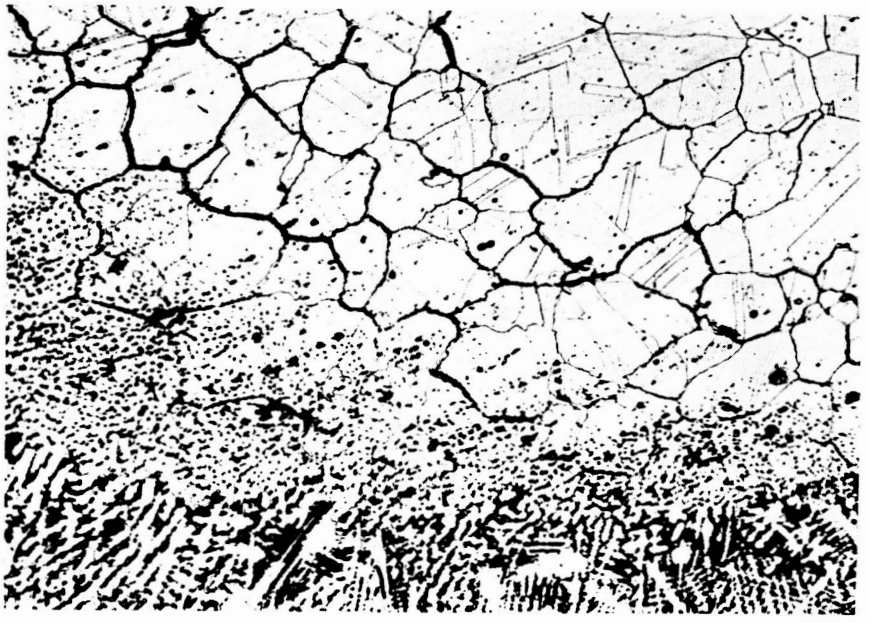

A

100X

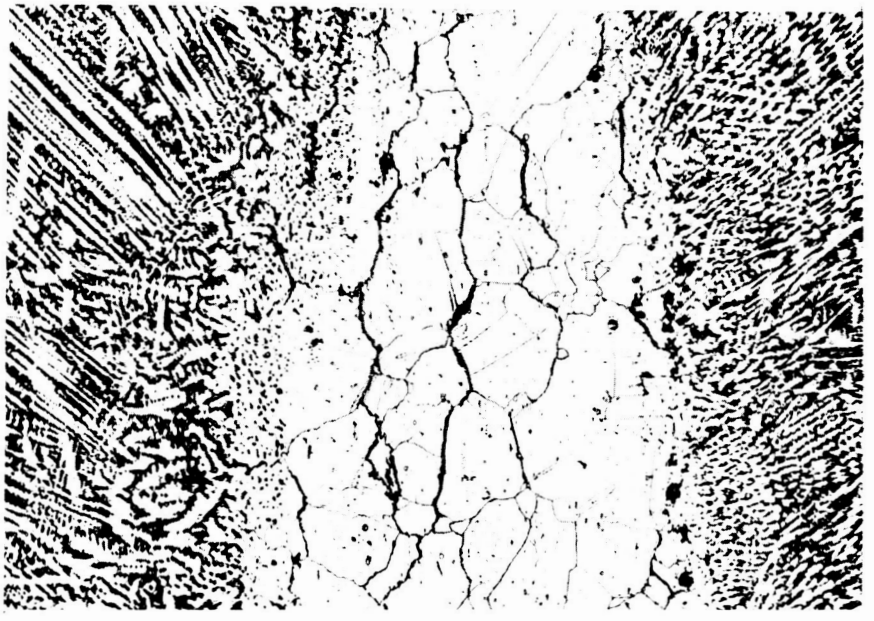

B

100X

FIGURE 60. RENE 41 BIAXIALLY STRAINED AT CONVENTIONAL STRAIN RATE

(A) PARENT METAL (Top), HEAT-AFFECTED ZONE (Center), and HASTALLOY W WELD METAL (Bottom). 5% ELONGATION. (Specimen R-8-5)

(B) PARENT METAL CENTER WITH HEAT-AFFECTED ZONE AND HASTALLOY W WELD METAL. 9% ELONGATION (Specimen R-11-4)

$HCl + HNO_3 + H_2O$ ETCH

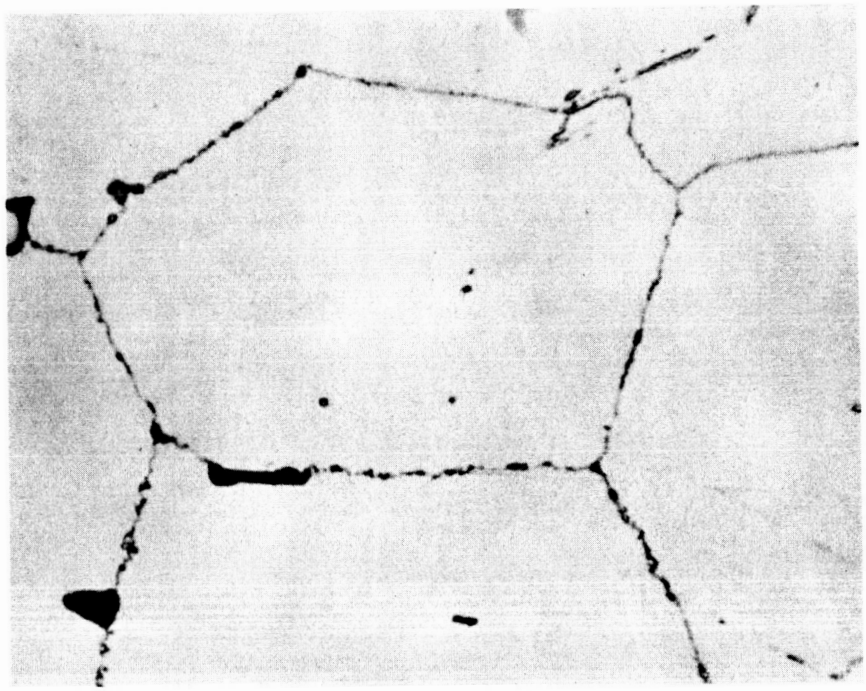

A

2000X

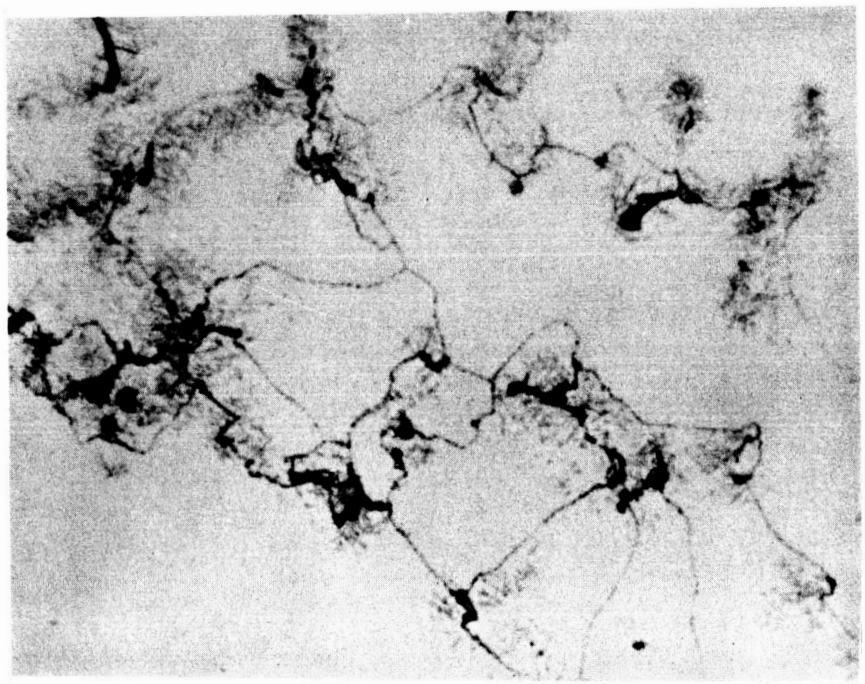

B

2000X

FIGURE 61. RENE 41 UNSTRAINED (Specimen R-51)

(A) PARENT METAL
(B) WELD ZONE OF HASTALLOY W

$K_4 (Fe CN)_6$ ETCH

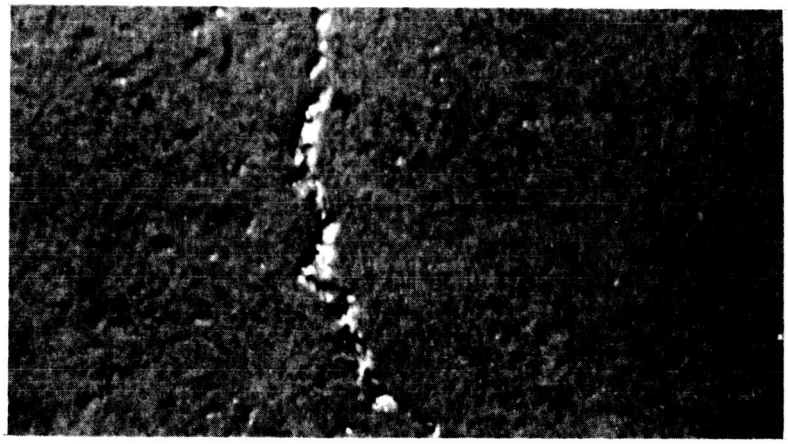

A

12,000X

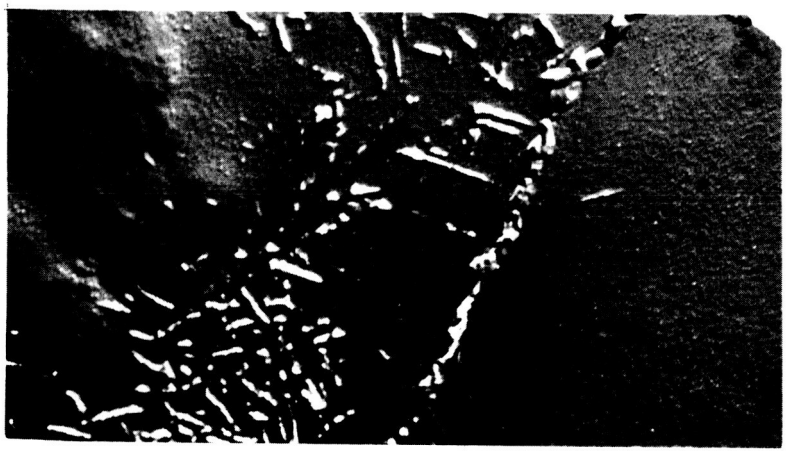

B

12,000X

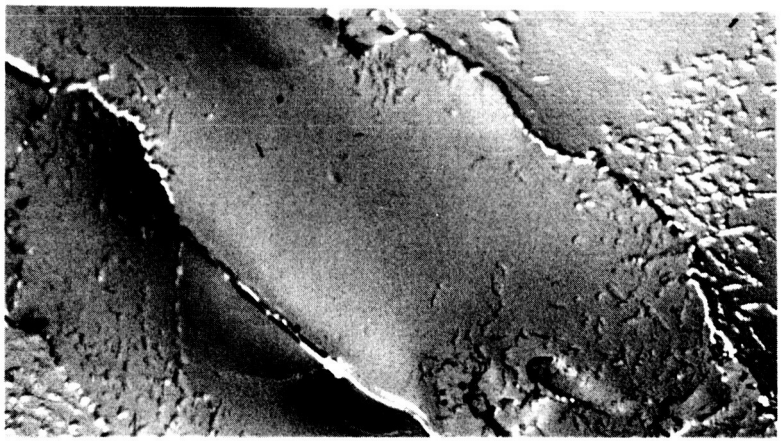

C

5,000X

FIGURE 62. RENE 41 UNSTRAINED (Specimen R-51)

(A) HEAT-AFFECTED ZONE
(B) WELD ZONE OF HASTALLOY W
(C) WELD ZONE OF HASTALLOY W

$HCl + HNO_3 + H_2O$ ETCH

DISTRIBUTION LIST

	No. Copies
National Aeronautics and Space Administration George C. Marshall Space Flight Center Huntsville, Alabama ATTN: M-P&C-CA	18
Aeronautical Systems Division ASTCMP-1 Wright-Patterson AFB, Ohio ATTN: Mr. K.L. Kojola	1
Watertown Arsenal Laboratories Watertown Arsenal Watertown 72, Massachusetts ATTN: Mr. P. Riffin	1
Defense Metals Information Center Battelle Memorial Institute Columbus, Ohio ATTN: Mr. R. Runck	1
Nuclear Space Program Division Lockheed Missiles & Space Company Sunnyvale, California ATTN: Dr. George Yasui Department 32-02	1
Los Alamos Scientific Laboratory P.O. Box 1663 Los Alamos, New Mexico ATTN: Mrs Helen F. Redman	1